



Aalborg Universitet

AALBORG UNIVERSITY
DENMARK

The PICO OWC Project

The full scale wave energy converter, that was in continuous operation for more than 7 years in roughest conditions and finally was very close to reach a load factor of 0,19

Winands, Victor Wolf Etienne

Publication date:
2019

Document Version
Publisher's PDF, also known as Version of record

[Link to publication from Aalborg University](#)

Citation for published version (APA):

Winands, V. W. E. (2019). *The PICO OWC Project: The full scale wave energy converter, that was in continuous operation for more than 7 years in roughest conditions and finally was very close to reach a load factor of 0,19*. Aalborg Universitetsforlag.

General rights

Copyright and moral rights for the publications made accessible in the public portal are retained by the authors and/or other copyright owners and it is a condition of accessing publications that users recognise and abide by the legal requirements associated with these rights.

- Users may download and print one copy of any publication from the public portal for the purpose of private study or research.
- You may not further distribute the material or use it for any profit-making activity or commercial gain
- You may freely distribute the URL identifying the publication in the public portal -

Take down policy

If you believe that this document breaches copyright please contact us at vbn@aub.aau.dk providing details, and we will remove access to the work immediately and investigate your claim.

THE PICO OWC PROJECT

THE FULL SCALE WAVE ENERGY CONVERTER, THAT WAS
IN CONTINUOUS OPERATION FOR MORE THAN 7 YEARS
IN ROUGHEST CONDITIONS AND FINALLY WAS VERY
CLOSE TO REACH A LOAD FACTOR OF 0,19

**BY
VICTOR WINANDS**

DISSERTATION SUBMITTED 2019



AALBORG UNIVERSITY
DENMARK

THE PICO OWC PROJECT

***THE FULL SCALE WAVE ENERGY CONVERTER, THAT
WAS IN CONTINUOUS OPERATION FOR MORE THAN 7
YEARS IN ROUGHEST CONDITIONS AND FINALLY WAS
VERY CLOSE TO REACH A LOAD FACTOR OF 0,19***

by
Dipl. Ing. Victor Winands

Dissertation submitted 19.08.2019

Supported by:
Duespan Wave- Engineering, WavEC Offshore Renewables, Técnico Lisboa and



AALBORG UNIVERSITY
DENMARK

Dissertation submitted: 19.08.2019

PhD supervisor: Associate Prof. Jens Peter Kofoed,
Aalborg University

PhD committee: Associate Professor Peter Frigaard (chairman)
Aalborg University

Associate Professor Luca Martinelli
University of Padova

Professor Gregorio Iglesias
University College Cork

PhD Series: Faculty of Engineering and Science, Aalborg University

Department: Department of Civil Engineering

ISSN (online): 2446-1636
ISBN (online): 978-87-7210-525-3

Published by:
Aalborg University Press
Langagervej 2
DK – 9220 Aalborg Ø
Phone: +45 99407140
aauf@forlag.aau.dk
forlag.aau.dk

© Copyright: Victor Winands

Printed in Denmark by Rosendahls, 2020



CV

Name: Victor Winands

Date of Birth: 11.04.1979

I have spend more than 10 years working on the Pico OWC. I'm a 39 years old mechanical engineer with a degree from the Technical University of Berlin. Beside that I have worked several years as a locksmith, carpenter and on various construction fields. As a father I have an interest in searching for sustainable ways of living and as a surfer I'm connected to the ocean. The combination of my manual skills, my engineering background and my personal motivation appears to have been a good combination to combine the wave energy theory with the demands of real world wave energy applications. My work experiences allowed to solve most of the problems of the Pico device without external support or essential budget. After reaching continuous autonomous operation in 2010 the desired external interest in the device remained very low, which we assumed to be caused by the low power production of the device. Therefore my college Kieran Monk and I started the power analyses and maximization for which I could find funding as a PhD student initially at the Technical University of Lisbon (Portugal) and later from the Aalborg University (Denmark). The last years of the project I earned my money by selling wave energy on the Azorean island Pico and working on construction fields in Germany.

My decision to work on Pico was not related to financial considerations. Before coming to Pico I was one of three owners of a well established construction company in Berlin (Germany) and therefore my financial situation was better than it is today.

Though it was a tough journey I hope there will be a chance to try it again, because I still believe that it is worth it.

ENGLISH SUMMARY

When comparing wave energy to the sector of wind energy it becomes obvious that wave energy has still not reached the technical breakthrough. In 2016 world wide about 430 GW of wind energy were installed while only approximately 1 MW of wave energy were installed. This is a large discrepancy especially because several estimations assume the energy resource of wave energy in the range of 10 percent of the resources of wind energy.

The main reason for the delayed development of the wave energy sector is often named to be the higher energy costs, which are caused by larger investment costs of maritime devices, the currently still low efficiency and expensive technical problems. However, it should be requested why so less effort is undertaken by the industry to develop the technology in order to overcome the prototype problems to reduce these costs. The author expects one essential reason for it to be the fact that till today no wave energy device could fully convince. Though since the 1970th it is professionally attempted to harvest wave energy, compared to wind energy, only a very small number of full scale devices was realized from which only very few were able to reach continuous autonomous operation. Theoretical some concepts appear very promising but in reality various devices could not withstand the ocean forces and only the devices with very low power predictions could reach the claimed expectations.

This thesis is the outcome of a 10 years lasting field study on the Pico OWC (oscillating water column) wave energy converter. In this field study it was attempted to develop a full scale wave energy converter, which can operate autonomously in rough sea conditions over a long period and can also prove the theory by delivering the claimed power levels. At the time of this study this was still possible and if it could have been reached the Pico OWC would have been a successful full scale wave energy converter, which might have helped to regain trust and related investment into the sector of wave energy.

The first part could be achieved because the Pico plant was in continuous autonomous operation since September 2010 and the wave climate on Pico is rough in winter time.

The long lasting history of problems on the Pico plant before 2010 were experienced to be problematic because this is still the better known part of the Pico project. However, this history has also positive aspects because it could be shown that positive results in terms of reliable operation do not require large investments.

The predicted power levels could not be reached in real device operation but in this thesis the significantly lower real device performance compared to the initial predictions was analyzed and could be explained based on a validated time domain model. Further it is shown that the reasons why the by the analysis proposed technical changes were not implemented to the real device were no technical ones.

The highest annual average grid power of the real device was 5,1 kW, which corresponds to approximately 5 % of the initial predictions of about 96 kW. In about 7 years of continuous operation the device fed 149 MWh to the grid. Though this is a respectable value compared to other wave energy converters it is far too low in comparison to the initial predictions, which were round 840 MWh per year.

However, it was possible to explain the low real device performance by use of the initial design theory. Therefore the theory appears to be proven. The problem that causes about 78 % of the total underperformance appears to be a reduced turbine efficiency. The reason for the reduced efficiency could not yet be detected but several reasons could be excluded in an analysis that is presented here. Currently, there is some evidence that the reason might be a scaling problem of monoplane Wells turbines. However, due to the fact that more recent monoplane Wells turbines are already introduced with significantly higher efficiency than the designed Pico turbine, it appears technically possible to correct this problem. Today after the collapse of the civil structure these changes cannot be realized at the Pico plant anymore but model results indicate an increase of the annual grid power of the Pico plant about a factor of 6,7 from currently 11,5 kW (with assumed full machine availability) to 77,5 kW. For this power increase exclusively the turbine performance has to be corrected, which appeared possible for the Pico plant within a reasonable effort. This was the case because, exclusively the substitution of the rotor blades by suitable ones appeared required and the blades of the Pico rotor were designed to be exchangeable. The 77,5 kW correspond to about 80 % of the initial power expectations, which is a respectable value for a prototype device. The other 20 % are lost due to a rotational speed limitation and defects on the chamber structure. Both effects can be avoided on future devices.

The found theoretical results should have been confirmed by developing, installing and testing suitable rotor blades for the Pico plant. This would have been the last remaining step to turn the Pico plant into a successful full scale wave energy converter. But this step was missed.

DANSK RESUME

”Når man sammenligner bølgeenergi med vindenergien, bliver det tydeligt at bølgeenergi stadig ikke har det nået et tekniske gennembrud. I 2016 blev der i hele verden installeret omkring 430 GW, mens det tilsvarende tal for bølgeenergi var ca. 1 MW. Dette er en stor forskel, især fordi flere estimerer tilsiger at bølgeenergiressourcen er i størrelsesordenen ca. 10 procent af vindenergiressourcen.

Hovedårsagen til den forsinkede udvikling af bølgeenergisektoren angives ofte at være den højere energiomkostninger, der skyldes større investeringsomkostninger for maritime enheder, den stadig relativt lave effektivitet og dyre tekniske udfordringer. Man må spørge sig selv om hvorfor der ikke gøres en større indsats i industrien for at udvikle teknologien og overvinde prototypeproblemerne, og dermed reducere disse omkostninger? Forfatteren mener at en væsentlig årsag til dette, skal findes i, at der til dato ikke er demonstreret overbevisende bølgeenergianlæg. Dette tiltrods for at der siden 1970'erne er arbejdet professionelt med forsøg på at høste bølgeenergi. Til sammenligning med vindenergi, er kun et meget lille antal fuldskalaanlæg blevet realiseret, hvoraf kun få har opnået en tilstand med kontinuerlig autonom operation. Teoretisk ser en del anlæg meget lovende ud, men i virkeligheden har mange ikke modstå havets belastninger og kun anlæg med meget lave forventninger til strømproduktionen har kunnet indfri disse.

Denne afhandling er resultatet af 10 års feltundersøgelse af Pico OWC (oscillerende vandsøjle) bølgeenergianlægget. I denne feltundersøgelse blev det forsøgt at udvikle et fuldskala bølgeenergianlæg, som kan operere autonomt i barske havforhold i lang tid og som også kan påvise leverance af hævdede ydelser. På undersøgelsestidspunktet var det stadig muligt, og Pico OWC anlægget kunne have været et succesfuldt fuldskala bølgeenergianlæg, som kunne have hjulpet med at genvinde tillid og relaterede investeringer i bølgeenergisektoren.

Den første del kunne opnås, fordi Pico-anlægget var i kontinuerlig autonom drift siden september 2010, og bølgeklimatet på Pico er hårdt om vinteren.

Den langvarige historie af problemer på Pico-anlægget i perioden før 2010 er uheldig, da dette udgør den bedst kendte del af Pico OWC projektet. Denne historie har dog også positive aspekter, fordi det kan godtgøres, at positive resultater med hensyn til pålidelig drift ikke kræver store investeringer.

De forudsagte ydelser kunne ikke nås ved brug af det realiserede anlæg, men i denne afhandling er den signifikant lavere reelle ydelse (i forhold til de oprindelige forudsigelser) blevet analyseret forklaret ve hjælp af en valideret tidsdomæne model. Det fremgår endvidere, at grundene til den lavere ydelse skal findes i at de nødvendige ændringer ikke er blevet implementeret, selvom dette rent tekniske er muligt.

Den højeste årlige gennemsnitlige ydelse til nettet fra anlægget 5,1 kW, hvilket svarer til ca. 5% af de indledende forudsigelser på ca. 96 kW. På ca. 7 års kontinuerlig drift har enheden leveret 149 MWh til nettet. Selvom dette er en respektabel værdi i forhold til andre bølgeenergianlæg, er det alt for lavt sammenligning med de indledende forudsigelser, som var omkring 840 MWh om året.

Det var imidlertid muligt at forklare denne lave reelle ydelse ved brug af den oprindelige designteori. Derfor synes teorien at være bevist. Problemet, der forårsager ca. 78% af den samlede underperformance ser ud til at være på grund af en reduceret turbineeffektivitet. Årsagen til den reducerede effektivitet kunne endnu ikke påvises, men flere grunde kunne udelukkes i en analyse, der præsenteres her. I øjeblikket er der nogle beviser for, at årsag kan være et skaleringsproblem med monoplan Wells turbiner. Men på grund af det faktum, at nyere monoplan Wells turbiner allerede er introduceret med betydeligt højere effektivitet end den designet til og implementeret i Pico OWC anlægget, synes det teknisk muligt at rette op på dette problem. I dag, efter sammenbruddet af betonkonstruktionen, kan disse ændringer desværre ikke realiseres på Pico OWC anlægget længere, men modelresultaterne indikerer en stigning i den årlige produktion til nettet på omkring en faktor på 6,7 fra i øjeblikket 11,5 kW (med antaget fuld maskine tilgængelighed) til 77,5 kW. For at opnå denne effektførelse, er det blot nødvendigt at korrigere turbineydelsen, hvilket syntes muligt for Pico-anlægget, med en overkommelig indsats (inden konstruktionen blev beskadiget). Dette var tilfældet, fordi hvad der krævedes var blot en udskiftning af turbinens rotorblade. 77,5 kW svarer til ca. 80% af de indledende forventninger af anlæggets ydelse, hvilket er en respektabel værdi for en prototype enhed. De resterende 20% går tabt på grund af upræcis styring af rotationshastighed og defekter på kammerstrukturen. Begge effekter kan undgås ved fremtidige anlæg.

De fundne teoretiske resultater burde have været bekræftet ved at udvikle, installere og teste passende rotorblade på turbinen i Pico OWC anlægget. Dette ville have været det sidste tilbageværende skridt for at gøre Pico-anlægget til et succesfuld fuldskala bølgeenergianlæg. Men dette skridt blev ikke opnået.”

ACKNOWLEDGEMENTS

I would like to say thanks to everyone who helped me along the years to keep the project alive. I would like to especially name the following persons who joint me on the way.

To my friend Tonecas Soares who has been there throughout all the years and helped me in numberless constructions.

To my friend Kieran Monk for going a long part of the way with me and for keeping the plant alive in the complicated times.

To my friend and former colleague Frank Neumann to involve me to the Pico project, to go through so many disappointing project periods with me and especially for his rear cover when opinions spread.

To the great people of the Cofaco tuna factory for permanent, free use of their installations throughout all these years. Especially to Manuel Marcos his advises and all the mechanical parts he build for me without hesitating, to Jose Manuel Viera for his support in electrical issues.

To the team of EDA for the support.

To Antonino for is invaluable knowledge support when analyzing the generator damage.

To Izan Le Chrom for all his help and effort such as the interesting diving experience we joint together.

To David Benhaim for his great help on one of our greatest challenges.

To Ana Neumann of WavEC for supporting the Pico project and giving me accommodation on her sofa all these times.

To Prof. Peter Fregard for offering me the possibility to write this thesis in Denmark and so financing my work for some time.

To Prof Jens Peter Kofoed for being my supervisor and guiding me through the for me less familiar part of this thesis.

To Prof. Antonio Falcao the father of the Pico plant for some impressive demonstrations of his knowledge and of course the realization of the Pico plant.

To the University of Lisbon IST (Institute Superior Technico) for the temporally support of my work.

Finally to Prof. Antonio Sarmento the Director of WavEC for his effort to keep the Pico plant alive.

To my family and especially my wife for tolerating and supporting my way of living.

LIST OF PAPERS WITH THE AUTHORS CONTRIBUTION

- Neumann F., Winands, V., Sarmiento, A.J.N.A., "Pico Shoreline OWC: status and new perspectives", proceedings of the 2nd International Conference on Ocean Energy (ICOE 2008), Brest, France, 15th -17th October 2008.
- Winands, V. and Fester, F. (2013) 'Challenging times for wave energy:Reasons and Solutions', in the Proceedings of the *EWTEC conference, Aalborg, 2013*
- F.Paparella, K. Monk, V. Winands, M. Lopes, D. Conely. "Benefits of up-wave measurements in linear short-term wave forecasting for wave energy applications", Proceedings of the IEEE Multi-conference on Systems and Control, Nice, October 2014
- F. Paparella, K. Monk, V. Winands, M. F. P. Lopes, D. Conley, and J. V. Ringwood, 'Up-Wave and Autoregressive Methods for Short-Term Wave Forecasting for an Oscillating Water Column', IEEE Transactions on Sustainable Energy, vol. 6, no. 1, pp. 171–178, 2015.
- Kieran Monk, Daniel Conley, Victor Winands, Miguel Lopes, Qingping Zou, Deborah Greaves Simulations and Field Tests of Pneumatic Power Regulation by Valve Control Using Short-term Forecasting at the Pico OWC– EWTEC 2015, 11th European Wave and Tidal Energy Conference, Nantes, France, Sep 2015.
- Monk, K., Winands, V. and Lopes, M. (2018) 'Chamber pressure skewness corrections using a passive relief valve system at the Pico OWC' *Renewable Energy*, Volume 128 (2018) 230-240

TABLE OF CONTENT

Chapter 1. Introduction	14
1. Thesis overview.....	15
2. Background.....	17
3. Objectives.....	19
3.1. Improve the sector of wave energy	19
3.2. Explain the reasons for the initial project problems.....	19
3.3. Share the experience of continuous operation	19
3.4. Present the detection of the main cause for the large device underperformance	19
Chapter 2. State of the art	20
1. Wave energy in general.....	21
2. The technology.....	24
2.1. The working principle	24
2.2. The bidirectionality of the Wells turbine and aerodynamic stall.....	24
2.3. control challenges due to aerodynamic stall.....	26
2.4. Control challenges due to grid constrains.....	26
2.5. Control procedure	27
3. The numerical model.....	28
4. Literature review.....	32
4.1. Historic Literature regarding the Pico plant.....	33
4.2. OWC papers Used to obtain the required theory.....	34
4.3. Recent studies relevant for this thesis	34
4.4. Obtained papers on performance analysis of WECs	34
Chapter 3. The Pico plant.....	35
1. Intro	36
2. Resource assessment.....	37
3. System specification.....	38
4. Available wave data in operation	45
Chapter 4. Data analysis and results.....	46
1. 14 Reasons for Realization problems	47
1.1. Background information.....	47
1.2. Initial troubleshooting during this field study.....	48
1.3. Root cause Analysis of the initial problems.....	49
1.4. Result discussion.....	54
1.5. Conclusion from troubleshooting.....	56
2. Continuous operation experience	57
2.1. Operation statistic.....	57
2.2. Production results.....	59
2.3. Failures in continuous operation	60
2.4. Discussion of the continuous operation results	63

2.5. Conclusions from continuous operation	64
3. Performance analysis.....	65
3.1. Purpose.....	65
3.2. Methodology.....	65
3.3. Execution and intermediate results.....	67
3.4. Power losses in Detail.....	79
3.5. Power evaluation	84
3.6. Discussion of Uncertainties.....	86
3.7. Discussion of the performance analysis results.....	87
3.8. Conclusions from the performance analysis.....	89
Chapter 5. Conclusions.....	91
1. Conclusions related to the thesis objectives.....	92
2. Scientific innovation	94
2.1. Scientific Innovation of the field study.....	94
2.2. Scientific innovation of the thesis	94
3. Future works.....	95
3.1. Further development on the Pico plant.....	95
3.2. Scientific studies.....	96
4. Advises for future projects	97
4.1. All PTO types.....	97
4.2. OWC in particular	97
5. Personal consideration.....	98

TABLE OF FIGURES

Figure 1.1 Project phases of a prototype.....	15
Figure 2.1 Installed wave energy capacity in 2016	21
Figure 2.2 Cross-sectional illustration of the Pico OWC.....	24
Figure 2.3 Schematic of a vertical Wells turbine.....	25
Figure 2.4 Forces at the blades of a Wells turbine.....	25
Figure 2.5 Flow diagram of the OWC wave to wire model	30
Figure 2.6 Characteristic curve of the designed Pico turbine	31
Figure 3.1 Device orientation	38
Figure 3.2 Civil structure cross section.....	38
Figure 3.3 Schematic of the self developed nearshore wave sensor.	39
Figure 3.4 Schematic of the Power electronics.....	40
Figure 3.5 Location plant and control unit.....	40
Figure 3.6 Independent security system	43
Figure 4.1 Pico turbine hall in 2007.....	55
Figure 4.2 Monthly operation statistic.....	58
Figure 4.3 Annual average power	59
Figure 4.4 Energy fed to grid.....	59
Figure 4.5 Pressure skewness.....	66
Figure 4.6 Generated power and RPM comparison	68
Figure 4.7 Measured turbine curve (green), best fit curve (blue), the designed curve (red).....	69
Figure 4.8 Model match of the “validated model” with real plant data.....	69
Figure 4.9 Different characteristic turbine curves.....	70
Figure 4.10 Theoretical RPM limitation approach.....	71
Figure 4.11 Influence of the hydrodynamic defects to the sea state classification. (Arrows: black:device performance with designed hydrodynamic performance; gray: performance with assumed hydrodynamic losses; green: stage of comparisons; yellow: input values; red: tendency to predict too large sea conditions).....	74
Figure 4.12 Chamber surface elevation spectra at high tide in average waves.....	74
Figure 4.13 Chamber surface elevation spectra at low tide in average waves.....	75
Figure 4.14 Chronological plot of the sea state classification.....	76
Figure 4.15 Chronological plot of the sea state classification.....	76
Figure 4.16 Power comparison in 44 sea states listed with increasing contained energy (applied classification). 77	
Figure 4.17 Power comparison in 44 sea states listed with increasing contained energy (offshore forecast data classification)	77
Figure 4.18 Power difference in 44 sea states listed with increasing energy content (applied classification) Sea states without real power value did not occur more than once in the observed period.....	77
Figure 4.19 Power difference between low and high tide (applied classification).....	78
Figure 4.20 Modeled losses and remaining grid power.....	80
Figure 4.21 Rotational speed margin and breaking procedure [real (red); theoretical approach (blue)]	81
Figure 4.22 Control strategy [theoretically optimal (red); real “best practice” (blue)]......	82
Figure 4.23 Characteristic turbine curve comparison	82
Figure 4.24 General scatter diagram of the Pico device today (Left: the used performance points (The filled and empty dots both indicate one performance point. Due to the classification procedure the points are sometimes overlapping. Therefore two different point types are used.); Middle: the real device average power per sea state; Right: Validated model average power per sea state).....	84
Figure 4.25 Pico scatter diagram for the device with corrected turbine efficiency (Left: modeled average power per sea state for the “Validated model”; Right: modeled average power per sea state for the “Model with corrected turbine”).....	85
Figure 4.26 Pico performance scatter diagram presented in (Pecher et al, 2011)	87
Figure 4.27 Pico scatter diagram with passive rectification valve (Monk, Winands and Lopes, 2018) (Hs and Tp values correspond to excitation flow surface elevation and not to outside wave).	88
Figure 4.28 Expected power increase	89
Figure 4.29 Generated power comparison per sea state.....	90
Figure 4.30 Factor 2,9 verification in real operation interval of 2 hours (Figure corresponds to Figure 4.8).....	90
Figure 5.1 Turbine curve of a recent Wells turbine which is adapted to the Pico plant (presented in (Falcao, Henriques and Gato, 2016)).	95
Figure 5.2 Curve comparison: Recent turbine to Pico design turbine.....	96

List of Tables

- Table 3.1 Local wave climate.....37
- Table 4.1 Failure log 1995-2007.....50
- Table 4.2 Failure log 2007-September 2010 part 1/2.....51
- Table 4.3 Failure log 2007-September 2010 part 2/2.....52
- Table 4.4 Root cause analysis for initial problems.....53
- Table 4.5 Root causes analysis for problems before 2010.....53
- Table 4.6 Annual operation statistic.....57
- Table 4.7 Section of the failure log for continuous operation.....61
- Table 4.8 Root cause analysis 09.2010-12.2016.....62
- Table 4.9 Root cause analysis (all events transformed into long down time events).....62
- Table 4.10 Root cause analysis 2016.....63
- Table 4.11 Root cause analysis 2017.....63
- Table 4.12 Detailed conversion chain analysis results.....80

NOMENCLATURE

Symbols:

•	D	Outer turbine diameter
•	F_D	Drag Force
•	F_L	Lift force
•	$f_p(\Psi)$	Characteristic turbine curve of the Wells turbine
•	H_D	Diffraction transfer function (used in (Brito-Melo et al, 2001))
•	h_r	Impulse responds function
•	$H_s \sim H_{m0}$	Significant wave height
•	$K(N)$	Wells turbine constant (depends on N)
•	K_1	Wells turbine constant (independent of N)
•	m_{-1}	-1 Moment (indication for the energy content in an ocean sea state)
•	N	Turbine rotational speed
•	p	Pressure (in the turbine and air chamber)
•	P_a	Atmospheric air pressure
•	P_e	Electric power / Generated power
•	P_{pneu}	Pneumatic power
•	P_t	Turbine power
•	$q(t)$	Total flow in the air chamber
•	q_i	Excitation flow (in some papers named Diffraction flow)
•	q_r	Radiation flow
•	q_t	Flow through the turbine
•	q_v	Flow through a turbine bypass valve
•	T_e	Energy period
•	T_p	Peak period
•	V_0	Air volume of the air chamber
•	α	Angle of attack
•	γ	Ratio of specific heats
•	ω	Radiation frequency
•	Π	Dimensionless turbine power
•	Ψ	Dimensionless pressure in the Wells turbine
•	ρ_a	Atmospheric air density
•	θ	Dimensionless flow through the Wells turbine
•	ζ	Surface elevation of the ocean (wave)

ABBREVIATIONS

- A.R.T.: Applied Research Technology was a company which build the Osprey OWC and the Pico OWC turbine. Later the company was transformed into Wavegen which collaborated later with Voith Hydro and with Siemens. This consortium build the Limpet OWC and the Mutriku OWC.
- DAQ: Data Acquisition
- EFACEC: Largest Portuguese Company for electric installations and equipment. Project partner of the Pico plant and designer, manufacturer and installer of nearly the entire electrical equipment of the Pico plant.
- EMEC: European Marine Energy Center / Test center for full scale wave energy and tidal energy devices on the island Orkney (UK)
- FRACAS: Failure Report, Analysis, and Corrective Action System
- GSM: Global System for Mobile Communication
- INETI: Instituto Nacional de Engenharia, Tecnologia e Inovacao
- I.S.T.: Instituto Superior Tecnico / Technical University of Lisbon (Portugal)
- PSD: Power Spectral Density
- PLC: Programmable Logical Controller
- PTO: Power Take Off
- RMS: Root Mean Square
- RPM: Rotations Per Minute
- TÜV: Technischer Überwachungsverein (German agency for technical safety inspection)
- WAVEC: Wave Energy Center
- Wave to wire: Theory of OWC devices. The model describing the complete conversion chain from undisturbed ocean waves to electrical power in the electrical grid.
- WEC: Wave Energy Converter

CHAPTER 1. INTRODUCTION

1. THESIS OVERVIEW

Content of the thesis

The here presented thesis is the outcome of a field study on the Pico OWC (oscillating water column) full scale wave energy converter between 2007 and 2018. Within the study it was attempted to reach the prior not achieved project goals in terms of reliable device operation and power production. The following Figure 1.1 shows a general schema of prototype project phases as the author assumes it to be suitable. In 2007 when the field study started the Pico project was stuck in the troubleshooting period. The prior realization phase was disturbed by significant problems, which required essential troubleshooting.

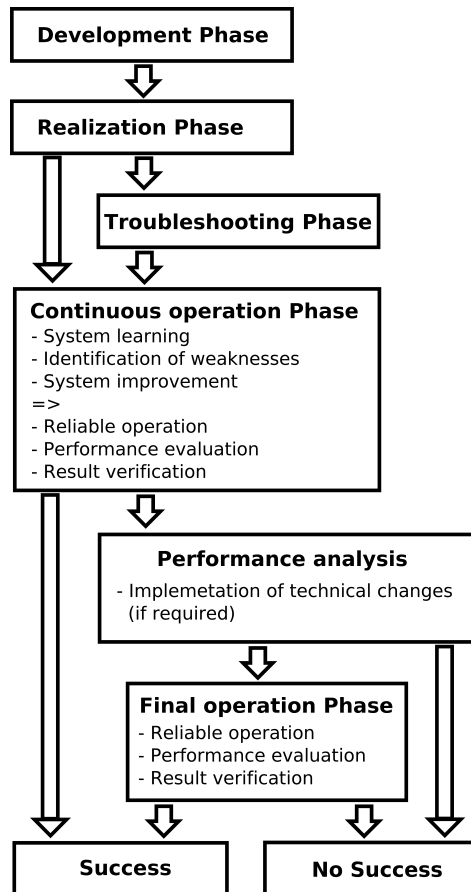


Figure 1.1 Project phases of a prototype

In 2018 after coming close to its foreseen lifetime the Pico OWC project and with it this field study ended when the concrete structure of the device collapsed due to increasing degradation without the required repairs. At this time the performance analysis was completed and efforts were undertaken to realize the final operation phase. However, the final operation phase was not realized though technical solutions were proposed within a reasonable financial effort.

The thesis address the following items:

- In Chapter 4.1 14 Reasons for Realization problems the executed troubleshooting is presented briefly. The required technical changes and repairs to complete the troubleshooting phase and reach the continuous operation phase in September 2010 are briefly introduced here. Further a root cause analysis for the dominating technical problems was executed to underline that the struggling was mainly caused because proven engineering solutions were not applied.
- In Chapter 4.2 Continuous operation experience the experiences of several years autonomous, remote controlled, continuous device operations is shared. Applied technical changes and repairs are presented and further a root cause analysis for the technical problems in continuous operation was executed.

CHAPTER 1. INTRODUCTION

Though the here presented in reality reached power levels are reasonable compared to other WECs they also reveal a essential shortfall compared to the theoretic power predictions.

- The theoretical core of the thesis that also reveals the main scientific achievement is the Chapter 4.3 Performance analysis. Here the in continuous operation observed essential power deficit is first quantified and in the following analyzed for its reasons. It will be shown that the majority of the power deficit compared to the initial predictions could be reproduced with a for this purpose developed numerical model. Due to the plausible results the performance analysis phase is assumed to be completed.
Further model results for the final operation phase are presented, which indicate possible 80 % of the predicted average power even with the fairly degraded device in the conditions of 2016. Hence they indicated a possible success.
- Finally the suggestions how to reach the final operation phase, which were proposed to the device owners in 2016 are presented.

Motivation for the thesis

The author applies the criteria of reliable continuous longer term operation within the predicted power levels to define the success of WECs. The predicted power levels should additionally indicate a possible economic viability in the future. Still today the in Appendix 2 presented attempt of the author to assemble those positive examples of realized large scale WECs was found to be a difficult task. The author experienced the consequence of the outstanding success of wave energy in general as a problem, which manifests in an generally decreasing industrial interest in the technology. Only some examples for this evolution are given here. The Sidar project was stopped after RWE pulled out in 2011 (The Globe and Mail. Inc., 2011), Wavegen was closed in 2013 (Wikipedia, 2018), Pelamis went into administration in 2014 (The Guardian, 2014) and Oceanlinx went into liquidation in 2015 (Tidal Energy Today, 2015). At the Pico project this interest decrease was clearly notable by missing funding, missing support from industry side and motivation deficits even within the project members. The author understands the missing interest in a technology, which struggles to prove its reliability, has high prototype costs and is supposed to be economically less viable than others renewable technologies. However, he also remembers similar problems for wind energy in the 1980th and 1990th. He assumes a comparable evolution as the one of wind energy likely as soon as the industrial interest returns and enables sufficient development. Thus it is this industrial interest that has to be returned.

Though opinions spread here the author believes that trust in the reliability of the technology and the involved companies is among others an important key factor. As long as the power levels indicate a possible economic viability in the future he believes reliable operating large scale WECs, which reliable reach these predicted power levels, to be the best instrument to gain trust.

Because the reason why this interest has to be gained is the missing interest and the corresponding poor funding situation, a reasonable possibility to reach the objective is to transform already existing large scale WECs to fulfill this purpose. This was attempted on the Pico WEC and could widely be realized during the field study. The author does not assume prototype problems as very negative as long as they can be overcome and solutions to prevent them in future machines can be established. However to gain trust it has to be shown that the lessons were learned. Therefore the dominating problems and their solutions should be reported transparently without hiding uncomfortable details.

About the study

Professional work requires reasonable budget and support. During the entire field study both was low on the Pico project. The author and his colleagues had to execute all steps of analysis, development, manufacturing, installation and testing of most systems without external support. Prior the project had sufficient funding but missing success denied income from energy revenues and did not favor further funding. This budget and support deficit is here expected to be the only reasons why no full machine availability could be reached, why the power analysis was finished so late and why the final operation phase in which the required final certainty could be gained was not realized anymore.

2. BACKGROUND

The Pico plant was a grid connected full scale onshore OWC prototype plant. Still in 2018 it was the oldest existing full scale WEC. It was build on the Azores island “Pico” (Portugal) between 1995 and 1999. Located at the North- West cost of the island (38°32'N, 28°32'W) in the middle of the Atlantic ocean it was exposed to a strong wave conditions during the winter months. The device collapsed in April 2018 due to monitored, increasing degradation of the concrete submarine walls. The device was build with the dual purpose of fulfilling the tasks of a prototype device but also to prove the feasibility of WECs in full scale by providing a remarkable part of the island energy consumption (Instituto Superior Tecnico, 1998). The development and the general design was widely developed by Antonio Falcao and the University of Lisbon (I.S.T.). It was funded with equal shares between the European Union and the utilities of Portugal (EDP & EDA).

The initial project was a “prestige” project in which several large Portuguese companies and the British company “Applied research technology” (A.R.T.) were involved. A.R.T. had build the Oस्पेरी and the Limpet 1 project before and later on was transformed into “Wavegen” and build the Limpet 2 and Mutriku OWC.

During the realization phase the project faced expensive technical problems, which could not be overcome. The major problems were turbine vibrations, which did not allow operation in the rated speed range, repeated destruction of the electric equipment by humidity and damage on the civil structure, that was assessed to provoke a collapse of the structure in the near future. In the consequence the project was practically abandoned. Only in 2003 Antonio Sarmiento was able to convince the former owners and the European Union to finance a second attempt to reach the project goals. This was possible because the civil structure did not collapse as predicted but remained without significant further damage. Details about this refurbishment project, for which the ownership of the device was transferred to the specially for this purpose founded and by Antonio Sarmiento leaded Wave-Energy- Center (WavEC), can be found in (Sarmiento, Brito-Melo and Neumann, 2006). The refurbishment project was based on the original design with few but essential changes. These changes could prevent the destruction of the electrical equipment by humidity and further enabled first machine operation in the lower end of the operation range. However a large number of additional before undiscovered design, engineering and execution issues disturbed the entire system. Therefore again no noteworthy operation periods could be achieved when the budget was widely spend.

When the reported field study started in 2007 the author experienced the reputation of the project as very low. The same applied for the interest in the project and even the motivation of involved persons to improve the situation.

However during this field study all operation preventing problems could be solved by systematic analysis of the system and the problems. This was possible within a small budget because the installed components could widely be utilized.

For autonomous remote controlled operation it was further required to install an originally not foreseen redundant safety backup system such as an also not foreseen remote control access system. Both system could be developed, realized and tested.

In September 2010 the device started autonomous, remote controlled continuous operation. Though component failures disturb operation from time to time the device remained in continuous operation till January 2018. However the real power levels could never get close to the theoretically predicted values. Finally in 2016 the reasons for the power deficit could be detected within the in Chapter 4. 3. presented power analysis. Only here it became clear that the device actually performs widely confirm with the underlying theory. The main cause for the underperformance could be detected to be a large discrepancy between predicted and realized turbine performance. Though the problem appears widely correctable within reasonable means and further offers a unique possibility, the abandonment of the device was scheduled already in 2015 to take place in June 2016. The reasons, which were claimed by WavEC were the financial situation, increasing structural damage and the completed theoretic learning.

Though the power analysis results changed the situation totally, WavEC stopped all financial support in June 2016 and discussed the process of dismantling with the responsible entities since then.

Because the machinery can not withstand the humidity and the salty environment without operation and maintenance the author continued device operation on his own costs to maintain the theoretic chance to still reach the final operation phase and close the case as a success. Though it was not a great business case, the income from energy revenues were still sufficient to pay the costs and a small income. In September 2017 the monitoring of the device degradation already indicated the collapse that occurred in April 2018. Therefore it was collectively decided to operate the device till the end of 2017 and than end the project with an official closing event while the device is still in continuous operation. The event was not realized for reasons which the author

CHAPTER 1. INTRODUCTION

did not understand and therefore the first official note about the end of the Pico project was the collapse in April 2018 but the operation was already ended at the first of January 2018.

3. OBJECTIVES

Below, the objectives of the conducted study are presented.

3.1. IMPROVE THE SECTOR OF WAVE ENERGY

This is the global objective, which results from reaching the other objectives. It was aimed to improve the wave energy sector by providing a positive example for a full scale WEC.

3.2. EXPLAIN THE REASONS FOR THE INITIAL PROJECT PROBLEMS

Here it is attempted to present the occurrences during the initial project realization phase as transparent as possible. A failure log was created to understand the mechanisms, which caused the determining problems. Further by showing the fact that continuous operation was reached it is shown that the problems could be solved or were less critical as expected. An executed root cause analysis reveals the main reasons for the problems and indicate how to avoid a repetition.

3.3. SHARE THE EXPERIENCE OF CONTINUOUS OPERATION

This experience is shared for two reasons.

- It is aimed to share the gained knowledge to avoid repetition of failures in future projects.
- It is aimed to present the still widely unknown evolution of the Pico project in order to finally get rid of the poor project reputation, which resulted from the well known failed initial realization attempt and the often presented low production figures. It is aimed to present that the device has reached reliable remote controlled continuous operation already more than 8 years ago and remained in it till 1 of January 2018. Further a comparison of the operation result to other devices allows to assess the quality of the Pico project.

The experiences are shared in form of production results and a failure log with an additional root cause analysis .

3.4. PRESENT THE DETECTION OF THE MAIN CAUSE FOR THE LARGE DEVICE UNDERPERFORMANCE

It is aimed to share the found results to raise interest, share opinions and gain trust. In an optimal scenario this would have lead to the final operation phase in which the results could have been verified and proven on the full scale real device.

The results of the power analysis are presented. In the analysis the prior not correctly quantified discrepancy between theoretic predicted power and real device power production was quantified and the losses are explained. This was done by the use of a time domain model, which was prior validated with instantaneous real device performance data. Because it was possible to explain the power losses for both, annual average and short term production reasonable, the theory is here expected to be sufficiently proven. Further the analysis results revealed new perspectives. This is the case because a large underperformance of the turbine was detected to be the main cause for power losses and it appears correctable within reasonable means. Therefore following the analysis results it appears possible that the device could have finally reach power levels in the predicted range.

CHAPTER 2. STATE OF THE ART

1. WAVE ENERGY IN GENERAL

The conversion of the energy contained in ocean wave into usable energy is named wave energy conversion. Mostly the usable energy is electrical energy but wave energy is also used for sea water desalination. The first patent appears to have occurred already in 1799 (Cement *et al.*, 2002) but only during the oil crisis in 1973 the efforts were concentrated. At this time several theoretic concepts were developed and tested in small scale. With the end of the oil crisis the effort was essentially reduced. However in the 1980 several first generation prototypes were tested, but unfortunately with little success. Some of these devices were the 500 kW Kavaerna OWC in Norway, the Tapchan in Norway and the 40 kW Saza OWC in Japan. While in Asia during the 1990th some further devices such as the 60 kW Sakata OWC the Kujukuri 30 kW OWC and the Vinzihnam 150 kW OWC were installed, the effort in Europe was very limited. Only in the late 1990 the effort increased again and several new full scale prototypes were build. In 1991 the Limpet 1 an 75 kW OWC was build in Scotland and in 1995 an attempted to build the A.R.T. Osperoy OWC in Scotland failed. Later around 2000 in Scotland the Limpet 500 (second generation onshore OWC) with 500 kW rated power, in Portugal the Pico onshore OWC with 400 kW rated power and in Japan the Mighty Whale a full scale floating OWC with about 110 kW rated power were installed. The information about the history of wave energy is obtained from (Brook, 2003). Since than several other devices followed but the total number of attempted devices is still very low compared to other technologies as for example wind energy. Some details about several more recent devices can be found in appendix 2.

Conversion principles from wave to usable energy

Different from wind energy where one dominant PTO type could be detected in wave energy various different PTO types exist. Today it is still difficult to say if one will become the dominating type. The presentation of these PTO types has been done in various other documents before. A reasonable overview of the different PTO types can be obtained in Wikipedia (Wikipedia, 2017 c) for example. Here no detailed explanation of the different PTO types is done because it is not directly required in the scope of this thesis. The present thesis exclusively deals with the technology of onshore OWC devices. Devices with other PTO types are exclusively presented with focus on their overall performance regardless of the PTO type.

Grid connected wave energy converters today

Though today the discussion about climate change caused large effort in the the sector of renewable energy, the effort in wave energy is dramatically reduced again. In 2016 world wide only very view full scale wave energy converters were still installed.

Following the World Energy Council, the total installed wave energy capacity in 2016 was about 1MW. Figure 2.1 (World Energy Council, 2016) shows the as installed considered wave energy devices in 2016. The devices in Ghana and Sweden are parks of the Swedish company Seabased for which the author could not find production figures or recent news. Additionally, but in the graphic not presented, in Australia another 240 kW device of Carnegie Energy appears to be in operation. The presented Portuguese and the Spanish values correspond with the Pico project and the Mutriku project.

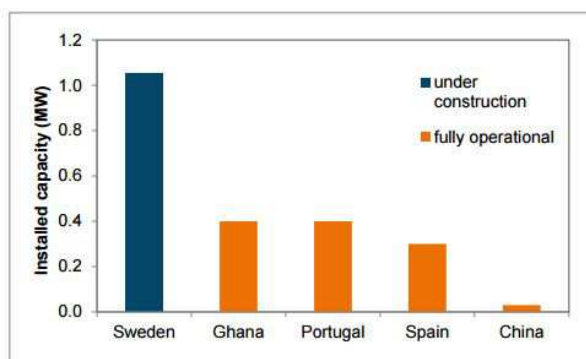


Figure 2.1 Installed wave energy capacity in 2016

In comparison to this low value, the world wide installed capacity in wind energy in 2015 is approximately 430 GW (GWEC, 2016).

Energy resource

Both renewable energy sources, wind and wave energy contain large resources for which the quantification is difficult. Therefore very different estimations for both sources can be found. However wind is the larger source but both are gigantic. Here rather conservative estimates are presented. In (Gunn, Stock- Williams, 2012) and (Mork, Barstow, Kabuth and Pontes, 2010) the global wave power resource is estimated between 2 and 3 TW. The 2 TW correspond roughly to 1/6 of the global energy consumption of 2013, which was approximately 12 TW (International Energy Agency, 2015).

In comparison the scientists of the Harvard and other Universities estimate the global wind resource to be in the range of 20 TW (Adams, Keith, 2013).

Summarized, the global resource appears to differ about a factor in the range of 10 but the installed capacity differs about a factor in the range of 430000.

Theoretical feasibility

Theoretically several promising wave energy converters with fairly high efficiency are developed. The probably most impressive concept is the duck of Steven Salter, which appears to have an overall efficiency of up to 90 % (Worldpress, no date). Further the efficiency can be obtained fairly spectacular in a video which is available at (Edinburgh wave power group, 1984). In theoretic models various converters appear to functioning reasonable. As can be obtained below in this section, the Pico plant for example shows a theoretic overall efficiency of about 50 %.

Realization of wave energy

To the authors knowledge hardly any wave energy device in larger scale could be realized satisfyingly. For various well known devices the theoretic performance expectations were missed essentially and several others devices struggled to survive the pure ocean forces. Only some full scale devices could reach continuous long term operation. Beside the Pico OWC plant, the Mutriku OWC in Spain, the Wave star in Denmark, the Waveroller in Portugal and possibly few other devices are these rather positive examples. However, for the three devices beside the Pico plant, the energy costs of each devices are obviously far to high due to the large structure compared to the small generated power. The initial power expectations for the other devices are unknown at this point but for the Pico plant it can be said that, because the technical changes, which are proposed in this thesis could not be implemented anymore, the real results remained far below the expectations.

Energy costs

Finally the essential problem appear to be the energy costs of wave energy. Today these costs are still fairly high. The international renewable energy agency (IRENA) estimates the costs between 0,33 and 0,63 €/kWh (IRENA, 2014). The anticipated energy costs for a significantly further developed wave energy sector still appear fairly high. The estimates are fairly different the Ocena Energy Council estimates the costs to be in the range of modern wind energy at about 0,045 €/kWh (Ocean Energy Council, no date), while IRENA estimates the costs between 0,11 and 0,23 €/kWh (IRENA, 2014).

Examples for realized full and large scale converters

In Appendix 2 a presentation of the majority of the important large scale wave energy converters of the recent past and the present can be found. Here basic information about the location, the PTO type, the state of development, the rated power and project results in form of production results and project problems can be found. As can be obtained there for most of the presented devices the author could not find reliable production figures.

The WEC with the larges accumulative energy production

The Mutriku breakwater OWC in Spain, which is also presented in more detail in Appendix 2, appears to be the

CHAPTER 2. STATE OF THE ART

wave energy converter, which fed in the largest amount of energy into the grid. Corresponding to their own web page (EVE, 2016) the device fed about 1,3 GWh accumulated energy into the grid between 2011 and end of 2016. This corresponds to approximately 215 MWh annually and approximately 25 kW average grid power, when assuming similar annual results. The device is supposed to be in smooth continuous operation. The installed capacity of the device is 296 kW, the capture wide is approximately 100 m and the local wave energy resource is approximately 8,8 kW/m. The technical information is obtained from (Torre- Encisio, Ortubia, Lopez de Aguilera and Marques, 2009) and (EVE, 2016). The corresponding load factor is 0,08 and the overall device efficiency is 2,8 %.

The Pico plant

In 2011 the performance of the Pico device was evaluated for the first time in (Pecher *et al*, 2011). Based on offshore wave data and generator power readings, the annual average generated power was estimated to be 28,2 kW for full device availability. This corresponds to about 28 % of the power predictions. As further explained in Chapter 4. 3.7. the results from 2011 differ from the results of the recently during this study executed performance evaluation. The reason for it is hear assumed to be no sign for further degradation but mainly caused by the data calibration in 2011.

The initial power predictions (Falcao, 2002) were approximately 100 kW. With an estimated average resource of 13,4 kW/m and a device wide of 15 m the available wave power is approximately 200 kW. Therefore the predicted overall efficiency is approximately 50 %. In reality the highest annual average power result that could be reached is 5,1 kW. This corresponds to an overall efficiency of 2,5 %. With compensation for down time periods the estimated annual average power is 11,5 kW (Chapter 4. 3.3. Execution and intermediate results). The corresponding overall efficiency is approximately 5,7 %.

2. THE TECHNOLOGY

2.1. THE WORKING PRINCIPLE

Typical realization of onshore OWC converters

The main plant structure consists of a tower, which stands on the sea floor and reaches up several meters above sea level. Above sea level the structure forms an closed air chamber, which is only connected to the atmosphere through an air turbine. Below the surface the structure has an always submerged opening towards the incident waves. The waves in the air chamber act as a piston compressing and expanding the enclosed air volume. The oscillating pressure inside the air chamber creates an reciprocal air flow through an air turbine, which is connected to a generator. In general either the air flow can be rectified to be used with an unidirectional turbine or a self rectifying turbine, such as the in Chapter 2. 2.3. introduced Wells turbine can be used without air flow rectifying valve system. Figure 2.2 shows a schematic of the Pico plant. Source: (Monk, Winands and Lopes, 2018).

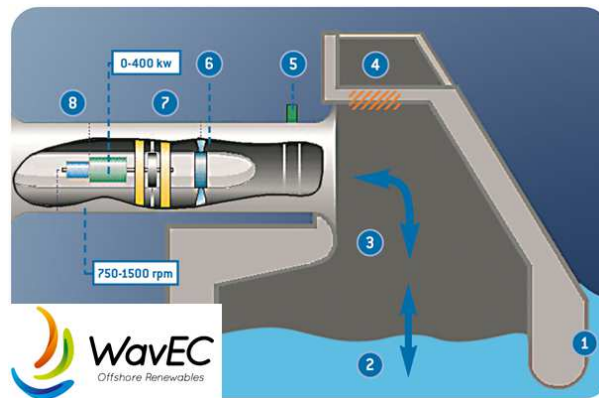


Figure 2.2 Cross-sectional illustration of the Pico OWC (1) the incident wave, (2) the chamber oscillation, (3) the bound air pressure chamber, (4) by-pass relief valve, (5) Main isolation valve, (6) Fast acting isolation valve, (7) Wells turbine, (8) Asynchronous generator

2.2. THE BIDIRECTIONALITY OF THE WELLS TURBINE AND AERODYNAMIC STALL

Figure 2.3 Is obtained in (Torresi *et al*, 2008). It shows the principle schematic of a vertical Wells turbine. The Pico device uses a horizontal Wells turbine but the principle is similar. An air flow is guided through the ring shaped turbine duct and hits the symmetrical Wells turbine blades perpendicularly. The exact occurrences and the the fact that the device is bidirectional can be obtained in Figure 2.4 where the cross section of a blade and the forces on it is shown. It is extracted from (Mohamed and Shaaban, 2013). It can be obtained that as long as the turbine is not spinning exclusively a drag force F_D (force in flow direction W) is created and therefore the turbine would theoretically not start to spin. Only when the turbine is spinning the in Figure 2.4 visible resulting direction of the flow W causes an angle of attack α between the chord of the blade and the flow W , which creates a lift force F_L (force perpendicular to the flow direction W).

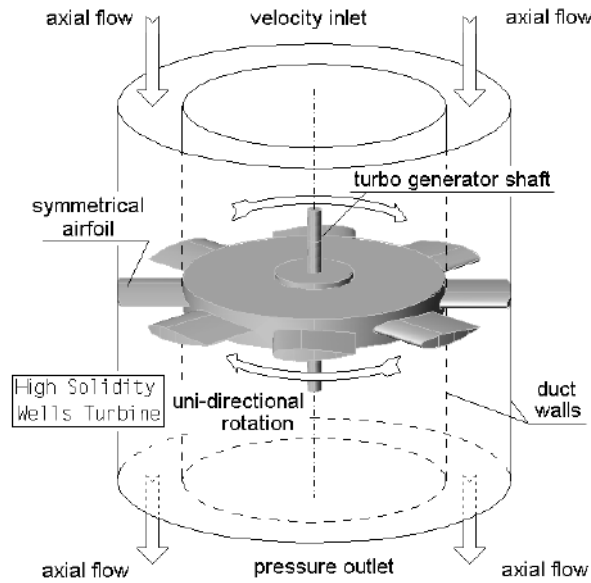


Figure 2.3 Schematic of a vertical Wells turbine

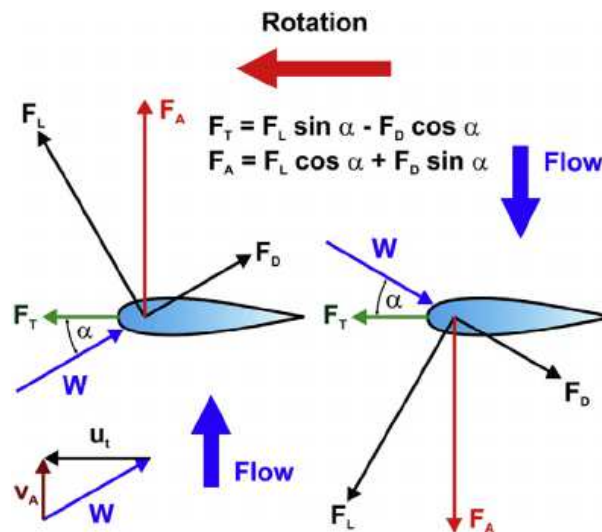


Figure 2.4 Forces at the blades of a Wells turbine

It can be obtained that the propelling force F_T increases with a larger angle of attack α because the lift force has a larger component in the spinning direction and further but not visible here the lift force increases with a larger angle of attack. For the Wells turbine without rotor guide vanes, which alter the angle of attack, the angle of attack for a constant air flow increases with reduced turbine velocity and decreases with higher velocity because the resulting flow component U_t varies while the flow component V_A remains constant. U_t is the blade velocity, which in combination with the air velocity V_A composes the resulting air flow velocity

W . As can be seen in Figure 2.4 the principle is valid for both flow directions and always results in a propelling force F_T in the same direction.

However the principle of increasing lift force for larger angle of attack is only valid until a certain threshold. When passing this threshold value only slightly the flow starts to separate from the blade profile and the lift force reduces immediately significantly. No large exceed is needed to cause the complete collapse of the lift force. Hence in moments in which the turbine is too slow for the current airflow, the angle off attack passes the threshold value. As soon as it passes this value slightly more the entire lift force and with it the propelling force is gone. This effect is called aerodynamic stall and is a large problem of Wells turbines. Beside the dramatic loss of the propelling force aerodynamic stall has a second very negative consequence. The separation of the airflow

from the turbine blades causes a highly turbulent airflow downstream of the rotor. These turbulence cause fatigue and noise issues due to vibrations of the turbine duct walls and all downstream installed components.

Aerodynamic stall is also the reason why Wells turbines do not use the entire duct area but as in Figure 2.3 visible only a ring section. The true velocity of a point close to the rotor axis is simply too slow. Here the flow resulting flow component U_r is too slow and hence aerodynamic stall would be the consequence most of the time.

2.3. CONTROL CHALLENGES DUE TO AERODYNAMIC STALL

The above explained effect of aerodynamic stall is a large disadvantage of Wells turbines. To avoid aerodynamic stall moments with too low rotational speed for the current pressure in the system have to be avoided. However as can be obtained from the characteristic turbine curve shown in Figure 2.6 moments with significantly too high rotational speed for the current pressure also cause a very low turbine efficiency. Therefore Wells turbines require a fairly exact ratio between rotational speed to pressure in the system.

To avoid full stall conditions and very low turbine efficiency in general the device has to be controlled in a way that the ratio between instantaneous rotational speed and instantaneous pressure in the system is always in the required range and does not exceed the threshold for aerodynamic stall. This introduces a significant challenge because the pressure in the system depends mainly on the incoming waves, which are naturally sinusoidal and irregular.

Corresponding to (Joustino and Falcao, 1999) the variations in ocean waves can be classified into the following three types.

- The sinusoidal character of ocean waves causes the instantaneous pressure to vary from zero to max over pressure to zero to max under pressure to zero within only one wave period of in average approximately 10 s. These variations are further referred as short term pressure variations.
- Wave grouping can cause large average RMS pressure variations from one wave to the successive wave. These variations are referred as mid term variations in the following.
- Finally the average RMS pressure above periods of 15 min (or larger) varies with the sea conditions. These variations are here referred as long term pressure variations.

Due to pressure variations in general, in order to maintain a high efficiency the device has to allow variable turbine rotational speed.

Especially the mid term pressure variations from wave to wave can introduce problems when the first wave is a smaller or average wave and the successive wave is a significantly higher wave. In order to keep the ratio between rotational speed and pressure in the optimal range the rotational speed is required to increase simultaneously to the pressure. To allow such a fast acceleration the inertia of the turbine rotor has to be small but as will be shown below rotational speed variations cause large fluctuations in turbine power, which create problems with the grid constrains in case no power smoothing strategy is applied.

2.4. CONTROL CHALLENGES DUE TO GRID CONSTRAINS

When feeding power to the electrical grid, constrains regarding the maximal allowed power fluctuations per time unit have to be respected. In case a turbine with a small inertia is used, which enables the almost instantaneous acceleration of the turbine, the turbine power P_t variations from one wave to a larger successive wave are very high due to a cubic influence of the rotational speed N to the turbine power for Wells turbines. The equation (1) is obtained from (Falcao, 2002) and shows the relation between rotational speed and turbine power for the Wells turbine.

$$P_t(t) = \frac{\rho_a N^3 D^5}{\Pi} \quad (1)$$

Here ρ_a is the atmospheric air density, D the outer turbine diameter and Π the non dimensional turbine power. The non dimensional power is for a given turbine related to the dimensionless pressure Ψ through the characteristic turbine curve (dimensionless turbine curve), which can be obtained in equation (14) and for the

CHAPTER 2. STATE OF THE ART

Pico plant in Figure 2.6. The dimensionless pressure depends only on the rotational speed and the pressure in the system by equation (11). Following equation (11) if the turbine could accelerate instantaneously it would double the rotational speed N if the pressure increases about the factor 4. Finally a 4 times higher pressure in the system would cause an eight times higher turbine power P_t .

Pressure variations of this range occur frequently but power variations of this magnitude cannot fulfill the grid constraints. Therefore some kind of power smoothing is required. This can be done in different ways.

- The turbine efficiency can be kept close to optimal by allowing the rotational speed to vary fast. The above explained large power fluctuations in this case can then be smoothed by successive power smoothing done by some kind of energy storage.
- Another possibility is pressure control to ensure an approximately optimal ratio between rotational speed and pressure. This can be realized by the use of a pressure relieve valve. Due to the released pressure this method can obviously not use the full available pneumatic power. The required opening frequency of the valve depends on the question if only long term pressure variations, mid term or short term variations are to be dealt with.
- Another method is the storage of energy in a flywheel directly on the rotor. This can be realized by a rotor with a large inertia. This concept combines two effects. First the large inertia disables the fast turbine acceleration, which is required to keep the turbine efficiency (the ratio) high. Therefore in the most unfavorable case of a large wave following a group of smaller waves the rotational cannot accelerate fast enough and causes a very low turbine efficiency, which avoids excessive turbine power peaks. However this causes the very unfavorable aerodynamic stall moments. The second effect is the return of energy, which was prior stored in the flywheel, in moments with less energetic wave input. Therefore the rotational speed can be kept fairly constant and the grid constraints can be respected but the average turbine efficiency is reduced and aerodynamic stall is favored.

2.5. CONTROL PROCEDURE

The turbine is controlled by the characteristic curve of the generator, which defines the electrical power (torque) depending on the rotational speed. In the following this characteristic generator curve is named the control strategy. The matching of the generator control strategy with the turbine is one of the essential control challenges of these devices. Therefore for the Pico turbine a generator was chosen for which the curve can be adapted to the turbine.

3. THE NUMERICAL MODEL

The underlying model is the wave to wire model for OWC technology presented in (Brito-Melo, Gato and Sarmiento, 2001) and (Joustino and Falcao, 1999).

In Figure 2.5 the basic structure of the OWC wave to wire model can be obtained in a flow diagram.

The OWC wave to wire model

The model describes the instantaneous relations between outside wave (surface elevation), chamber wave (surface elevation), pressure inside the system $p(t)$, rotational speed $N(t)$, extracted pneumatic power P_{pneu} , turbine power P_t and generated power P_e . The incoming wave causes a water volume flow $q(t)$ inside the chamber. If no turbine bypass air flow through a bypass valve $q_v(t)$ is considered the air flow through the turbine $q_t(t)$ is the only air flow leaving the system. Due to friction and the turbine as an obstacle this airflow $q_t(t)$ is smaller than the water flow $q(t)$ entering the chamber. Therefore the system is pressurized and the air inside the chamber is compressed. The size of the air flow through the turbine and with it the pressure inside the system depend on the turbine characteristics, which itself depend on the turbine rotational speed. The pressure in the system causes a contra acting force on the water surface inside the air chamber and thus reduces the surface elevation inside the chamber and following the water volume flow $q(t)$ and the air volume flow $q_t(t)$ through the turbine.

The extracted pneumatic power at the turbine is:

$$P_{pneu}(t) = q_t(t) * p(t) \quad (2)$$

For a constant rotational speed, Wells turbines have a proportional relationship between pressure and flow. The proportional constant is named $K(N)$.

$$K(N) = p(t, N) / q_t(t, N) \quad (3)$$

The size of $K(N)$ depends on the rotational speed. The conversion from available pneumatic power P_{pneu} to mechanic turbine shaft power P_t depends on the turbine performance, which can be obtained in the dimensionless characteristic curve Figure 2.6 of dimensionless power Π versus dimensionless pressure Ψ in the section [The Wells turbine] of this paragraph. In both values, dimensionless power and dimensionless pressure the rotational speed is already included and therefore this curve is independent of the rotational speed.

If no losses are considered, the electrical power P_e at a certain rotational speed depends only on the characteristic generator curve (control strategy). In case at a certain rotational speed N the electrical power P_e is larger than the mechanical turbine power P_t the rotational speed of the turbine decreases. For $P_e < P_t$ the rotational speed N increases.

Following the linear wave theory the water flow q inside the air chamber can be decomposed into two theoretic flow components the excitation flow q_i (in (Brito-Melo, Gato and Sarmiento, 2001) it is called the diffraction flow) and the radiation flow q_r .

$$q = q_i + q_r \quad (4)$$

The excitation flow is the theoretical flow that would be caused by the waves in case now pressure would be present in the air chamber. In a theoretic model the chamber is assumed without roof, which causes atmospheric pressure in the system. In this assumption the second theoretic flow component is the radiation flow, which is caused by the pressure oscillation inside the chamber is zero. Hence the excitation flow corresponds to the total flow q . In the case of only excitation flow the extracted pneumatic power is zero because the pressure in the system is zero.

The second theoretical flow component is the radiation flow. The radiation flow is the theoretic water flow that

CHAPTER 2. STATE OF THE ART

leaves the air chamber in the theoretic case that no outside waves are present but the pressure oscillation inside the chamber is present and causes oscillating forces to the water surface.

The excitation flow is an into the chamber incoming flow and the radiation flow an from the chamber outgoing flow (or better a the incoming flow reducing component).

The radiation flow can be seen as a measure of the extracted pneumatic power power because both the radiation flow and the pneumatic power for a Wells turbine at constant speed only depend on the pressure in the system.

The complete equation of the hydrodynamic model is.

$$q_i(t) + q_v(t) = q(t) - \frac{V_0 dp(t)}{\gamma P_a dt} \quad (5)$$

Here V_0 is the chamber air volume, γ is the ratio of specific heats and P_a the atmospheric air pressure.

The term $\frac{V_0 dp(t)}{\gamma P_a dt}$ describes compressibility of air.

When the Wells turbine proportionality between flow and pressure is implemented it follows:

$$\frac{p(t)}{K(N)} + q_v(t) = q(t) - \frac{V_0 dp(t)}{\gamma P_a dt} \quad (6)$$

The radiation flow q_r depends on the pressure oscillation in the chamber in the past approximately 30s. It can be obtained by the use of an impulse responds function hr.

$$q_r(t) = \int_{-30s}^t hr(t-\tau) \frac{dp}{dt}(\tau) d\tau \quad (7)$$

The excitation flow depends exclusively on the outside wave and the constant hydrodynamic coefficients of the device which depend on the chamber geometry and the chamber water depth.

Here the equation,

$$q_i(\omega) = H_D(\omega) \zeta(\omega) \quad (8)$$

which corresponds to the equation 15 in (Brito-Melo et al, 2001), is used to compute the excitation flow from the outside surface elevation $\zeta(\omega)$. ω is the radiation frequency of the incoming wave. To compute the excitation flow the outside surface elevation has to be transferred into the frequency domain and the equation above has to be integrated over all possible frequencies, which are included in ocean waves.

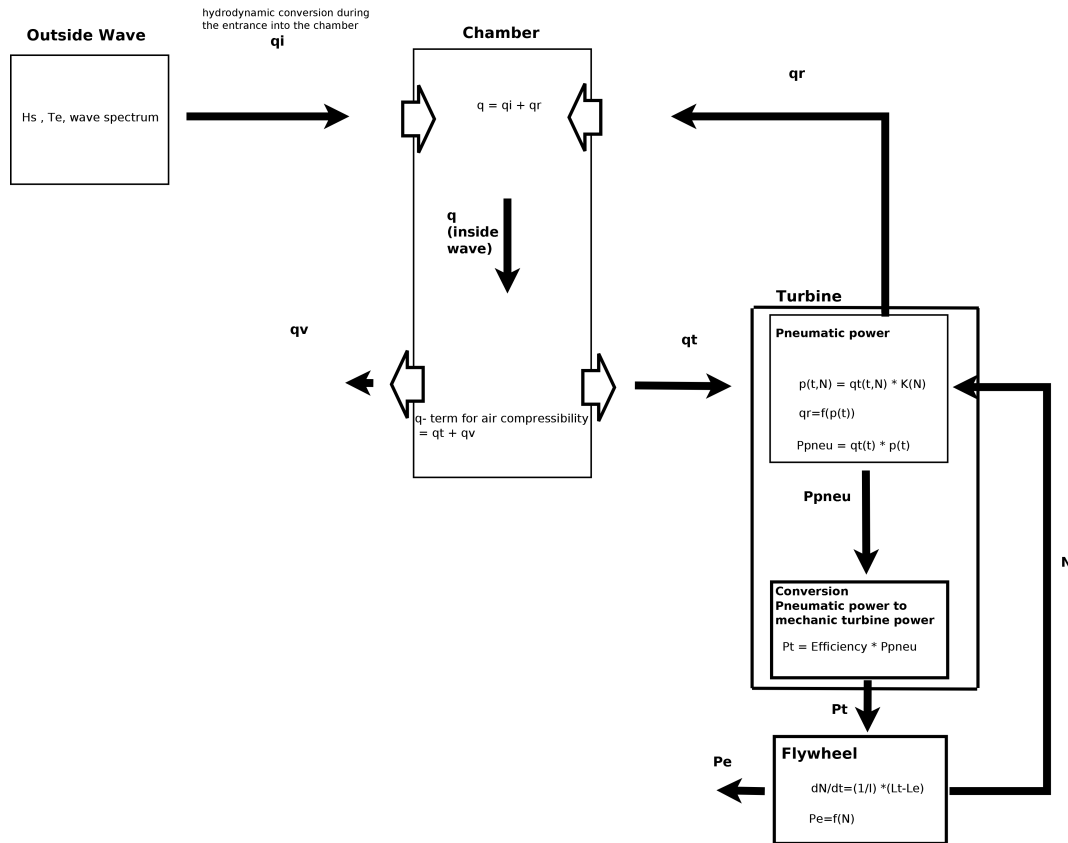


Figure 2.5 Flow diagram of the OWC wave to wire model

The Wells turbine

As stated above the Wells turbine at constant rotational speed has a proportional relationship between pressure and flow.

$$K(N) = p(t, N) / q_t(t, N) \quad (9)$$

To remove the influence of rotational speed it is common to write the turbine power, the turbine pressure and the turbine flow in dimensionless form as done in (Joustino and Falcao, 1999), (Falcao, 2002) and (Brito-Melo, Gato and Sarmento, 2001).

Dimensionless turbine flow:

$$\Theta = \frac{q_t(t)}{N D^3} \quad (10)$$

Dimensionless pressure:

$$\Psi = \frac{p(t)}{\rho_a N^2 D^2} \quad (11)$$

Dimensionless turbine power:

$$\Pi = \frac{P(t)}{\rho_a N^3 D^5} \quad (12)$$

Relations between the dimensionless values:

$$\Theta = K_1 \Psi \quad (13)$$

Here K_1 is a turbine constant which is different from $K(N)$ and not depend on N anymore.

$$\Pi = f_p(\Psi) \quad (14)$$

With f_p being the characteristic turbine curve.

For the Pico turbine the designed characteristic curve can be obtained in Figure 2.6, which can be found in (Falcao, 2002).

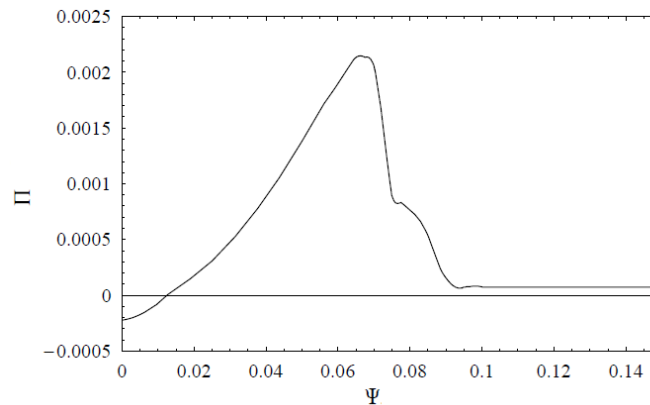


Figure 2.6 Characteristic curve of the designed Pico turbine

How to read the curve:

Every single operation condition of the Wells turbine is defined by a point on the characteristic turbine curve. The position of the point is defined by the dimensionless pressure, which depends only on the pressure and the rotational speed. The turbine power at this point is defined by the corresponding dimensionless power and the current rotational speed. As follows from equation (11) the dimensional pressure increases with increasing pressure and decreasing rotational speed (and the opposite). Hence, when for example at a certain rotational speed a significantly larger wave enters the chamber and creates a higher pressure the operation point moves towards the right side on the characteristic curve if the rotational speed remains approximately constant. It can be obtained that the curve drops down sharply on the right side of the peak. This is the zone of the curve, which describes the aerodynamic stall described in Chapter 2. 2.2. .

4. LITERATURE REVIEW

The initial part of this study in which all technical problems were removed and the continuous operation was executed was mainly engineering. Therefore here mainly historic literature such as (Instituto Superior Tecnico, 1998), (Falcao, 2000) and others were reviewed to back statements. A suitable way to compile, evaluate and present the problems was found in form of a failure log in (Kenny et al, 2017).

The performance analysis was the part that required the scientific literature review. As already stated in Chapter 1 during the continuous operation it became obvious that the real device performance is fairly poor. After obtaining the initial theoretic annual average power predictions in (Falcao, 2002) it became obvious that the real device performance is far too low. The initial theoretic power predictions are computed with a frequency domain model of the Pico plant with theoretic, stochastic wave input based on a prior measured local wave climate and linear wave theory.

Due to the type of give power predictions a comparison between real device and theoretic predictions was difficult. The problems were the following. As can be obtained in Chapter 4.3. Performance analysis the real device showed several damages and variations compared to the theoretic device, which were all assumed to somewhat lower the performance. Additionally no real time wave data on site was available to enable a performance comparison between model and real device for short periods in similar wave conditions. The remaining possibility of comparing the annual average power introduces generally large uncertainties due to annual wave climate variations and further requires real performance data of an entire year without large machine downtime, which could never be sufficiently achieved with the Pico plant.

It was assumed that the power losses have various different reasons, which are located in different parts of the conversion chain. This together with the fact that the real device performance was so far off from the predictions made it impossible to evaluate if the theory is suitable or where the problems originate from.

The power predictions coming from the initial frequency domain model indicated a clear problem in the conversion chain from wave to electrical power but the type of model did not allow to validate steps of the conversion chain isolated to detect the main problem.

For this purpose it was more suitable to set up a time domain model of the Pico plant. With a time domain model it is possible to validate the entire conversion chain or parts of it with real measured time series. In the case of the Pico plant it was not possible to validate the entire conversion chain due to the absence of local real time wave measurements but it was still possible to validate the conversion from pressure inside the air chamber to electrical power fed to grid. This approach was already done before in (Monk *et al*, 2015). Here it was aimed to increase the power of the Pico plant by air flow control. Here a time series of the only theoretic excitation flow was computed from real time series of the measured pressure inside the air chamber and the plant performance. This time series was then used to drive the time domain model, which was strictly based on the theory proposed in (Falcao, 2002). In (Monk *et al*, 2015) a good match between model and real device performance was found for the verified part of the conversion chain, which confirmed the theory of this part. The large obvious power shortfall was not the focus of the study but the good model match indicated that it originates very likely in the hydrodynamic conversion from wave to pressure inside the system, a faulty wave climate expectation or a general problem in the theory regarding the made assumptions.

Similar to the model used in (Monk *et al*, 2015), the time domain model that was developed for the present thesis is also based on the theory presented in (Falcao, 2002), (Joustino and Falcao, 1999) and (Brito-Melo et al, 2001). The model was validated for a good match in the conversion from pressure inside the air chamber to electrical power fed to grid by comparing the real device performance and the model performance based on the excitation flow such as done in (Monk *et al*, 2015) before. Different from the results found in (Monk *et al*, 2015) the here used model could not confirm the theory for this part of the conversion chain. On the contrary the modeled power results were essentially higher than the real device results. Close verification of the codes used here and in (Monk *et al*, 2015) revealed a mistake in the code used in (Monk *et al*, 2015) which unfortunately by coincidence returned a good model fit. The mistake in the code regarded the turbine performance and was corrected in the follow up study (Monk, Winands and Lopes, 2018).

To achieve a good model match, now all already prior introduced variations between theoretic model and real device such as the new found turbine performance problem had to be modeled. The so validated model was then fed with the similar theoretic annual wave input as was done in (Falcao, 2002). This was done to observe if the low annual average power of the real device can already be reproduced by the problems in the conversion chain from pressure in the chamber to electric power and assuming no problems in the conversion from outside wave to pressure in the air chamber. The annual average power of the real device was estimated by superposition of real device performance data of a 6 month performance period. Having in mind the large introduced

uncertainties but also the very large underperformance of the real device the majority of the power losses could already be reproduced with this model.

By afterwards running the validated model in the theoretic conditions (hence without the variations between theoretical and real device) the quality of the power predictions in (Falcao, 2002) was validated to be reasonable. By further modeling each variation between theoretic and real machine isolated, the influence of each variation was obtained.

To reduce the high level of uncertainty, which was introduced by the comparison based on annual average values, in the following it was aimed to evaluate the real device performance in different sea conditions and to compare it to model results of similar sea conditions.

If reliable wave data on site is available this can be done by a performance analysis of the equimar type as proposed in (Pecher and Kofoed, 2016) but in the Pico case only offshore wave forecast data was available at the time of the study. A performance analysis of this type based on offshore forecast data was already executed for the Pico plant in (Pecher et al, 2011) but the variation from offshore wave to near shore wave and the forecast itself introduce new very large uncertainties. Therefore this type of performance evaluation was not suitable with the objective of reducing the uncertainties. Though methods exist to model the nearshore wave data from offshore data there is still a large uncertainty and the uncertainty of the forecast character of the data can also not be removed with these methods.

To keep the uncertainties in the sea state classification of real operation periods as low as possible it was here chosen to use real measured data time series of the surface elevation inside the air chamber and to concluded from it to the undisturbed wave before entering the air chamber. Of course this method also introduced uncertainties because the variation from theoretic and real device conversion from undisturbed wave to chamber surface elevation is unknown. However it was assumed here that the energy transmitted in the waves is not altered significantly by this variation.

By the use of a spectral analysis the sea state inside the air chamber is classified similar to the classification of the surface elevation outside the air chamber in the Equimar method proposed in (Pecher and Kofoed, 2016). To specify the corresponding sea state of the undisturbed wave outside the air chamber the numerical model was driven with a large number of different theoretically computed outside sea states to return the surface elevation inside the air chamber. The spectral analysis of the so computed surface elevation inside the air chamber returns the sea state data inside the chamber. The corresponding outside sea state, which returned the best fit for the inside sea states, was chosen as the most likely outside sea condition of the operation period. The results were further compared to the corresponding outside forecast data and showed a plausible match.

Again the hydrodynamic losses of the real device could not be modeled directly because the theoretic hydrodynamic performance had to be assumed in the model calculations. However, the found results for the single losses, which were prior found for the annual average values could be confirmed for the majority of the verified sea conditions. Though still significant uncertainties are introduced by the chosen sea state classification the results are clear enough to indicate that the performance analysis revealed the main contributor for the losses to be a faulty turbine performance.

Finally with the purpose of showing that the turbine underperformance, which was found to be the main contributor for the losses, can be removed even though the reason for it is not fully understood the recent case study of the Pico plant with different turbines (Falcao, Henriques and Gato, 2016) was consulted. Here a more recent mono plane Wells turbine is already theoretically adapted for the Pico plant and shows a significantly better performance as the the installed turbine is theoretically supposed to have. Therefore it appears likely that the correction of the performance deficit is possible.

4.1. HISTORIC LITERATURE REGARDING THE PICO PLANT

- Falcao, A.F.O. (2000) 'The shoreline OWC wave power plant at the Azores', In: Proceedings of the Fourth European Wave Power Conference, Energy Centre Denmark, Danish Technological Institute, Tastrup, 42–48, Denmark, paper B1.
- INSTITUTO SUPERIOR TECNICO (1998) 'EUROPEAN WAVE ENERGY PILOT PLANT ON THE ISLAND OF PICO, AZORES, PORTUGAL. PHASE TWO: EQUIPMENT', *Contract JOR3-CT95-0012 PUBLISHABLE REPORT*.
- Monk, K. (2012) 'A review of the Pico project 2010 to 2012- mistakes, milestones and the future '
- Neumann, F. and Brito- Melo, A. (2009) 'MOERI - WavEC Collaboration Research for Safety Design and Optimal Operation of OWC-WEC Pilot Plant in Korea',
- Neumann, F. and Le Crom, I.(2011) 'Pico OWC - the Frog Prince of Wave Energy? Recent autonomous operational experience and plans for an open real-sea test centre in semi-controlled environment', in:

CHAPTER 2. STATE OF THE ART

Proceedings of the 9th European Wave and Tidal Energy Conference (EWTEC 2011), Southampton, UK, 05-09 September 2011.

- Neumann, F., Brito-Melo, A. and Sarmento, A.J.N.A. 'Grid connected OWC wave power plant at the Azores, Portugal', In: Proceedings Int. Conf. Ocean Energy: *from innovation to industry*, OTTI, ISBN 3-934681-49-2, pp. 53-60, 2006.
- Sarmento, A. J. N. A., Brito-Melo, A. and Neumann, F. 'Results from sea trials in the OWC European wave energy plant at Pico, Azores', in Invited paper for WREC-IX, Florence, Italy, 2006, pp. 1–6.
- Sarmento, A.J.N.A (2006) 'Engineering, analysis and monitoring of full-scale and prototype plants (performance, safety and environmental impacts)', Deliverable 06 report for the FP7 ITN 215414 – wavetrain2 project.

4.2. OWC PAPERS USED TO OBTAIN THE REQUIRED THEORY

- Brito-Melo, A., Gato, L.M.C. and Sarmento, A.J.N.A. (2002) 'Analysis of Wells turbine design parameters by numerical simulation of the OWC performance'
- Falcao, A.F.O. (2002) 'Control of an oscillating-water-column wave power plant for maximum energy production'
- Justino, P.A.P. And Falcao, A.F.O. (1999) 'Rotational speed control of an OWC plant'

4.3. RECENT STUDIES RELEVANT FOR THIS THESIS

Theoretic development on OWC devices is still ongoing. Studies are executed for more example on efficient turbines and on pneumatic power regulation by valve control.

Several studies were recently executed based on the Pico plant. Two studies with the contribution of the author were executed by Kieran Monk on the topic of pneumatic power regulation.

- A first study “Simulation and Field Tests of Pneumatic Power Regulation by Valve Control Using Short- term Forecasting at the Pico OWC” (Monk *et al*, 2015) deals with a power optimization of the Pico plant by the use of neural networks and the during this study developed active bypass relieve valve system. An initially during the here presented field study developed active valve system that was based on wave information of a submerged nearshore pressure sensor was transformed for this study. The nearshore sensor information was substituted by a information coming from a neural network based on exclusively plant operation data. At the time of this study the here in Chapter 4. 3.3. explained main reason for the device underperformance was still unknown. At this time still defects on the plant structure and reduced water depth were assumed to be the main contributors. The study showed a possible power improvement of about 15 % such as a relevant reduction of aerodynamic stall.
- A second study again on pneumatic power regulation was executed on the Pico plant in 2016. It is named “ Chamber pressure skewness corrections using a passive relief valve system at the Pico OWC” (Monk and Winands, 2016). At the time of this study the here in Chapter 4. 3.3. presented power analysis had already revealed the essential reason for the power shortfall on the Pico plant. The study aims the partially correction of the influences from pressure skewness Chapter 4. 3.2. by the use of a passive one way valve in series with the pressure relive valve.
- Another study “ Air turbine optimization for a bottom- standing oscillating water column wave energy converter” (Falcao, Henriques and Gato, 2016) is a case study in which recent bidirectional air turbines are theoretically implemented into the Pico plant for performance comparison. Results from mini turbine tests are up scaled and adapted to the Pico plant requirements. Though this is the same method as was initially done for the original Pico turbine, the study does not remark that the original Pico turbine could not deliver what the mini turbine tests suggested. However a recent monoplane Wells turbine with high efficiency is introduced and a bi radial impulse turbine found to be the most efficient turbine for the tested case.

4.4. OBTAINED PAPERS ON PERFORMANCE ANALYSIS OF WECS

- Pecher, A. and Kofoed, J.P. (2016) *Handbook of Ocean Wave Energy*.
- Pecher, A., Kofoed, J. P., Le Crom, I., Neumann, F., and Azevedo, E. de B. (2011) 'Performance Assessment of the Pico OWC Power Plant Following the Equimar Methodology'

CHAPTER 3. THE PICO PLANT

1. INTRO

The Pico plant was a free standing, bottom fixed, full scale, concrete OWC equipped with a large horizontal mono plane Wells turbine. It was implemented in the rocky coastline on the north west coast of the Azorean island Pico. The civil construction was terminated in 1998 and was designed for a 25 years lifetime (Instituto Superior Tecnico, 1998). The structure collapsed in April 2018 after about 20 years. It was aimed to be equipped with two different 400 kW Wells turbines, which were meant to be operated only one at a time (The carbon trust report, 2005). Due to problems during the project realization the foreseen second Wells turbine with a variable pitch rotor was never realized. Therefore the only installed turbine is a 2,3 m diameter monoplane 400 kW Wells turbine equipped with guide vanes on both sides. Neither rotor blades nor guide vanes can be pitched. For air flow control a slow turbine bypass valve in parallel is installed.

The project aimed the learning about the technology and the prove of the feasibility. Concrete production predictions were given in (Falcao, 2002) and (Instituto Superior Tecnico, 1998). It was aimed to produce annual average grid power of approximately 100 kW which allows to cover about 8 % of the islands energy consumption of 1995. A brief project review is given in Chapter 1. 2. .

2. RESOURCE ASSESSMENT

The local wave climate for the Pico plant was measured for a period of 2 years during the project development in the 1990th. The resulting estimation for the local energy resource in terms of wave power flux is 13,4kW/m (Falcao, 2002). Based on these measures also a local wave climate, which contains 44 different sea states, was defined. These sea states are was defined by its significant wave height H_s , energy period T_e and probability and can be obtained in Table 3.1.

During the summer months usually south swells are dominating while in winter time the more frequent north swells are dominating. The location of the device on the north west coast of the island is sheltered almost completely from south waves. Therefore the wave climate on the device location varies significantly between summer and winter. During the summer months of June, July and August waves on location are usually very small while large swell are frequent in winter.

Annual local wave climate			
sea state number	T_e [s]	H_s [m]	Probability [%]
1	6,6	1,2	0,1
2	8,1	0,5	1,8
3	8,1	1,0	4,7
4	7,9	1,6	2,2
5	7,5	2,3	0,4
6	7,5	2,8	0,1
7	8,5	0,5	2,2
8	8,8	0,9	5,6
9	8,8	1,4	8,7
10	8,7	1,9	2,3
11	8,7	2,1	0,1
12	8,5	3,3	0,1
13	8,5	3,8	0,1
14	9,5	0,5	1,1
15	9,9	0,6	3,5
16	9,7	1,0	8,6
17	9,7	1,4	5,0
18	9,5	2,3	3,0
19	9,5	2,8	2,3
20	9,5	4,3	0,2
21	10,9	0,5	4,4
22	10,9	1,5	3,2
23	10,7	1,9	9,0
24	10,6	2,2	3,8
25	10,5	2,8	2,3
26	10,5	3,3	1,4
27	10,5	4,3	0,3
28	11,4	0,7	1,7
29	12,1	1,4	1,8
30	11,8	1,9	5,5
31	11,9	2,4	2,7
32	11,5	2,8	4,2
33	11,5	3,3	3,2
34	11,5	3,8	0,3
35	11,5	4,3	0,1
36	13,5	1,9	0,3
37	13,2	2,2	0,7
38	13,3	2,6	0,8
39	13,1	3,0	1,1
40	12,5	3,8	0,3
41	12,5	4,3	0,1
42	13,5	4,3	0,3
43	14,7	2,6	0,1
44	14,5	4,3	0,2

Table 3.1 Local wave climate

3. SYSTEM SPECIFICATION

Civil structure

The device was designed to be built in prefabricated concrete blocks but was finally realized as a reinforced concrete structure. It consisted one air chamber with an area of 144m^2 ($12\text{m}\times 12\text{m}$) and a volume of 1050m^3 . The structure contains the air chamber, a closed turbine hall and a basement, which initially housed the electrical equipment. The structure is built into a rocky coastline with a connection to the land only at one lateral side. The device entrance is from this lateral side. Water depth inside the chamber was scheduled to be about 8m but has decreased due to bolder movement to about 6m or less. In Figure 3.1 and Figure 3.2, which are both extracted from (Falcao, Henriques and Gato, 2016), the orientation and a cross section of the device structure can be found.

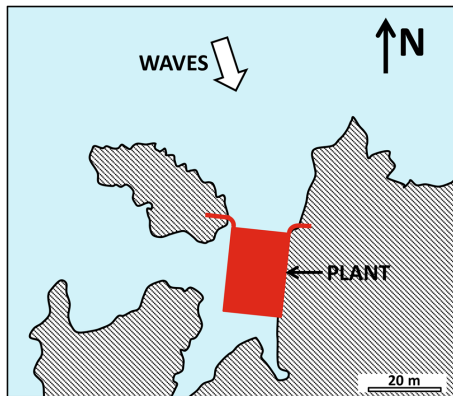


Figure 3.1 Device orientation

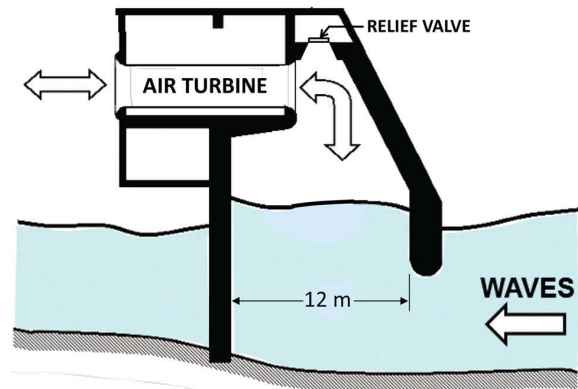


Figure 3.2 Civil structure cross section

The civil structure suffered significant damage during the construction phase for various reasons. The result was a civil structure with several holes in the submarine walls and large areas in which the reinforcement steel was exposed to the sea water. Initially the damage was assessed to limit the life time of the structure dramatically but it finally reached 20 of 25 scheduled years. However the damage increased significantly with the years and in early 2017 a large storm has finally removed large parts of the western submarine wall. This removed submarine wall was about one year later the reason for the collapse of the civil structure. However, the collapsed wall was only the last step but already before holes and an additional damage on the submerged front wall caused air passage during larger wave trough at low tide. This and the decreased water depth always influenced the hydrodynamic performance of the device negative with increasing impact.

PTO

A 2,3 m diameter monoplane Wells turbine with one set of guide vanes on both sides directly drives a 400 kW double fed inductive asynchronous generator. A design problem caused the destruction and removal of the downstream guide vane. Another faulty design in the power electronics caused the limitation of max power to 200 kW. Beside that, pitch corrosion caused significant degradation of the rotor blade surfaces and even partly the profile shape.

Operation speed

The device was foreseen to operate with variable rotational speed between 750 and 1500 RPM. Due to a specification issue the power electronics switch of the generator at exactly 1500 RPM. Therefore the available rotational speed limit is maximum 1400 RPM to enable slight exceed of the limit which is caused by the non static air flow conditions.

Power smoothing

For midterm power smoothing the rotor is equipped with a large inertia to provide a flywheel and for long term smoothing it is equipped with a stationary (slow) pressure relive valve in parallel with the turbine. For short term

smoothing a fast acting relieve valve was foreseen to be installed and tested (Instituto Superior Tecnico, 1998) but this could never be realized. During the study the stationary pressure relieve valve was used as an active valve, which allowed pneumatic power smoothing in significant larger waves. For this purpose the slow relieve valve was coupled with a sensor, which measured the incoming waves about 80 m before reaching the device. A schematic of the system can be seen in Figure 3.3, which is extracted from (Monk, 2012). This gave sufficient time to partly open the valve automatically in case a significant higher successor wave was detected. As can be found in (Monk *et al.*, 2015) the system was later on controlled by a neural network instead of the sensor. However the type of valve caused the limitation of moving cycles which limited the effect of the neural network attempt.

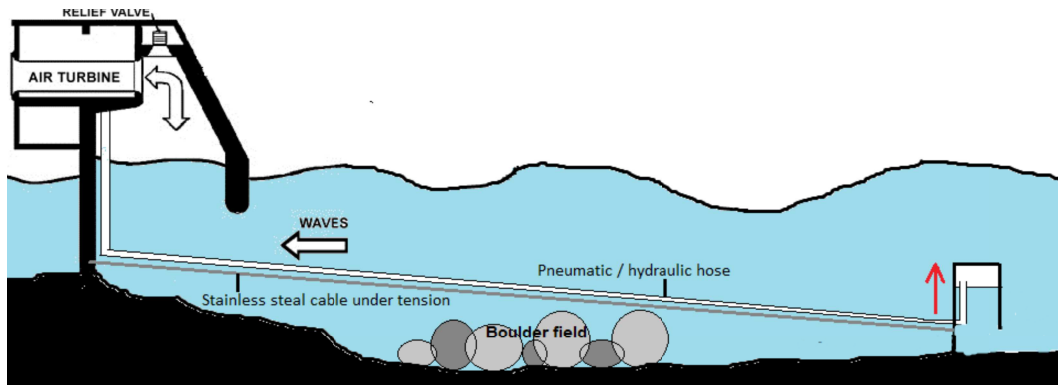


Figure 3.3 Schematic of the self developed nearshore wave sensor.

Operation range

The in Chapter 4. 3.3. further explained turbine underperformance prevents operation with positive power transfer to the grid for smaller wave conditions. Therefore the lower limit for operation is currently theoretically in the range of $1\text{m } H_s$ at T_e about 8 sec at location or in real device operation at roughly $1,5\text{m } H_s$ at about 10 sec T_e swell from north west to north east in offshore forecast. On the other side the device is operated in all large sea conditions without limit.

Detailed information obtained from (Falcao, 2002)

- rotational speed range 750 RPM - 1500 RPM
- Rotor diameter outside: 2,3 m; inside: 1,36 m
- Number of blades: 8
- Blade chord: constant 0,375 m
- Blade section profile: not clearly defined: Once reported as specially designed NACA 0015 or similar profile (Instituto Superior Tecnico, 1998)
- Rotor inertia: 595kg/m²
- Guide vane:
 - Cylindrical shape
 - 59 guide vanes in each row
- 400 kW double fed inductive asynchronous generator
- air chamber area: 144 m²
- air chamber volume 1050m³
- capture wide 15 m
- air chamber wide 12 m

Power electronics

The stator of the applied double fed inductive asynchronous generator is directly connected to the grid phases with the use of two transformers which lower the voltage from 15 kV to 380V. The coils on the rotor deliver a alternating potential, which is rectified with the use of a spinning diode rectifier inside the generator. The dc currents are later transferred into the alternating grid currents by the use of current converter (based on IGBT technology). A schematic of the system, which originates from the original device documentation, can be seen in Figure 3.4.

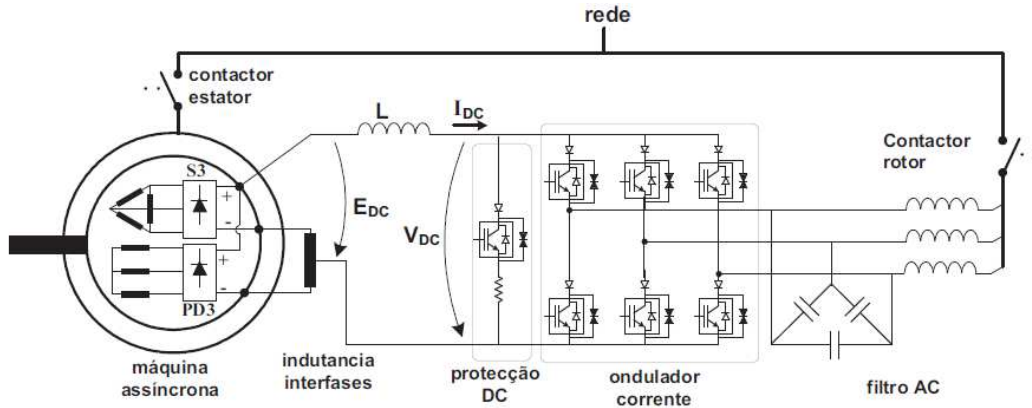


Figure 3.4 Schematic of the Power electronics

Control equipment

All electronic equipment, hence also the control equipment was initially located inside the plant structure (in the basement). During the refurbishment project it was transferred into two shipping containers, which are located about 100 m inland for humidity protection. A schematic location plan can be seen in Figure 3.5. The control equipment, the power electronics (beside the generator), the remote access equipment and parts of the DAQ equipment are located in the containers. The turbine, all related auxiliary systems, the generator and all sensors beside the generator-current and voltage meters are located inside the plant. Since 2014 also a part of the DAQ system, which captures the values of the sensors located inside the plant, was located inside the plant again.

The main control unit is outdated. It was designed in 1995 and is still based on windows NT technology. The unite contains an automate that controls the power electronics and the auxiliary systems. This is either done automatically based on the input data from the Instrumentation and a control algorithm or manually by operator commandos. The system also contains a battery backup for the case of grid failures.

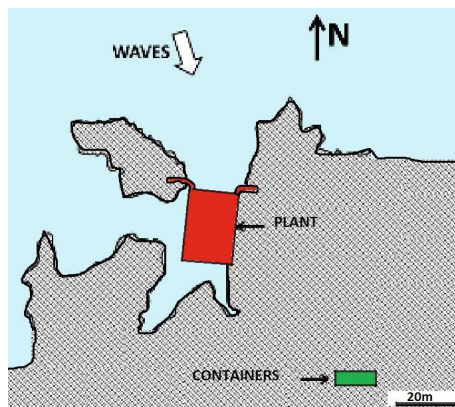


Figure 3.5 Location plant and control unit

Auxiliary systems

A schematic of the basic plant system is presented in Figure 2.2.

- The turbine can be isolated from the air chamber by two independent duct valves. Both valves are

CHAPTER 3. THE PICO PLANT

actuated pneumatically. The main duct valve, which is in direct contact with the chamber is executed as a strong but fairly slow (30 sec closing time) vertical slide valve. The second valve is a much faster (2 sec) butterfly valve. The pneumatic pressure is delivered by an air compressor.

- The system is equipped with an air pressure relive valve in parallel to the turbine. It is executed as a hydraulic horizontal slide valve actuated by a hydraulic pump.
- The turbine bearings are lubricated in an closed oil circuit while the generator bearings are lubricated only with grease.
- The turbine hall is equipped with power supplies, a light system, a fresh water reservoir and a crane for works on the turbine.

Instrumentation

The installed instrumentation has changed in the lifetime of the Pico plant. Initially a large number of monitoring sensors were installed. Especially due to the financial situation during the here presented field study the number of installed sensors was essentially decreased. Sensors which were not absolutely relevant for safety or data post processing were not repaired or substituted after damage. But also some as required assessed and before not installed safety or control relevant sensors and systems were installed for performance optimization.

Initially monitored vital values for device control (not necessarily stored data)

- Inductive end stop sensors at both duct valves
- An inductive linear sensor to indicate the exact position on the pressure relive valve
- A mechanic oil level and two inductive oil flow sensors at the bearing oil circuit
- Temperature sensors at all bearings
- Temperature sensors at the generator coils
- Generator brush sensors to detect critical wear
- A mechanic rotational speed sensor at the generator shaft
- Horizontal acceleration sensors to obtain the vibrations at both turbine bearings and the generator and an additional diagonal sensor at the generator
- Produced active power
- Produced reactive power
- Generator currents and voltage etc.
- Several further vital values of the power electronics
- Several further vital values of the control system
- For longer periods in 2012 an air pressure sensor was installed, which measured the pressure in an air chamber that was fixed on the sea floor about 80 m in front of the plant. The signal was used to control the above introduced active pressure relive valve (see point Power smoothing of this section)

CHAPTER 3. THE PICO PLANT

Budget reasons have caused the reduction of sensor equipment. Since the beginning of 2016 the device is monitored only with the required minimum because damaged sensors, which were assessed as disposable, were not replaced. However an important second rotational sensor was additionally added.

Monitoring sensors since 2016

- One inductive end stop sensors at the main duct valve
- An inductive linear sensor to indicate the exact position on the pressure bypass valve
- A mechanic rotational speed sensor at the generator shaft
- A second inductive rotational speed sensor at the turbine
- Horizontal acceleration sensors to obtain the vibrations at both turbine bearings and the generator and an additional diagonal sensor at the generator
- Produced active power
- Generator currents and voltage etc.
- Several further vital values of the power electronics

For performance evaluation acquired data and used sensors

- surface elevation inside the air chamber is measured with an ultrasonic sensor
- pressure inside the chamber is measured with two pressure sensors
- static pressure inside the turbine is measured on both sides of the turbine with one pressure sensor per side (initially 2 sensors were installed per side)
- Air flow is measured via the dynamic pressure, which is measured with Pitot sensors on both sides of the turbine (initially 3 sensors per side now only 2 per side)
- The temperature inside the turbine duct was measured till the sensor was destroyed in 2011
- Rotational speed
- The relive valve position
- Produced active power
- For a short period in 2010 and 2011 an aquadopt wave sensor was installed

For post processed troubleshooting acquired data

- vibration on the weaker turbine bearing support
- second rotational speed value (at the turbine)

Data acquisition system (DAQ)

The initial DAQ system was developed by INETI and was based on windows NT. Already in 2007 to begin of this study a fiber optic system was installed to transmit the analog sensor data from the device to the control unit. Before the installation of this system the noise was reported to be very high. However even with the fiber optic system the noise remained high and required significant filtering. Because the DAQ system suffered damage and was not correct functional anyway a new system based on one "labjack U9" and one "labjack U12" DAQ boxes and the belonging software "DAQ factory" was installed. Not all installed sensors share a common ground, which led to noise problems in the old system. Therefore the sensors with common ground were installed on one DAQ box and the differential signals on a separated box. This already improved the situation but only in 2012 the noise level could finally be reduced to a acceptable level after some analysis and removal of problem sources. However in 2014 a lightning destroyed the system including the expensive fiber optics. Because a replacement was impossible, the DAQ system had to be changed again. One Laptop and two "labjack" DAQ boxes were then installed in a water proof cabinet inside the plant where the analog data was acquired directly. The connection of this computer to the internal network that was located in the control unit was impossible with

a simple LAN cable due to the long distance. However a system could be installed that hijacked a simple power cable to provide an internet connection inside the power plant. Finally two separated DAQ systems were operated and could both be accessed via the internet. Only in post processing the data was compiled. The new system enabled to remove a before by the fiber optic system introduced time delay of approximately 3 seconds. The acquired data quality of most values was good.

Safety systems

Safety systems were not installed or foreseen on the device. Only a control system was installed, which was not suitable to also address safety functions. Due to the not reliable automatic system and the attempted remote controlled operation it was required to develop and install a suitable redundant safety system. To indicate the possible worst case failures, a risk analysis was executed. A initial schematic of the developed system can be seen in Figure 3.6. The finally installed system reacted on elevated vibrations, over speed (which was measured with the rotational speed sensor at the turbine), low oil level (this function was later removed) and the loss of connection between the main control unit to the device. When ever a failure was detected relays were deactivated which in turn caused the closing of the duct valves via solenoid valves. All relays and solenoid valves were doubled, the same was the case for the duct valves and also applies for the event of over speed because the consequence was elevated vibrations. Hence the system was redundant and has never failed.

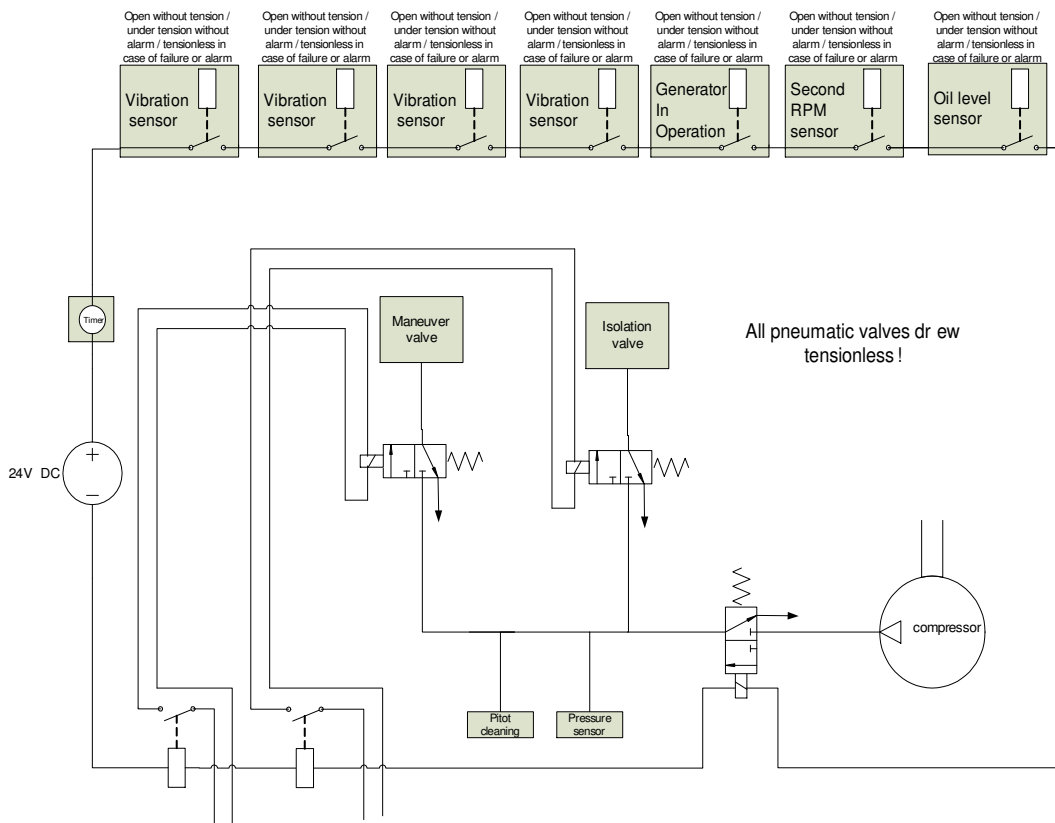


Figure 3.6 Independent security system

Remote control system

Similar to the safety system a remote control system was not foreseen or installed at the device. For the purpose of continuous long term operation this system had to be developed and implemented. Because the system was based on not sufficiently reliable components it was attempted to execute it redundant.

The machine operated automatically and was additionally observed by the above introduced independent safety system. In case of a shut down either by the automatic functions or the independent security system the remote operator was informed via a landline telephone system. To minimize the risk of landline failures, which prevent the transmitting of the alarm, beside the alarm calls periodic calls were executed to confirm the function of the telephone system.

The remote operator could always access the device via a standard landline internet connection. The operator

CHAPTER 3. THE PICO PLANT

used a remote access software as for example “teamviewer” to access a standard laptop close to the control unit. This laptop was connected to the main control unit via a local network and could be accessed with the use of the windows standard program “VNC viewer”. Here the operator could executed all required actions to ensure a safe shut down and additional all troubleshooting and restart tasks which did not require manual intervention. For redundancy two standard laptops were installed.

The case of an internet failure was addressed by a mobile phone based GSM switch that could either reset the internet router or execute an emergency device shut down when called by the operator. Temporally an additional mobile internet router was installed that could back up the internet in case of a primary connection failure but this system was later removed.

In case a manual intervention was required and an operator was not on the island a local part time employer executed the simple tasks and for larger repairs the operator had to travel to the island.

4. AVAILABLE WAVE DATA IN OPERATION

During the continuous operation period local wave data was captured only for short periods in 2010 and 2011 with an deployed aquadopt sensor. A study using this data can be obtained in (Le Crom *et al*, 2009). Until 2012 a wave rider buoy was located in the region ($38^{\circ}25.26'N$, $28^{\circ}32.26'W$), which delivered regional wave measurements. Since 2012 the only available data is offshore forecast data.

CHAPTER 4. DATA ANALYSIS AND RESULTS

1. 14 REASONS FOR REALIZATION PROBLEMS

Detailed information about the here briefly presented problems, analysis and solutions can be found in Appendix 1.

1.1. BACKGROUND INFORMATION

Situation at the end of the project realization in 2000

The project realization was disturbed by expensive and time consuming problems regarding the civil construction and the electrical equipment. In 1998 the civil construction was finalized. However, it showed already essential damage. The first operation attempts in 1999 revealed another large problem regarding the turbine function. A second flood destroyed the electrical equipment already the second time and ended the first operation attempts. First solution attempts for the turbine vibrations could not improve the problem essentially during the second operation attempt in 2000 (Sarmiento, Brito-Melo and Neumann, 2006). These problems were already briefly introduced in Chapter 1. 2. . Additionally the next expensive electrical accident followed only few weeks later (Falcao, 2000). At this time the device was fully nonoperational and the civil structure was assessed to collapse soon ¹. In the consequence the project owners appear to have lost the interest in the project and the trust in a possible success. Therefore the device was practically abandoned and no further actions took place.

The following three problems were the main reasons for the situation.

- The majority of the entire electrical equipment was destroyed already 3 times due to floods and humidity.
- Excessive vibrations in the turbine support structure prevented turbine operation in the aimed operation range.
- The civil structure was seriously damaged during construction and was later assessed to collapse in the near future.

Situation to beginning of this field study in 2007

The civil structure did not collapse as predicted but remained without essential further degradation. This had enabled the execution of a refurbishment project. The project was initiated by Antonio Sarmiento and took place between 2003 and 2005 (Sarmiento, Brito- Melo and Neumann, 2006). The project shared similar goals as the initial project and only few technical changes were implemented. Basically it was attempted to overcome the already discovered three main problems. After a short assessment the civil structure was now assumed to resist. The humidity problem of the electrical equipment was addressed by a location change of the equipment. The majority of the equipment was moved out of the device into an external control unit about 100 m inland. Only the generator and large parts of the Instrumentation remained inside the device. Also the turbine vibrations were attacked by further vibration measurements and turbine structure reinforcements.

Beside these changes a new set of electrical equipment based on the original design was installed and the mechanic components were recovered after having suffered corrosion and ocean loads several years without maintenance.

In the first operation tests in 2005 the rotor guide vanes were destroyed under normal operation loads. These were replaced by new redesigned guide vanes but the unexpected costs consumed remaining budget.

At this time the vibrations in a ring structure around the turbine rotor could be eliminated but the vibrations in the rotor support structure remained. Therefore the machine still remained hardly operational. With the reinforced structure the machine vibrations now only started to occur in the lower end of the foreseen operational speed range instead of below, as it was the case before.

The same applied for the electrical system. The situation was improved because the system was never flooded again and consequently did not suffer complete destruction by humidity. However a large quantity of malfunctions especially in the control equipment such as the DAQ equipment prevented automatic machine operation fully..

¹ A internal report about this issue exist and was studied by the author years ago. The same assessment was used again in 2008 to terminate another planed recovery project. The report is not officially available and no reference could be found.

CHAPTER 4. DATA ANALYSIS AND RESULTS

In the consequence the device could be operated with strongly reduced rotational speed with an operator permanently observing the system ready for emergency interaction. But even operation of this type was permanently disturbed by elevated vibrations and electrical and mechanical failures. Operation periods of more than one or two hours at a time were hardly possible.

A prior existing large electrical noise problem in the DAQ system could already be improved by the installation of a fiber optic system.

Beside that it was hardly attempted to solve the existing system failures. Only new occurring damage which interrupted even the poor operation was still repaired.

1.2. INITIAL TROUBLESHOOTING DURING THIS FIELD STUDY

Between summer 2007 and September 2010 all problems, which avoided serious operation could be solved. This was done by executing the following steps.

- Initially reasonable working conditions were created.
 - Recovering the damaged light system and the power sockets
 - Cleaning up the turbine hall which was obviously not done since years
 - Removing unnecessary damaged or corroding material and components from the turbine and turbine hall
- Basic improvements of humidity problems
 - Cables were removed from the wet floor.
 - Connections were executed water prove and solid.
 - Systems were physically protected from spray water and strong air flow.
- Reviewing the entire wiring of the device with the following purpose:
 - Creating a reliable documentation, which did not exist
 - Detecting installation mistakes (wrong or loose connections)
 - Gain certainty that the cabling is done as expected
- Systematic analysis, development and installation of solutions for each subsystem (step by step)
 - Turbine vibrations could be solved by a modal and FEM analysis and a special designed reinforcement.
 - Generally the humidity problems were solved by suitable water prove connection boxes, submarine connectors and suitable cable ways and fixation.
 - A large electrical interference problem that caused frequent faulty alarms and in the consequence disabled automatic operation was systematically analyzed and solved by changes in the system setup.
 - The not suitable control algorithm was studied and adapted to the requirements of the device.
 - A not suitable general safety concept was corrected.
 - Further many other smaller problems were solved.
- Developing, installing and testing required but missing systems.
 - A completely missing independent security backup system was developed, installed and tested from the scratch.
 - A remote access system was developed, installed and tested from the scratch.

After having finished these tasks the continuous operation phase was started and was technically only interrupted by new damage till operation was stopped in January 2018.

1.3. ROOT CAUSE ANALYSIS OF THE INITIAL PROBLEMS

The number of solved problems was large but because the analysis was executed in retro perspective several years after the occurrence most of the small trivial issues cannot be recapitulated with certainty anymore. Therefore only the larger determining problems were observed for the analysis. The failures, which caused these problems, were compiled in a failure log in dependence to the FRACAS method as was done in a similar way in (Kenny et al, 2017) before.

Used information regarding the problems, that were already overcome before 2007, was compiled in retro perspective by studies of old internal project documentation and conversation with various project members. Information about the technical failures, which were not solved in 2007, result from the authors problem analysis.

The focus of the analysis was on the question why it took so long to reach continuous operation.

The compiled failure logs are presented in Table 4.1, Table 4.2 and Table 4.3. The main failures, which caused others to follow, are here marked in red and later on referred as primary failures. Grey background in the log indicates problems solved by the author.

Log of failures which caused the practical abandonment of the Initial project				Particular involved failures											
Sub Assembly	Component	Failure Effect	Final Solution	Solution type	Detection method	Root Cause	Failure Mechanism	Resp.	Failure Mode	Failure Symptom					
Civil structure	sub marine structure	Initial abandonment of the device / Reduced life time due to structural damage / Performance losses due to holes and reduced water depth	no solution	no solution	observation after occurrence	Standard design mistake	change of design not prevented	PM	too complicated construction method / too high risk for failure	underwater concrete works required / temporarily dam required					
											temporarily dam designed to weak	Sub	collapse of temporarily dam	strong damage due to bolder impacts from collapsing dam	
											required concrete quality to low	Sub	Locally poor concrete quality washing out of cement	several holes	
											installation mistake	Sub	time limit between two concrete layers exceeded	poor concrete quality and time limit exceeded	
											insufficient removal of the remaining rocks from the collapsed dam	Sub	sea floor / chamber floor covered in rocks which do not belong there	reduced water depth / permanent bolder impacts on the walls / chipping of concrete	
											inadequate calculation methods were applied	PM	wrong life time assessment	no more trust in the civil structure	
											Standard design mistake	Not against humidity protected electrical equipment located 4m above sea level / device not designed water proof	PD	flooding of the electrical equipment through the openings to the chamber	destruction of the first equipment
											wrong assessment	installation of electrical equipment before the turbine hall was closed against the chamber (in winter)	PM	flooding of the equipment through a not adequate entrance door	destruction of the second equipment
											wrong assessment	Equipment reinstallation without changes	PM	Equipment location change / still inside the humid device	destruction of the third equipment
											Turbine structure	rotor support structure	turbine not operational in the designed operation range	reinforcement installation / structure changed towards triangle shape	applying of proven engineering solutions
					wrong assessment	turbine vibration tests executed during construction without the large generator weight in place	Sub	Confusion about the source of the vibrations							
					installation mistake	accidental drop down of the turbine during transport	PM	Discussion about responsibility							

Table 4.1 Failure log 1995-2007

Log of failures which practically prevented operation between 2007 and 2009

Sub Assembly	Component	Failure Effect	Final Solution	Solution type	Detection method	Particular involved failures				
						Root Cause	Failure Mechanism	Resp.	Failure Mode	Failure Symptom
Turbine	Rotor guide vane	on first occurrence long and expensive down time / later slight reduction of turbine performance	removal of the downstream guide vane / including tube section repair into the maintenance procedure	Redesign / substitution	observation after occurrence	unexpected loads	aerodynamic stall causes unexpected high vibrations to the guide vanes	PD	cracks in the guide vanes	destruction of guide vane / sucked into the rotor / superficial rotor damage
			Guide vane substitution by a tube section / accepting performance reduction	maintenance	Standard design mistake	Standard design mistake	Welding lines substitution tube section cracked under vibrations	PtcT	cracks in the substitution guide vanes	
Electrical equipment	low voltage equipment	no reliable function of many systems / complicated trouble shooting	installing suitable connection boxes, connectors / changing equipment position review and re documentation of the entire low voltage equipment	applying of proven engineering solutions	observation in system review / after occurrence	Standard design mistake	Not suitable against humidity protected electrical equipment in humid environment	PD	corrosion and short circuits	Frequent sensor and auxiliary system malfunction and damage
			correcting the mistakes	system review	installation mistakes	plenty cables were either wrong or not connected		Sub	system malfunctions	faulty alarms / no alarm / systems not responding etc.
					installation mistake	the documentation was not correctly updated after location change		Sub	Plenty mistakes in the documentation	useless documentation
					missing authority	no enforcement for final system check		PM	no final system check	risk of malfunctions
Entire device	maintenance procedure	device operation often disturbed /down time / costs	implementing a suitable maintenance procedure	applying of proven engineering solutions	observation	Standard design mistake	correct maintenance was impossible due to accessibility and was neither planned nor executed before 2007	PD / PM	Missing maintenance	detection of component damage only after occurrence
Electric	Instrumentation and control electric	automatic device operation impossible due to permanent shut downs caused by faulty alarms / no continuous operation possible	changing the wiring schematic of all alarm cables correcting the mistakes	applying of proven engineering solutions	systematic analysis	Standard design mistake	all rules to prevent electromagnetic interference were not respected	PD	High electric noise in all alarm cables due to interference	permanent faulty alarms during operation attempts
			adapting the algorithm and updating it during operation	correcting the mistakes	installation mistake	installation mistake	the shields of all alarm cables were disconnected	Sub	Disarmed alarms showing correct function	High risk for operation attempts
					installation mistake	various alarm functions wires were disconnected and bridged but documented as connected		Sub	Even without faulty alarms the automatic mode functions were not suitable	Faulty operation in automatic mode attempts
					Standard design mistake	Standard design the control algorithm was not adapted to the requirements of the device		PD		

Table 4.2 Failure log 2007-September 2010 part 1/2

structure	Device (initially control unit) access	high human risk when accessing the device in stronger sea conditions / strong limited access to the device	design of a wave deflector / creating a shelter for the operator during access	new design	observation	Standard design mistake	The opening direction of the heavy duty entrance door of the device is towards the ocean	PD	Overtopping waves hit the entrance door	uncontrolled opening of the door with overtopping waves during operator access / operator exposed to the waves forces / large amounts of water entering through the open door
PTO	Safety concept	high risk for device destruction especially in automatic mode function	development of an independent, redundant safety system	development of a permanent verification system, triggering the safety system	system review and risk analysis	Standard design mistake	no independent safety system foreseen and control unit not suitable for this purpose	Sub	Freezing of the control unit	Loss of connection between control unit and PTO
			change the wiring concept and the programming	concept change		Standard design mistake	fail safe concept not respected	Sub	alarm cables wiring of the alarm cables	no alarm signals transmitted in case of any damage on cable or power supply.
Duct valves	Isolation valve	heavy reinforcement required (only emergency recovery possible) further damaged expected	reinforcing the housing structure / repairing it frequently	reinforcing the design / frequent repair during maintenance	maintenance	unexpected loads	the isolation valve housing is not correctly sealed against the air chamber and therefore is pressurized (not designed for it)		cracking of the valve housing	the stainless steel case of the isolation valve blows up as a balloon and is sucked back with every wave cycle

Table 4.3 Failure log 2007-September 2010 part 2/2

Analysis Results

To evaluate the results of the failure log the failures are divided into two groups of failures. The primary failures, which are the real source of the final problem, and secondary failures, which include follow up failures or smaller failures, which would not cause a large impact when occurring alone. Design and installation failures such as wrong assessment are ranked as human caused failures.

Table 4.1 shows the root causes of the failures, which caused the failing of the initial realization phase and the following practical abandonment.

Root causes for the initial problems before the "abandonment"		
	total	%
Primary failures	3	
caused by failed standard design	3	100
caused by unexpected loads	0	0
Secondary failures	12	
caused by failed standard design	0	0
caused by installation mistakes	4	33
caused by unexpected loads	0	0
caused by wrong assessment	7	58
Total amount of human caused mistakes	14	93

Table 4.4 Root cause analysis for initial problems

It can be found that more than 90 % of the larger mistakes were caused by human failures. Further it can be obtained that all primary failures were caused by failed own design solutions for applications, where known reliable solutions existed.

The second large failure type "wrong assessment" emerges among the secondary failures. These failures are mostly related to wrong assessment of the destructive ocean forces and makes up for 58 % of the secondary failures. One example is the underestimation of humidity inside the device. The last large group of failures is caused by installation mistakes. About 33 % of secondary failures were caused by it.

Failures caused by corrosion, unexpected loads or the new technical challenge did not contribute essentially to the initial project abandonment.

Table 4.2 and Table 4.3 show the detected root causes of all important failures, which prevented the start of continuous operation before 2010. The initial failures from Table 4.1 are again included here.

Root causes for all problems which disabled continuous operation before 2010		
	total	%
Primary failures	10	
caused by failed standard design	8	80
caused by unexpected loads	2	20
Secondary failures	22	
caused by failed standard design	5	23
caused by installation mistakes	8	36
caused by unexpected loads	0	0
caused by wrong assessment	7	32
Total amount of human caused mistakes	29	91

Table 4.5 Root causes analysis for problems before 2010

A similar result emerges when observing all problems, which avoided continuous operation before September

2010. Still about 80 % of the failures are caused by own failed design solutions for applications were reliable solutions exist. Additionally again about 90 % of all failures are caused by human mistakes.

1.4. RESULT DISCUSSION

To answer the question for the reason why so many mistakes were done and why they could not be overcome for such a long time would involve personal speculation. Therefore only some observations of the author with a short interpretation of the situation are presented together with the solutions in general and some of the problems in detail.

To begin of the field study in 2007 the author found the following:

- A machine that was hardly operational
- The floor of the turbine hall was covered in a solid layer mixed of sand, corrosion, oil, salt, water and garbage (remaining from the refurbishment project in 2004).
- Two different light systems were installed but none was functioning.
- All power sockets were damaged.
- No fresh water system existed in the device to clean the machine from salt.
- The turbine hall was used as a storage of corroding materials as can be obtained in Figure 4.1.
- Only few of the bolts in the turbine were installed but bar clamps were installed instead.
- Works were focused on the DAQ system and the new guide vanes.
- No concept and no employer existed to change this situation.
- Project engineers were concentrated on scientific tasks.
- Engineering problems were only reported and transmitted to mostly not local sub contractors.

This caused the authors impression that non scientific tasks were simply not attended correctly. Consequently in the following these non scientific but technical tasks were attended with priority by the author and his colleagues. With a systematic in house troubleshooting concept, which reduced the requirement of external support to a minimum, it was finally possible to solve all problems.

Due to all these observations, detected problems and found solutions it is here assumed that at least the struggling to overcome the technical problems during the refurbishment project was strongly influenced by the mostly scientific intentions of the project members. This caused the focus to be on the final scientific goals but not on the prior required engineering tasks. The troubleshooting concept involved external, not local sub contractors to solve the engineering problems. At least for the Pico project with its remote location and its sub contractors this was a not very effective but time and budget consuming strategy.



Figure 4.1 Pico turbine hall in 2007

Examples for failed design concepts

- It is common standard to build harbors or breakwaters in prefabricated concrete structures because it ensures a high concrete quality and reasonable short construction periods. This was the initially chosen design concept for the Pico plant but it was later on changed by the sub contractor, which had reportedly never build a maritime structure before. This concept change was the source for all problems regarding the civil structure.
- The electrical system was initially designed to be in a separated control structure but for political reasons the designers were forced to install it inside the device (Instituto Superior Tecnico, 1998). Though the maximum waves were estimated to be 7,5m a proper protection from humidity was not foreseen. The executed humidity protection standard for the electrical system was less than usually used in bathrooms. Meanwhile the equipment was installed about 4 m above sea level in a not properly sealed building. The problem could be widely solved by removing the majority of the equipment out of the device into a separated control unit and by increasing the humidity protection of the remaining system to marine application standards.
- The 2,3 m turbine is equipped with a large inertia rotor and therefore has a large rotating weight. Large rotating (oscillating) weight requires stiff support structures to ensure sufficiently high natural frequencies. The favored design solution for bearing supports of large weight rotors is a triangle shape to cope with horizontal forces. For the Pico turbine a mono pile bearing support structure was chosen. The result were exactly these low natural frequencies in horizontal direction. The final solution was a large bearing reinforcement structure that basically changed the concept to be triangle shaped.
- A large electrical interference problem that prevented automatic operation was caused because several rules to prevent electrical interference were not respected. The removal of the most important mistakes improved the situation in a way that it never caused problems afterwards. The solution did not require any new equipment but exclusively a correction of the wiring concept.

Corrosion

Finally it should be said that the result that corrosion appears to be no problem is probably slightly misleading because the device is fairly corroded. However, only corrosion in not correctly protected electrical cables and components contributed to the essential problems that prevented operation. However corrosion is an issue that requires permanent attention.

1.5. CONCLUSION FROM TROUBLESHOOTING

It appears unlikely that the Pico project would have suffered a similar fate if the developers would have selected well known reliable design solutions. The quantity of failing “standard” design solutions caused a complex structure of problems with only few certainly known facts. This caused a not trivial troubleshooting for which the project management was initially not prepared. The remote location complicated the situation but was not the main reason for the problems.

2. CONTINUOUS OPERATION EXPERIENCE

As already stated before the Pico OWC was in continuous operation from September 2010 till January 2018.

Operation procedure

The device executed all operation related tasks automatically. In case of failures the device shut down automatically and informed a remote operator for restart interaction via telephone. This interaction was mostly done via internet access. In case of required manual intervention either the operator or a local employer had to interact at location.

Maintenance

In 2008 a regular maintenance procedure was established and adapted to the means of the device. The procedure includes a two month, an annual and a biannual intervention and was executed regularly from 2010 till July 2012 and again from January 2014 till July 2016. Afterwards maintenance was reduced to an absolute minimum.

2.1. OPERATION STATISTIC

Machine availability

Beside some political decisions mainly some remaining design weaknesses caused machine downtime since 2010. In Fehler: Referenz nicht gefunden the large periods without machine operation and availability from July 2012- February 2014 and the down times in 2017 were caused by political decisions. In this figure it can additionally be seen that the machine availability in summer is usually significantly higher than in winter. This is caused by essentially smaller loads and operation time in summer such as faster respond time due to easy device access and work conditions. This seasonal variation results from the already in Chapter 3. 2. explained seasonal variation of the local wave climate. The orange columns in Fehler: Referenz nicht gefunden indicate this effect. Here the percentage of operation days compared to days with machine availability is displayed. It can be obtained that these value is very low during the summer month and increases significantly in winter.

The annual results for machine availability and operation time is displayed in Table 4.6.

Annual availability and operation results			
	Availability [%]	Operation days [%]	Operation days / available days [%]
2010	not known	16	not known
2011	18	9	49
2012	36	12	33
2013	0	0	0
2014	50	23	45
2015	73	27	37
2016	69	26	38
2017	19	13	67

Table 4.6 Annual operation statistic

CHAPTER 4. DATA ANALYSIS AND RESULTS

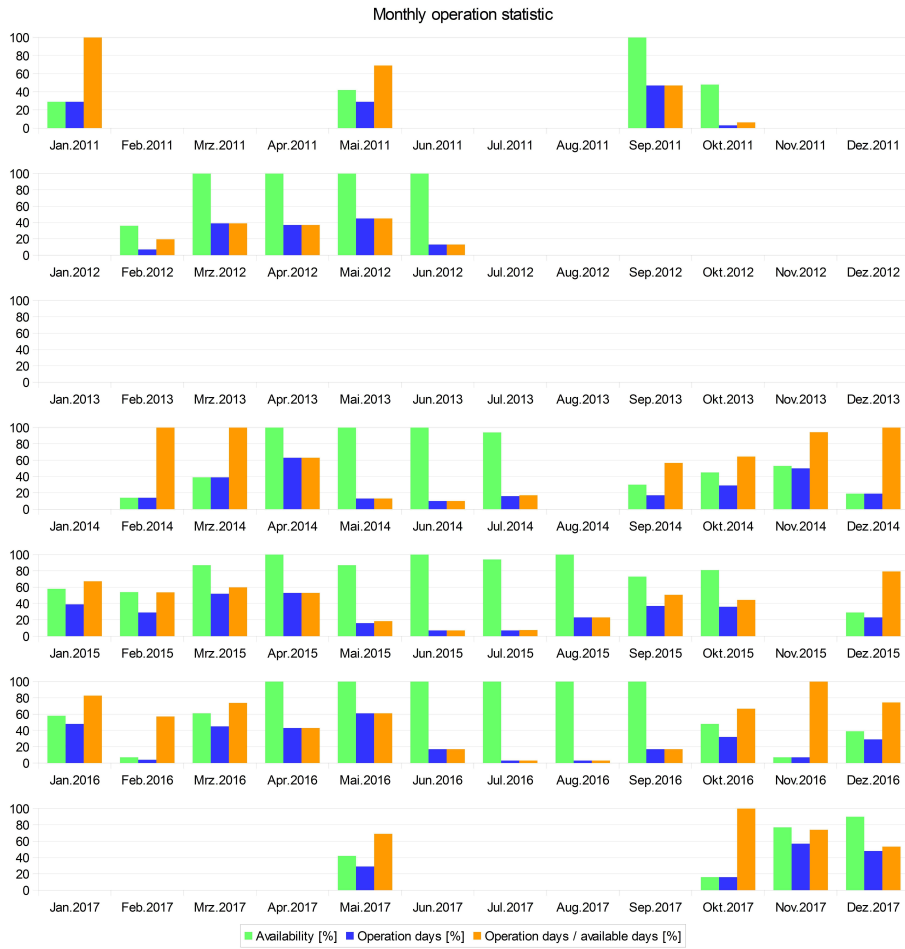


Figure 4.2 Monthly operation statistic

2.2. PRODUCTION RESULTS

The presented values are obtained from grid readings on utility side and agree with the invoiced values.

The annual values are strongly influenced by machine downtime and therefore do not represent the average power of a fully available device. Further, as it will be shown in Chapter 4. 3. , the real device always showed an essential turbine underperformance. This appeared to be likely correctable and therefore the here presented values do not represent the theoretically designed device. These values exclusively represent the performance of the real device with its turbine problem.

Average power production

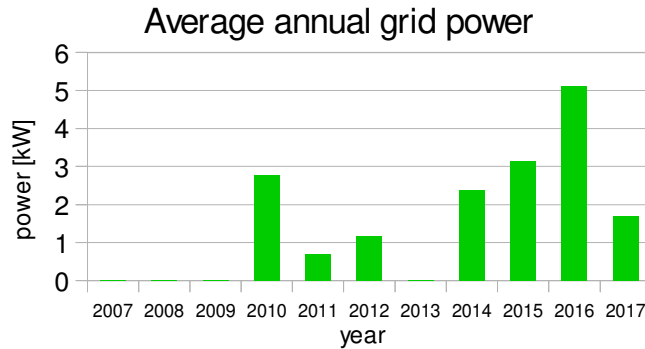


Figure 4.3 Annual average power

Figure 4.3 shows the annual average grid power from 2007 to 2016. The maximum average production could be reached in 2016 when 5,1 kW were fed to the grid in annual average. However, the initially predicted annual average grid power is approximately 96kW (Falcao, 2002).

Delivered energy

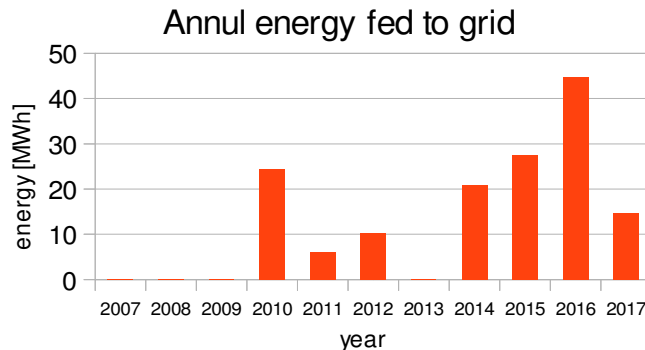


Figure 4.4 Energy fed to grid

Figure 4.4 shows the annually delivered energy to the island grid till 2017. The in 2016 reached maximum production was 44,8 MWh.

The cumulative energy production since September 2010 is approximately 149 MWh. In contrast to this value, the foreseen annual energy production was about 840 MWh.

Load factor and overall efficiency

The here presented values correspond to the results of 2016.

With 400 kW installed capacity and an average power production of 5,1 kW the corresponding load factor is 0,013. The overall efficiency is 2,4 %. From the theoretical predictions of approximately 96 kW average power a load factor of 0,24 and an overall efficiency of approximately 50 % was aimed.

Maximum short period average power

For a 15 min period the maximum reached average is 80 kW while 48 kW for the period of 24 h could be reached. Both values were achieved in Mai 2016.

2.3. FAILURES IN CONTINUOUS OPERATION

As prior mentioned the continuous operation was interrupted frequently by technical defects. The documentation of the problems during the operation time was done with the focus of problem elimination. Hence large problems were analyzed documented and solved while smaller issues were simply solved with only short remarks in the logbook. Here for the purpose of a root cause analysis, a failure log for the continuous operation period was compiled in retro perspectives similar as already done in Chapter 4. 1.3. . The objective is to point out the main weaknesses of the system such as the presentation of occurred and solved problems in order to prevent the repetition.

Because all failures could be solved with small means the essential influence of the defects was the loss of power production caused by machine down time. Therefore the failures are ranked by length of the resulting machine downtime.

Failures, which resulted in downtime smaller than 24h, were not ranked. Downtime between 24h and 72h were ranked as short downtime, between 72h and 7 days as medium, between 7 days and 3 weeks as large and longer than 3 weeks as very large downtime. Only two events with 18 and 32,5 weeks of down time were ranked as extreme events.

Here only a short example of the complete failure log is shown in Table 4.7. The complete failure log such as further details to several of the compiled failures can be found in Appendix 1.

Log of failures in continuous operation										
Sub Assembly	Component	time	Failure Effect	Final Solution	Solution type	Detection method	Root Cause	Failure Mechanism	Failure Mode	Failure Symptom
Control unit	Main PLC	2010	overheating of the PLC	No repair of the air condition/ installation of a second PLC fan / improving the heat isolation of the control room and painting the roof white	design change / continuing with degraded system	observation after occurrence	component failure	Air condition damaged causing high temperatures inside the control room in summer around noon	air condition of control unit damaged	Heating of the control unit in summer around noon peeping warning signal
Instrumentation	Oil level sensor	2010	Faulty machine shut down	sensor removed	continuing with degraded system	observation after occurrence	corrosion /degrading	cable damage directly at sensor entrance / cable degraded	sensor malfunction	faulty alarms for missing oil
Pressure bypass valve	hydraulic hosts	2010	no function of the valve / pollution	Substitution / protecting the hydraulic hosts externally and fixing them better	Substitution / design improvement	observation after occurrence	Standard design mistake	host moving on concrete due to the air flow through the valve / friction damaged the host mechanically	host damaged	oil leaking and blow n out of the device with the valve airflow
Turbine	Downstream guide vanes	December 2010	long down time (21 days)	substitution of the guide vanes by a simple tube section	continuing with degraded system	maintenance	Prototype design mistake	manufacture notches caused cracks in almost all blades	cracked guide vanes	increasing cracks
Control unit	Containers	End 2010 beginning 2011	humidity entering the control unit	recovering of the containers and construction of a wooden house around the unit	Repair / design improvement	maintenance	corrosion	walls and roofs corroded through	containers not prove against rain	rain entering into the control unit
Instrumentation	Pilot	January 2011	No dynamic pressure measures on downstream side	new designed Pito installed	new design	observation after occurrence	changed loads	after downstream guide vane removal the turbulent air reached the downstream Pitot	sensor damaged	visible sensor damage / wrong pressure transmission
Instrumentation	Duct temp sensor		No duct temp measures	sensor removed	continuing with degraded system	observation after occurrence		after downstream guide vane removal the turbulent air reached the downstream installed duct temp sensor	sensor damaged	visible sensor damage / no temp signal
Turbine	Downstream guide vanes	January 2011	Medium downtime	repairing and reinforcing the tube section	repair and reinforcement	maintenance	unexpected loads	vibrations caused cracks in the tube section	cracked tube section	increasing cracks
Turbine	Downstream guide vanes	since January 2011	required repair from time to time in maintenance	Regular repair during maintenance	maintenance	maintenance	fabrication mistake	vibrations caused cracks with roots in welding lines which were executed with too much heat	cracks in the tube section	small cracks
Power electronics	Generator	January 2011	extreme down time (32.5 weeks)	disassembling and removing of the generator / substituting the damaged components / Full Maintenance / water protection on turbine outlet installed	Repair / maintenance / improved design	analysis after occurrence	Prototype design failure / humidity / component degradation / wear	combination of carbon dust from fast worn out rotor brushes with humidity caused sticky conductive bridges on the poor electrically isolated spinning rectifier	short cut on rectifier diode (inside the generator)	Immediate failure of start up attempts with damaged fuses
Pneumatic system	Compressor	2011	Short down time / repair required	substitution of compressor motor	repair	observation after occurrence	component failure	overheating	no pneumatic pressure	valves does do not open / compressor pumps continuously

Table 4.7 Section of the failure log for continuous operation

Root cause analysis

The failure log was evaluated to detect the long and very long down time events and the belonging failure roots. As can be seen in the complete failure log in the Appendix 1 the root cause is often a design mistake. However, it can also be seen that the majority of the design mistakes in the electronics and especially the power electronics were causing the majority of the very long and long down time events. The power electronic equipment was a prototype design at the time when the device was developed in the 1990th. Today reliable standard equipment exists, which could easily be implemented to the device. Therefore these failures were assessed as annoying but not critical because they will not occur in future devices. To point out how much problems and down time can be avoided with proper equipment these failures are especially ranked as power electronic or control electronic malfunctions and not as simple design mistakes.

Though the continuous operation continued in 2017 the results of the failure log only concern the time before 2017 because in this year the financial conditions were too low to create meaningful results.

Results of the root cause analysis

Table 4.8 shows the failure roots for all longer down times in this period.

Downtime causing failure events between between 2010 and 2016		
	total	%
Extreme down time events	2	
power electronic malfunctions	2	100
Very long down time events total	4	
power electronic malfunctions	2	50
control electric malfunction	1	25
insufficiently attended small engineering problem	1	25
degraded large components	0	0
human operation mistake	0	0
normal wear	0	0
failed mechanical prototype design	0	0
long down time events total	11	
power electronic malfunctions	4	36
control electric malfunction	0	0
insufficiently attended small engineering problem	2	18
degraded large components	2	18
human operation mistake	1	9
normal wear	1	9
failed mechanical prototype design	1	9

Table 4.8 Root cause analysis 09.2010-12.2016

Already here it is visible that most of the longer down times are caused by the power electronics and only few events were caused by other issues.

However to obtain the full extend of the problem the three different down time event types are transferred into only one type. Here the long events are chosen. The approximated average duration of all long events is 15 days, while it is 37 days for very long and 261 days for extreme events. In Table 4.9 the very long and the extreme events are transformed into long events by the corresponding multiplication factor.

	total	%
Long down time events (with transformed very long and extreme events)	39,6	
power electronic malfunctions	32,6	82
control electric malfunction	2,5	6
insufficiently attended small engineering problem	4,5	11
degraded large components	2	5
human operation mistake	1	3
normal wear	1	3
failed mechanical prototype design	1	3

Table 4.9 Root cause analysis (all events transformed into long down time events)

CHAPTER 4. DATA ANALYSIS AND RESULTS

Here it is visible that about 82 % of the entire technical down time in this period was caused exclusively by malfunctions in the power electronics. The roots for these malfunctions are design mistakes. Together with problems in the control electronics, which are also caused by design mistakes, these mistakes caused almost 90 % of the technical down time.

To obtain the learning curve, results are presented for the year 2016 and 2017. In this period no very long or extreme technical down time events occurred mainly because the repair and protection procedures for the power electronics were understood. 2016 is a representative year while 2017 had long political down time periods and had therefore only reached about 25 % of the power production of 2016. However in Table 4.10 it can be seen that the power electronic problems caused only 33 % of the down time in 2016. In 2017 no technical down time due to the power electronics occurred as can be obtained in Table 4.11.

Downtime causing failure events in 2016		
	total	%
long down time events total	6	
power electronic malfunctions	2	33
control electric malfunction	0	0
insufficiently attended small engineering problem	1	17
degraded large components	1	
human operation mistake	1	17
normal wear	1	17
failed mechanical prototype design	0	0

Table 4.10 Root cause analysis 2016

Downtime causing failure events in 2017		
	total	%
long down time events total	2	
power electronic malfunctions	0	0
control electric malfunction	0	0
insufficiently attended small engineering problem	0	0
degraded large components	2	
human operation mistake	0	0
normal wear	0	0
failed mechanical prototype design	0	0

Table 4.11 Root cause analysis 2017

2.4. DISCUSSION OF THE CONTINUOUS OPERATION RESULTS

Power production

During the continuous operation period from September 2010 to January 2018 the Pico device remained clearly far below the initial power predictions. In the best achieved annual result it could deliver only about 5 % of the theoretical predictions. Though this is a poor result it should be seen in context with other WECs. As shown in Chapter 2. 1. the Mutriku OWC, which is according to their own web side (EVE, 2016) the WECs with the highest accumulated energy production, shows an overall efficiency of approximately 2,8 % with stated correct machine function while Pico showed 2,5 % even with about 16 weeks of technical downtime and the turbine underperformance. Further it should be seen that there is no reason to believe that the theoretic goals cannot be widely achieved after correcting the turbine underperformance problem (see Chapter 4. 3.).

Machine availability

About 82 % of the technical down time was caused by design faults of the power electronics. This caused especially extreme down times on the first occurrence because the system had to be analyzed to detect the detailed failures. The entire electrical equipment of the device is outdated and includes various faulty design issues but still since some changes were executed it is generally operational. Thus it was no priority issue anymore and a substitution was not possible due to available budget. Never the less the understanding of the failure processes and some smaller design changes helped to reduce the related down time essentially. Finally in 2017 these issues did not occur anymore. Though also the operation time was reduced significantly the achievement is expected to be likely caused by the latest design changes.

Several technical failures often cause machine shut downs or small down time events but the majority of these

CHAPTER 4. DATA ANALYSIS AND RESULTS

issues are related to outdated and worn out equipment and therefore do not require to be named here. The regular maintenance procedure usually prevents large operation failures because the majority of the failures are detected before problems occur.

Several technical down time events were caused or extended due to the remote location and no reasonable stock of spare components.

2.5. CONCLUSIONS FROM CONTINUOUS OPERATION

When regarding the power electronic issue as not relevant because today reliable equipment exists and when assuming a reasonable budget to execute the maintenance procedure and to substitute components with detected design problem there is no reason to believe that a machine availability of 90 % or higher can not be reached with the assembled knowledge.

In case it is possible to correct the turbine underperformance as proposed in Chapter 5. 3.1. Further development on the Pico plant there is no reason to expect significantly more technical damage because the loads on large parts of the device are rather reduce.

Especially the security systems have never failed and therefore the device operated without large unexpected accidents. The remote control systems failed several times because they depend on the local internet connection and cheap equipment. For an offshore application the remote system is not sufficient and requires more attention.

Overall the operation was fairly smooth especially when regarding the small available budget.

3. PERFORMANCE ANALYSIS

3.1. PURPOSE

The performance of the real Pico plant is far below the theoretical predictions. This is obviously visible in device operation and was prior already assessed in (Pecher *et al.*, 2011) and roughly in (Monk *et al.*, 2015). The reason for this performance deficit was not fully understood before this analysis. So far as for example done in (Monk *et al.*, 2015) the focus was on the hydrodynamic performance, which is negatively influenced by damage on the chamber structure and reduced water depth. Some information on these effects is given in Chapter 4. 3.2. .

Beside the above mentioned damage on the chamber structure, the real device shows various variations compared to the theoretic model, which appeared all likely to influence the performance. Especially because the underperformance was so essential, the author did not believe in the hydrodynamic losses as the one major reason.

Here to begin of the analysis not even a problem in the theory itself was excluded due to some performance observations. Details on it can also be found in Chapter 4. 3.2. .

To gain certainty about the power losses and in order to understand how these can be overcome the here presented performance analysis was executed.

3.2. METHODOLOGY

Type of methodology

The performance analysis is done by validating a model with real device data. The validated model is then used to observe the effect of real device variation from the original design and to compute future power predictions.

Abstract of the methodology

The performance analysis could not be executed straight forward by comparing the real device performance to model results of the same real data set or similar sea conditions. The simple reason is that no reliable real time wave measurements existed at the Pico plant at the time of the analysis. With the purpose of analyzing a visible underperformance, the available offshore forecast data introduced to large uncertainties.

Because no possible source for the performance deficit was excluded, mistakes in the underlying theory and the applied local wave climate were also considered possible. Additionally the possibility of still undiscovered variations between the real and the theoretical machine was taken into account.

To prove the correctness of the underlying theory it was required to develop a model that returns the machine performance when fed with real data input. The rawest available real data input that is suitable for that purpose is the pressure inside the air chamber. Therefore a time domain model that first computes the excitation flow from real chamber pressure time series and in a next step simulates the theoretic conversion from excitation flow to grid power was developed. By implementing only the already prior known differences between the theoretic and the real device it was impossible to achieve a satisfying match between the model and the real device performance. Only after implementing a prior unknown large turbine performance deficit into the model it was possible to achieve a reasonable match between the real and the modeled performance. This turbine performance deficit was detected during the process of model validation. The finally found reasonable match indicates no larger problems in the underlying wave to wire theory. This validated model is successively named the “validated model”.

In a next step all physical differences between the real and the designed machine were removed from the “validated model” and the model was run with the same theoretic annual wave input as was done for the initial power predictions. The approach to model the theoretic wave input can be found in (Falcao, 2002). The theoretic waves are modeled based on the linear wave theory and the local wave climate. In the following the so modeled input is named the “theoretically computed wave input”.

The results were used to verify the correctness of the initial annual power predictions based on the local wave climate. The initial annual production predictions could be reproduced reasonable and therefore no evidence for problems in this part could be detected.

In order to understand if the model results are able to explain the magnitude of the real device underperformance, annual production results of the real device were compared to results of the validated model with “theoretically computed wave input”. The magnitude of the losses could be confirmed. Therefore no evidence for a mistake in the local wave climate was expected.

However the prior as large assumed hydrodynamic losses could not be modeled directly by this approach. These losses were assumed to contribute alone or among others to the losses, which could not be explained by the model. The comparison was again done based on annual average values. The losses due to the defects on the chamber structure were found to be small compared the losses of the already detected turbine performance deficit.

To gain more confidence in the results a second analysis was executed. Now the short term performance of the real device in different sea conditions was compared to the predictions of the “validated model” with “theoretically computed wave input” of corresponding sea conditions. Here uncertainties due to the missing local wave measurements are introduced during the process of local sea state classification. This classification is done based on chamber air pressure, chamber surface elevation and turbine rotational speed.

In this second analysis the prior for the annual average values found magnitude of the again not directly modeled hydrodynamic losses could be confirmed. Therefore the results are expected to contain a sufficient level of confidence.

Evidence for possible sources of performance losses

- **Reasons to assume elevated hydrodynamic losses**

Pressure asymmetry (skewness) can be obtained with increasing influence at low tide. The pressure asymmetry is at least partly caused by intermittently emerged holes in the submarine chamber walls, which create non linear air passage to the atmosphere. Further influence is assumed to be caused by wave shoaling due to a reduced water depth from bolder movement on the sea floor and possible other hydrodynamic inaccuracies. Figure 4.5 below is extracted from (Monk, Winands and Lopes, 2018). Here detailed information about the pressure asymmetry can be found.

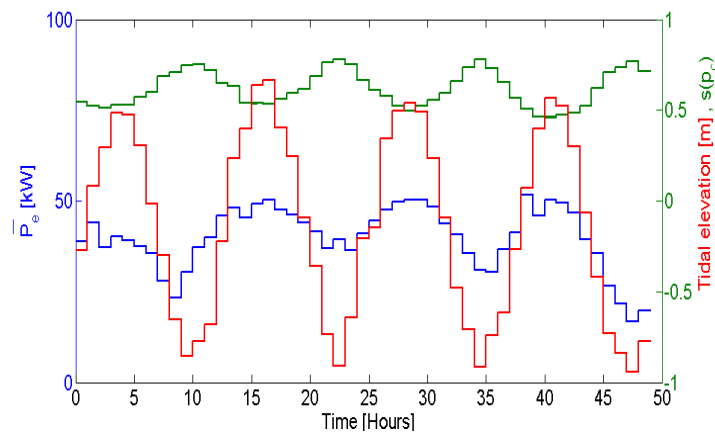


Figure 4.5 Pressure skewness
Tide (red), pressure skewness (green), power (blue)

In Figure 4.5 it can be obtained that with decreasing tide the pressure asymmetry (skewness) increases and the power production decreases.

Further indication for large losses in the hydrodynamic conversion or problems with the local wave climate were introduced by a prior in (Monk *et al*, 2015) introduced time domain model. This model also returned the conversion from chamber pressure to generated power for the Pico plant and accidentally showed a reasonable fit with the real device performance due to the at this time still undiscovered turbine performance deficit. However at this time it appeared to confirm the correct conversion in this part of the conversion chain. The discovery of the turbine performance deficit is explained in Chapter 4. 3.3. .

- **Reasons to assume a possible theoretic problem**

When implementing the in (Falcao, 2002) as optimal suggested control strategy to the real machine, it remains almost constantly in aerodynamic stall. Therefore the machine cannot be operated with this strategy. In operation various empirically developed control strategies were tested. The best performing strategy is used in most of the operation periods. Here it is referred as the “best practice” control strategy and and some additional details can be found in Chapter 4. 3.4. .

- **Reasons to assume an influence by a wrong use of the turbine**

The machine is operated with a significantly reduced rotational speed limit compared to the theoretical assumptions due to inaccurate assumptions and design specifications. Further details can be found in Chapter 4. 3.4. .

3.3. EXECUTION AND INTERMEDIATE RESULTS

Step 1

Development of a suitable time domain model

To be able to prove the underlying theory with real time performance data it was initially required to develop a suitable time domain model. The development was required because the in (Falcao, 2002) introduced initial design model is a frequency domain model, which does not allow real time input.

The here used model code is based on the wave to wire model, which was presented in Chapter 2. 3. and the hydrodynamic coefficients of the Pico plant, which were obtained in tank tests and can be found in (Brito-Melo et al, 2001).

The main code of the developed model starts the calculations with an excitation flow time series $q_i(t)$ as model input and follows strictly the wave to wire model.

The required excitation flow time series can either be computed theoretically by the use of the linear wave theory and a defined outside sea state or from real measured chamber pressure and rotational speed time series.

The possibility to calculate the excitation flow from device measurements allows to validate the model results directly with real device performance data.

The possibility to use theoretically computed excitation flow as input for the before validated model allows to compare the real device with all its problems to the theoretic expectations. Further it enables the opportunity to quantify the annual losses caused by different effects and to estimate possible improvements.

The methodology to compute the excitation flow from real pressure and rotational speed time series is similar to the approach that was done in (Monk et al, 2015). The model assumes no unforeseen bypass air flow $q_v(t)$ and therefore the air flow through the turbine $q_t(t)$ follows from equation (5) to be equal to the sum of the total air flow $q(t)$ and the term for compressibility of air. By equation (3) the air flow through the turbine follows from the pressure time series and the turbine rotational speed. The radiation flow $q_r(t)$ can be obtained by equation (7) from the pressure time series. With the knowledge of the total flow $q(t)$ and the radiation flow $q_r(t)$ the excitation flow $q_i(t)$ follows from equation (4).

The basic schematic of the code can be found in the diagram shown in Figure 2.5.

Step 2

Validating the model / Proving the theory and detecting all involved problems in the conversion chain from excitation flow to grid power

The initially developed model code was developed on the exact theoretic design. In order to adapt it to the real device, it was required to implement all variations between the real device and the initial modeled device into the code.

Initially it was impossible to find a reasonable match between the model results and the real device performance.

In contrary the above mentioned prior in (Monk et al, 2015) introduced code, which shared the same theory, showed a reasonable fit. Detailed study of both codes revealed a mistake in the code of Monk, which

accidentally divided the turbine performance by two. Once the mistake was removed both codes showed similar results but were far from the real device performance. Consequently the real device performance matched with the model performance when reducing the modeled turbine power by the factor two. This can be obtained in Figure 4.6, which shows a comparison of a 2 hours plot between the real device (blue), the “validated model” (green) and the validated model with designed turbine performance (red). The generated power and the rotational speed is displayed.

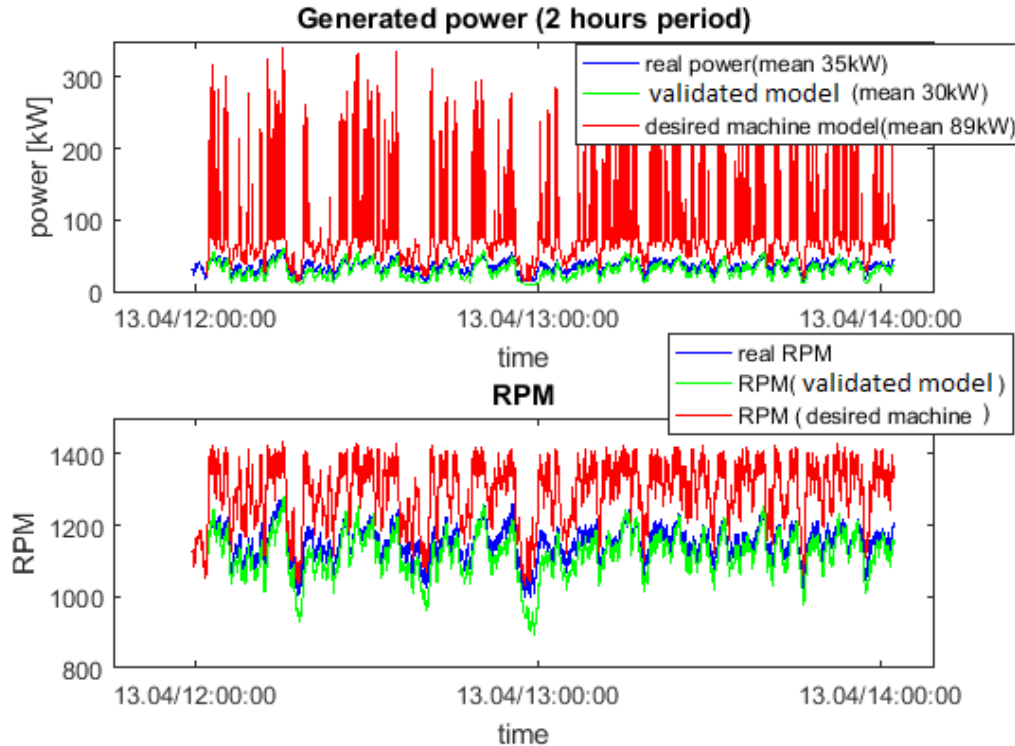


Figure 4.6 Generated power and RPM comparison (real device (blue), “validated model” (green) model with designed turbine (desired) (red))

In the following both codes were scanned systematically for further mistakes, which could not be detected. Additionally essential effort was undertaken to vary all possible parameters into the extreme cases in order to understand, which parameter could cause such a dramatic loss of power. Finally the only effect that could reproduce the real device performance was the turbine performance, that was reduced about the factor 2.

Because this was an essential discovery and hard to believe, the characteristic turbine curve of the real turbine was captured with the available equipment. This was already done in the past but misinterpretation of the measured results excluded the turbine as a potential problem source. The measurement of the characteristic turbine curve is not trivial because no torque meter is available and the quality of the rotational speed measures is not optimal for this purpose. However it was possible to measure the curve and confirm the extremely reduced performance compared to the theoretic turbine. It was further attempted to detect the reason for the reduced turbine performance in a first turbine performance analysis, which can be found in Appendix 3. The final reason for it could not be detected but degradation and missing rotor guide vane could be widely excluded as possible reasons. The drawn conclusion is that the rotor design causes the poor performance but the reasons for it remains unclear. Figure 4.7 shows the measured and already significantly filtered real turbine curve compared to the designed curve.

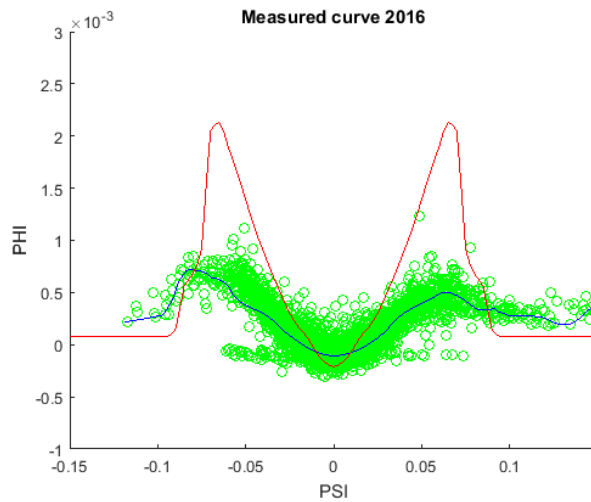


Figure 4.7 Measured turbine curve (green), best fit curve (blue), the designed curve (red)

From that point in time the reduced turbine performance was regarded as real and introduced into the model. The finally for the “validated model” used characteristic turbine curve corresponds to the measured curve, which was multiplied by factor of 1,5 to compensate filtering effects. The factor 1,5 was found empirically and appears reasonable. The model fit can be obtained in Figure 4.8 and in Figure 4.9 it can be seen that this turbine curve is in the range of the initial curve divided by two.

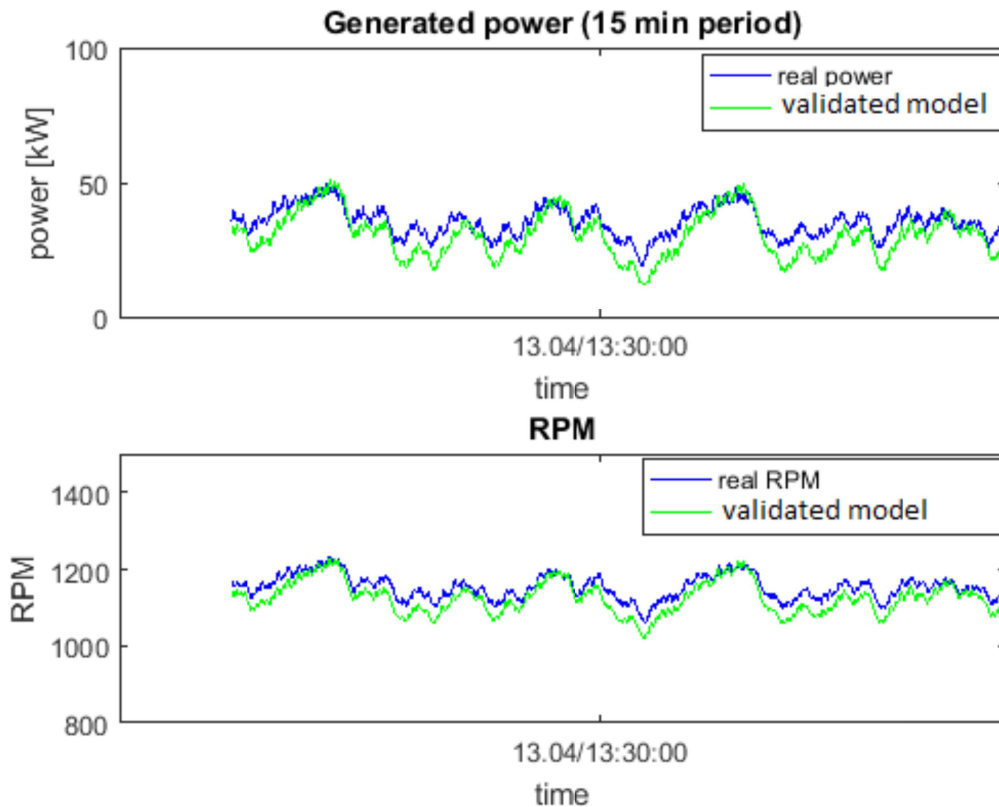


Figure 4.8 Model match of the “validated model” with real plant data

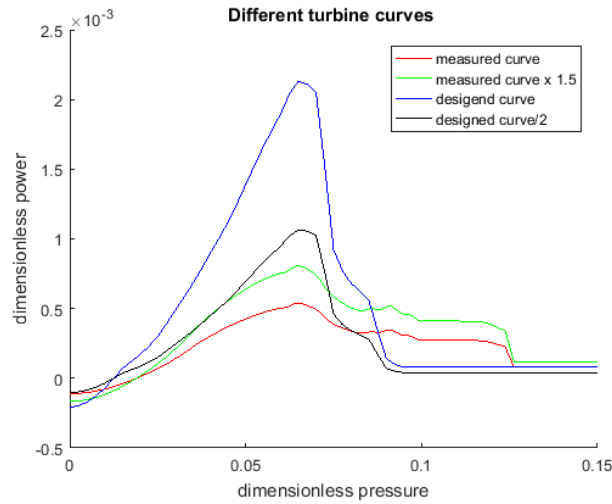


Figure 4.9 Different characteristic turbine curves

Intermediate results

- Concluded from the reasonable model fit, the theoretic conversion from excitation flow to generated power could be confirmed with the real device performance. *The average error of the “validated model” for average generated power over several operation periods is in the range of 15 to 20 percent of the real produced average power. This corresponds to an absolute average error in the range of 4kW.*
- A before undiscovered problem in the turbine design appears to reduce the turbine power by the factor two.

Step 3

Verifying the correctness of the annual power predictions based on the local wave climate.

For this purpose the “validated model” was adapted to represent the machine in design conditions. Therefore the turbine performance was corrected and all other implemented differences between the real and the designed machine were removed. To obtain the annual average the so created “validated design model” was fed with the “theoretically computed wave input” for annual power.

It was possible to reproduce a similar annual average power result with the “validated design model” as was predicted. The in (Falcao, 2002) predicted annual average generated power is 100 kW. Here 104 kW could be modeled with some assumptions regarding the procedure of breaking the turbine close to rated speed in order to avoid over speed situations. It was found that the results are fairly sensitive to this breaking procedure. In the frequency domain approach used in (Falcao, 2002), moments with speed above the max speed of 1500 RPM are simply regarded with max speed. This is impossible in reality and in a time domain approach. The here selected method can be obtained in Figure 4.10. The generated power is increased about approximately 500 kW in the operational speed range from 1498 to 1500 RPM. The required installed capacity to provide this breaking torque is about 600 kW but only 400 kW are installed. This strategy cannot fulfill the grid constrains of allowed power fluctuations and additionally cannot avoid over speed completely. Thus the “validated design model” is only a theoretical approach, which cannot be realized.

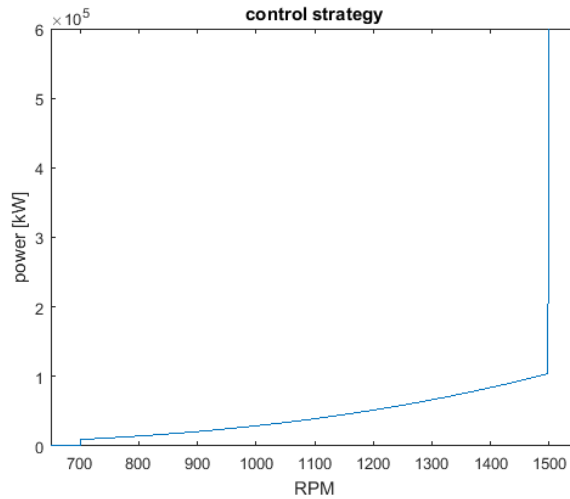


Figure 4.10 Theoretical RPM limitation approach

In order to estimate the quality of the applied breaking procedure approach, the same approach was applied to a second also in (Falcao, 2002) presented model. This second model includes a theoretic approach of an fast acting relive valve, which is not further subject of this study. However the “validated design model” with the selected breaking procedure and the proposed approach for the fast acting relive valve could return similar annual average results as the frequency domain model in (Falcao, 2002). This result caused confidence in the breaking procedure approach.

Intermediate results

It was possible to reproduce the initial power predictions done in (Falcao, 2002) with the “validated design model”. Therefore no problem in the initial power predictions could be found.

Step 4

Observing the magnitude of the annual production difference between real device and “validated model” results in order to estimate the possible correctness of the results and the possible correctness of the local wave climate.

For this purpose the “validated model” was fed with the “theoretically computed annual wave input”. The computed generated annual average power was 33 kW, which corresponds to approximately 23 kW power delivered to grid. The electrical losses are further explained in Chapter 4. 3.4. .

The local wave climate is defined only for the full calendar year therefore for the comparison it is required to evaluate the annual real device production for at least one full calendar year. As could be obtained in Chapter 4. 2.1. though in continuous operation for several years the Pico plant could never operate for one calendar year without significant machine down time. Therefore the machine down time periods have to be theoretically removed by superposition. Obviously this introduces additional uncertainties to the anyway included annual fluctuations. Never the less the superposition of continuous operation data in a representative longer time period is expected to be sufficient to quantify the magnitude of the annual average power due to the essential losses.

Estimation of the real achieved annual average power with removed machine down time

The estimation is based on energy fed to grid in the period from 01.01.2016 till 30.06.2016.

Assumptions

- The local wave climate of the first half year period and the second are approximately similar. Therefore the observed half year period is representative for the annual local wave climate.
- January, February and March belong to the most energetic months of the calendar year.
- The different machine tests do not influence the overall power production significantly.

Calculation

In the 91 days of the period between 01.01.2016 and 01.04.2016 the device was 39 days available and

52 down. In this period 14 MWh could be fed to grid, which corresponds to a average production of 360 kWh per available day. The superposition of this value for the 52 days of machine down time returns 18,7 MWh. This superposed value is added to the 31,9 MWh, which were fed to grid in the entire observed period from 01.01.2016 till 30.06.2016. The resulting 50,6 MWh are the assumed power production in the first half of 2016. Following the estimated annual energy production is 101,2 MWh which corresponds to an annual average power of approximately 11,5 kW.

Plausibility observation

The quality of the result appears reasonable though especially the assumption of the similar wave climate in the first and the second halve year period is rather weak and might lead to a slight overestimation. On the other hand the majority of the downtime occurred during February and the beginning of March, which is expected to be the best operation period due to less extreme conditions compared to January. Further from operation experience the 360 kWh daily average production in winter periods appear reasonable because in energetic sea conditions the daily energy production of an operation day can reach up to about 1000 kWh. For the entire year 2016 the real reached average grid power is 5,1 kW and here the second part of the year was again strongly limited due to the abandonment plans of the device and another 60 days of technical machine down in the energetic month of October, November and December.

Intermediate results

No evidence could be found for any problems in the local wave climate. The found model results are only about 11,5 kW higher than the estimated real device results, which still do not include the certainly existing losses caused by the hydrodynamic defects.

Step 5

Estimation of the losses caused by the hydrodynamic defects

As found in step 4 the discrepancy in annual average power between “validated model “ and estimated real device is only 11,5 kW. This corresponds to approximately 12 % of the predicted average grid power. The predicted average grid power is here assumed to be 96 kW and corresponds to the annual average power obtained by the “validated design model” with included 8 kW direct electrical losses.

Compared to the other losses of 73 kW these losses do not appear to be essential.

Step 6

Comparison of the real device short term performance to results of the validated model, which is fed with theoretic waves of similar sea conditions.

The purpose of this step is to quantify the losses caused by the hydrodynamic defects of the real machine in different sea conditions to observe the quality of the results of step 5.

For this purpose a set of 123 two hour real device operation records of a continuous operation period between 17.03. 2016 and 15.04.2016 were analyzed. In all operation periods the same best practice control strategy was applied and the turbine bypass valve was fully closed.

The real achieved average power includes all losses of the real device. This real average power in each operation period is compared to results of the validated model, which is fed with “theoretically computed wave input” of similar wave conditions, which do not include the by defects caused additional losses of the conversion from outside surface elevation to excitation flow .

Due to the prior mentioned absence of local wave measurements the local wave conditions outside the device had to be obtained from device measurements. This process is assumed to introduce uncertainties but it is the best that could be done with the available equipment and data.

Methodology how to obtain the outside local wave conditions of each operation period

The definition of the wave conditions (surface elevation) of a sea state is commonly done by a spectral analysis of the surface elevation $\zeta(t)$. The resulting significant wave height H_s and the energy period T_e are the parameters, which define a sea state sufficiently.

Because no time series of the outside surface elevation is available it would be required to compute it from

available measures inside the device, but this is in general not trivial and here impossible due to the unknown hydrodynamic conversion caused by the structural defects.

Therefore here the following alternative approach was chosen.

For a before defined set of predefined sea states the hydrodynamic conversion from outside surface elevation $\zeta(t)$ to surface elevation inside the air chamber $\zeta_{internal}(t)$ were computed by the use of the “validated model”. This code assumes the hydrodynamic conversion to be as designed.

Consequently with assumed designed hydrodynamic performance of the device, for each outside sea state the inside sea state is known and can be defined again by H_s and T_e .

It was chosen to use these spectral parameters H_s and T_e of the internal surface elevation as the stage of comparison between the real operation data to the theoretically predefined set of outside sea states. Based on these values each of the 123 operation periods is classified to belong to one of the predefined sea states.

The comparison was selected to be at the stage of internal surface elevation because this values can easily be obtained and because it is a real value that can be used for plausibility observations.

Note: The stage of comparison could have been selected to be the spectral parameters H_s and T_e of the excitation flow q_i as well. Different than for the internal surface elevation for the excitation flow it was possible to detect a theoretic approach, which predicts the outside wave conditions exactly. This approach computes the excitation flow from the measured pressure time series and the measured internal surface

elevation time series. q_r follows from equation (7) $q_r(t) = \int_{-30s}^t hr(t-\tau) \frac{dp}{dt}(\tau) d\tau$ and q_i follows

from equation (4) $q = q_i + q_r$. Because both values are real measures the introduced mistake is assumed low. However this approach could not be used because the quality of the measured internal surface elevation time series is fairly poor and is difficult to be used in the time domain. Therefore again a large uncertainty would have been introduced, which would have been difficult to evaluate because the excitation flow is only a theoretic value.

Methodology to obtain the spectral data H_s , T_e and m-1 moment of the surface elevation inside the chamber for the real operation data.

The internal surface elevation can be obtained in two methods.

- The real measured time series can be used directly.
- It can be computed from only the pressure time series. From equation (3) follows the turbine flow q_t and from equation (5) $q_t(t) + q_v(t) = q(t) - \frac{V_0 dp(t)}{\gamma P_a dt}$ with the assumption of no bypass

air flow q_v follows the total flow q which is directly proportional to the internal surface elevation $\zeta_{internal}(t)$.

As will be explained below, both methods tend to predict the internal surface elevation different to what would be predicted if the hydrodynamic conversion of the device would be as designed.

In order to not underestimate the losses coming from the hydrodynamic defects it was selected to use the measured surface elevation values directly. As will be explained below this method tends to predict the outside sea conditions to large, which causes rather too high model results and consequently a larger difference between real device and model results. The second method would tend to underestimate the losses coming from hydrodynamic defects. This effect can be seen in the Figure 4.12 and Figure 4.13 were the power spectrum for two different real operation periods is plotted for both methods.

Basic Influence of the hydrodynamic defects

In moments when the holes in the submarine chamber walls emerge in large wave troughs or medium wave troughs at low tide, a not foreseen air flow leaves the air chamber. This air flow is similar to the air flow through the pressure relive valve q_v and is assumed as such for this theoretic model. Obviously these effects are non linear but because only the general tendency is observed for this observation they are assumed linear. In Figure 4.11 it is attempted to display this effect. The black arrows show the normal occurrences without hydrodynamic

defects. The gray arrows show the altered occurrences due to the bypass air flow through the holes in the chamber walls. The difference in length of the arrows shows the tendency of the alteration of each value.

Due to the bypass airflow q_v , the airflow through the turbine q_t is reduced, which causes a reduced pressure in the system. The reduced pressure in the system causes a reduced radiation flow q_r or in other words causes a smaller contracting force to the chamber surface movements. This causes larger surface elevations inside the air chamber as would be present without the hydrodynamic defects.

The tendency of this selected method, to predict too large outside sea states can be observed by the red arrows in Figure 4.11. In the figure the green arrow shows the stage of comparison and the yellow color shows the chosen input values for the comparison.

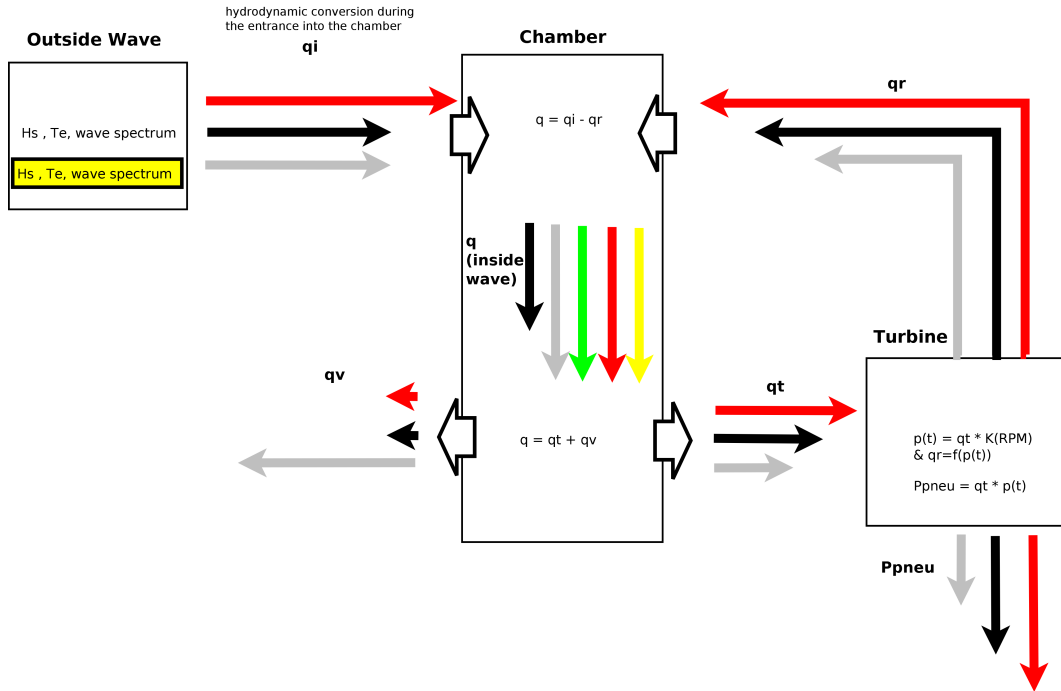


Figure 4.11 Influence of the hydrodynamic defects to the sea state classification. (Arrows: black:device performance with designed hydrodynamic performance; gray: performance with assumed hydrodynamic losses; green: stage of comparisons; yellow: input values; red: tendency to predict too large sea conditions)

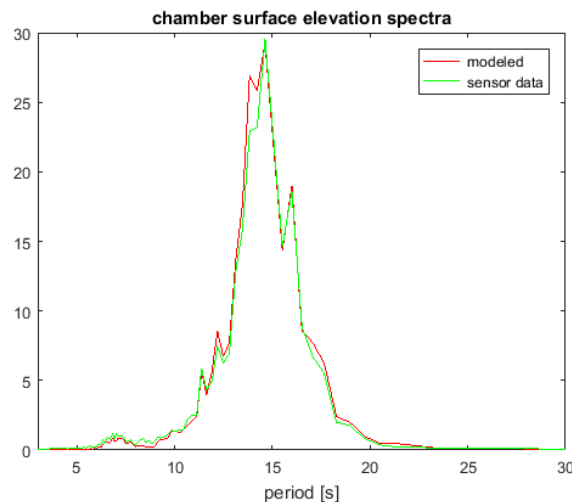


Figure 4.12 Chamber surface elevation spectra at high tide in average waves

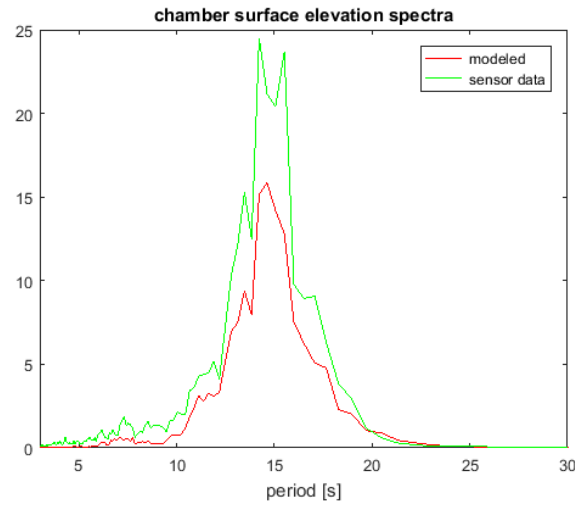


Figure 4.13 Chamber surface elevation spectra at low tide in average waves

Execution of the classification

Used data

A set of 123 operation periods with a duration of 2 hours per period are classified into a set of 44 predefined sea states. These 44 sea states correspond to the defined 44 sea states of the local wave climate, which are shown in Table 3.1.

Sequence

- For each of the 44 predefined sea states the spectral data H_s , T_e and m-1 moment of the internal surface elevation are computed by the use of the “validated model” and a power spectral analysis.
- For each of the 123 real operation periods the spectral data of the internal surface elevation H_s , T_e and m-1 moment are calculated from the real measured internal surface elevation and a power spectral analysis.
- By comparing the spectral data of the internal surface elevation, each of the 123 operation periods is classified into one of the 44 predefined sea states.
- If more than one operation period is classified into one of the 44 sea states, the power values are averaged.
- For each of the 44 sea states these average values are compared to the results of the validated model for this sea state.

Classification criteria

- Each operation period is classified into the predefined sea state, which shows the smallest difference in H_s and T_e of the internal surface elevation.
- Within the limit of 20 % variation in H_s , T_e and m-1 moment all operation periods could be merged into the sea states.

CHAPTER 4. DATA ANALYSIS AND RESULTS

- Because the overall performance is observed in this classification all available 123 records regardless of the tide are used.
- To cope with uncertainties in the match with single sea states the two best fitting states were considered. Therefore most data records appear twice in the classification.
- Sea states, for which only one real operation period could be found, are not considered.

Additional observation

In order to verify the increasing power losses with increase pressure asymmetry the classification was repeated for low and high tide records separated. The number of data points for this classification is very limited therefore only some trend observations are regarded.

Applied methods to create further reference data for plausibility verification of the found classification

It is assumed that the local (onshore) wave conditions are less energetic than offshore conditions. However it was chosen to execute a second classification with the assumption that the offshore wave predictions are valid for the location of the Pico plant. The result of this offshore classification can be compared to the results of the selected classification.

Intermediate results

- The found classification appears plausible because the found local wave conditions follow the general trend of the forecast offshore sea conditions but with significantly lower energy content. This can be obtained in Figure 4.15 where a chronological plot of the found local wave conditions is shown. The green points shows the two best fitting of the 44 predefined sea states when using the measured surface elevation inside the chamber as base for the classification. The blue points show the two best fitting of the 44 predefined sea states when the offshore forecast sea conditions are used as local wave condition. On the Y axis the 44 predefined sea states are arranged with increasing energy content.

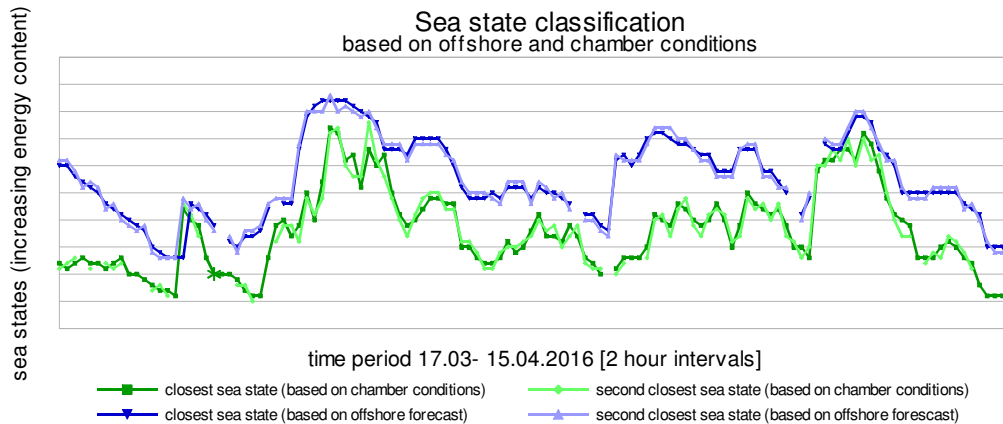


Figure 4.15 Chronological plot of the sea state classification

- Further evidence for the reasonable quality of the classification can be found when comparing the power production results of the “validated model” to the real production in the single sea states. When doing this for the applied classification the power results show a reasonable match. When doing it for the alternative classification based on offshore forecast data it can be obtained that the pattern is shifted as expected towards more energetic sea states. These observations can be found in Figure 4.16 and Figure 4.17.

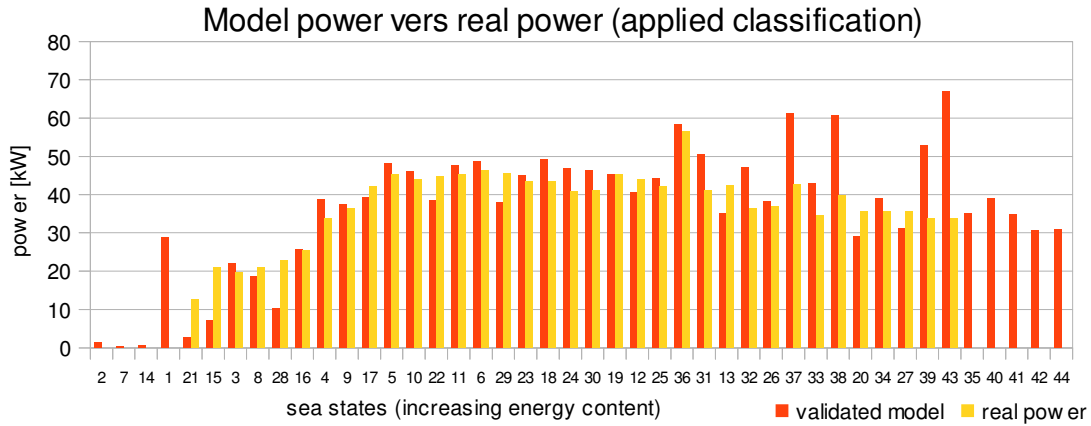


Figure 4.16 Power comparison in 44 sea states listed with increasing contained energy (applied classification)

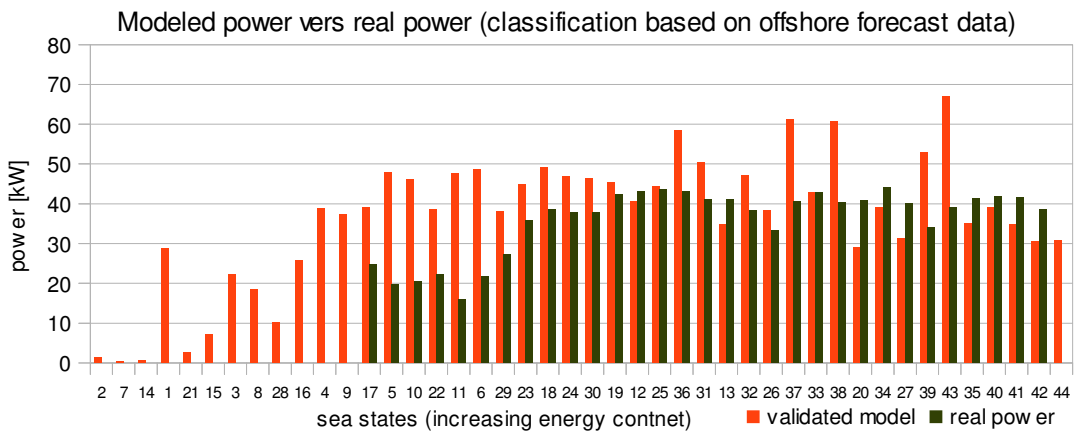


Figure 4.17 Power comparison in 44 sea states listed with increasing contained energy (offshore forecast data classification)

- The differences, which are assumed to be caused by the hydrodynamic defects, are fairly low. This can be obtained in Figure 4.16 and Figure 4.18. For the majority of the sea states it is in the range of 20 %, which corresponds to an absolute values in the range of 7 kW (whit 36 kW average power over all sea states).
- Only for very energetic sea states an increasing power difference of up to 50 % can be obtained. This corresponds to a maximal found difference of approximately 35 kW.

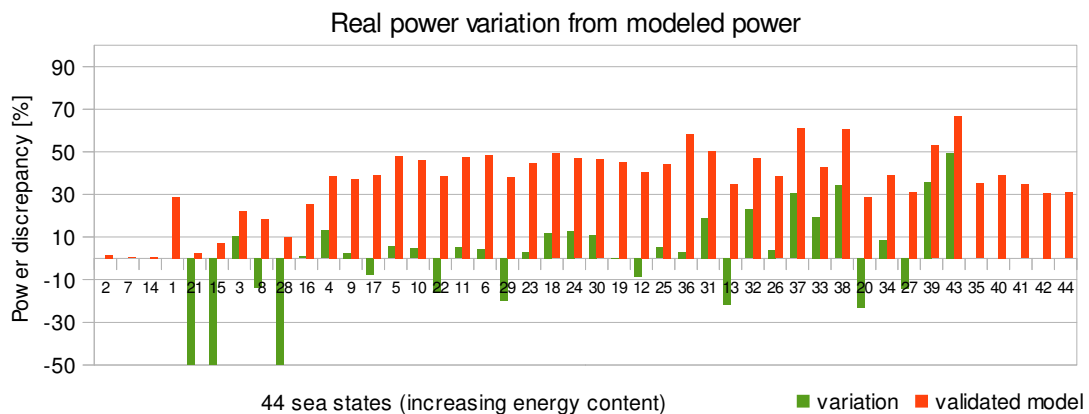


Figure 4.18 Power difference in 44 sea states listed with increasing energy content (applied classification) Sea states without real power value did not occur more than once in the observed period.

CHAPTER 4. DATA ANALYSIS AND RESULTS

- For low energetic sea states the match of the classification is poor.
- The expected increasing influence of the hydrodynamic defects with low tide and more energetic sea states could be confirmed as can be seen in Figure 4.20. Here the classification is done for low tide and high tide periods separated and the results are compared. It can be observed that for all more energetic sea state the real power in high tide is significantly larger than in low tide. Only for very small sea states it is in a similar range. The observation of absolute values here is assumed nonsense due to the high influence of classification mistakes caused by the small number of real data sets.

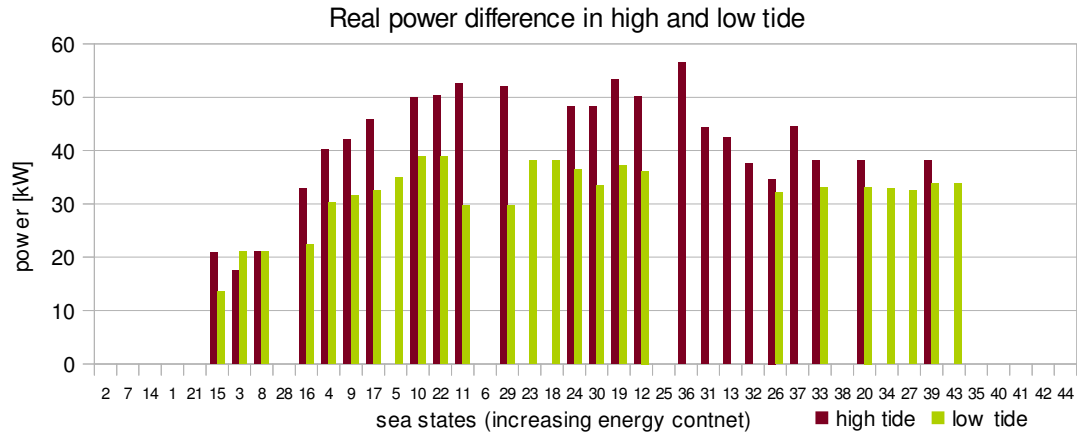


Figure 4.19 Power difference between low and high tide (applied classification)

Intermediate result interpretation

- No evidence could be found that the hydrodynamic defects causing losses which exceed the in step 5 found 11,5 kW in annual average.
- The second analysis confirms the results of the first analysis.

3.4. POWER LOSSES IN DETAIL

Total losses

The analysis could confirm the theoretical power predictions of approximately 100 kW generated power. The validated model that was used for the purpose of analyzing the different losses predicted 104 kW generated annual average power. Because this model is the base for the here executed analysis of the losses the 104 kW are used as starting point. The superposed annual average grid power of the real device is 11,5 kW while the “validated model”, which does not account for the hydrodynamic defects, returned 23 kW annual grid power average. Following, for the real device total losses in the range of 92,5 kW have to be explained.

Expected losses (Direct electrical losses)

The initial predictions were done for generated power and consequently do not include the electrical losses. These were found to be fairly high in operation, which is probably caused by the low generator efficiency in the low power range in which the device is used. In average over a large number of operation periods direct electrical losses in the range of 8 kW could be found.

Unexpected losses

Following 84,5 kW of unexpected losses have to be explained.

Analyzed effects

- Rotational speed limitation
- Different control strategy
- Indirect electrical losses
- Turbine performance deficit
- Hydrodynamic defects

Details about the effects and the method how to model them can be found in Contributing losses in detail in the bottom of this section.

Detected losses

Figure 4.20 gives an overview about the occurrences. The graphic displays the occurrences with the in reality used “best practice” control strategy. The size of each displayed value corresponds to the length of each colored beam. The detailed losses can be found in the table of Table 4.12.

- Approximately 73 kW of the total 84,5 kW power losses can be reproduced by the “validated model” where hydrodynamic defects are not taken into account. (with the “best practice” control strategy)
- The dominating losses are caused by the deficit in turbine performance. This effect alone makes up for approximately 64 kW of the 73 kW losses. (with the “best practice” control strategy)
- The not foreseen lower rotational speed limit causes losses in the range of 7 kW (with the Best practice control strategy)
- Further 2 kW are caused by the indirect electrical losses (with the “best practice” control strategy)
- Only remaining 11,5 kW cannot be explained by the validated model for the conversion chain from chamber pressure to grid power.
- The analysis of the device operation in defined sea states confirmed a influence of the hydrodynamic

CHAPTER 4. DATA ANALYSIS AND RESULTS

defects in this range. Therefore the hydrodynamic defects are alone or among others expected to make up for the losses in the magnitude of the unexplained 11,5 kW.

- The optimal control strategy shows marginal power increase (below 1 kW) when applied to the machine with the designed turbine performance.
- When the optimal control strategy is applied to the machine with the turbine performance deficit it even increases the losses for further 15 kW down to zero in annual average even without assumed hydrodynamic defects.

CHAPTER 4. DATA ANALYSIS AND RESULTS

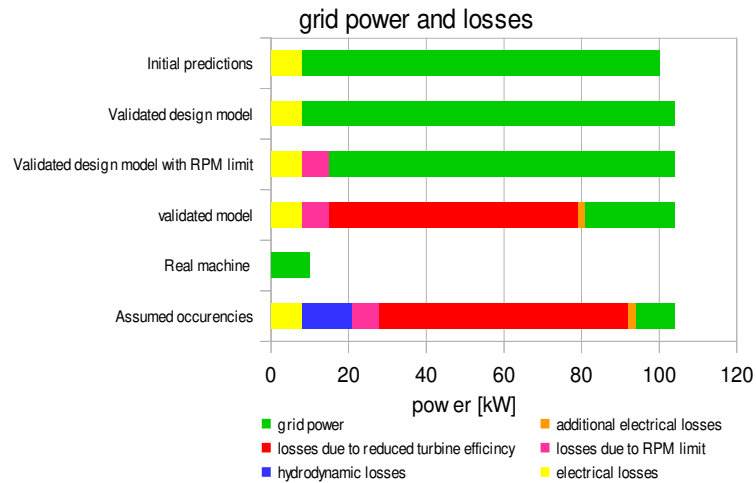


Figure 4.20 Modeled losses and remaining grid power

power losses						
different machine setups		Modeled losses	generated power		power to grid	
			control strategy		control strategy	
			optimal	real	optimal	real
Validated design model	Contributing power losses [kW]	rotational speed limitation				
		measured turbine curve				
		electrical losses direct			8	8
		electrical losses indirect			0	0
	power	annual average power [kW]	104	104	96	96
		Total losses [kW]	0	0	8	8
	power [percent of desigend conditions]	100	100	100	100	
Validated design model with RPM limit	implemeted effects	rotational speed limitation	7	7	7	7
		measured turbine curve				
		electrical losses direct			8	8
		electrical losses indirect			0	0
	power decreases	annual average power [kW]	97	97	89	89
		Total losses [kW]	7	7	15	15
	power [percent of desigend conditions]	93	93	93	93	
Validated model without hydrodynamic losses	implemeted effects	rotational speed limitation	7	7	7	7
		measured turbine curve	79	64	79	64
		electrical losses direct			8	8
		electrical losses indirect			2	2
	power decreases	annual average power [kW]	11	33	8	23
		Total losses [kW]	86	71	96	81
	power [percent of desigend conditions]	11	34	8	24	
Validated model with assumed hydrodynamic losses	implemeted effects	rotational speed limitation	7	7	7	7
		measured turbine curve	79	64	79	64
		electrical losses direct			8	8
		electrical losses indirect			2	2
	power decreases	hydrodynamic losses	13	13	13	13
		annual average power [kW]	5	20	-5	10
	Total losses [kW]	99	84	109	94	
	power [percent of desigend conditions]	5	19	-5	10	

Table 4.12 Detailed conversion chain analysis results

Contributing losses in detail

Rotational speed limitation

The real Pico converter has a strict rotational speed limitation exactly at rated speed of 1500 RPM due to a faulty design specification. Additionally the designed rated power of 400 kW is reduced to 200 kW by an additional faulty design in the power electronics. In the consequence the real machine has a significantly reduced breaking

torque compared to the designed machine. In order to still guaranty the respect of the rotational speed limit at 1500 RPM a significant rotational speed “breaking” margin is required to allow further excess energy storage in the flywheel. The resulting smoother breaking procedure also copes better with the grid constrains for power fluctuation. In operation a minimum margin of 100 RPM was successfully tested for short periods and a more conservative margin of 150 RPM is generally used. Accordingly the real rated speed in most operation periods was 1350 RPM. The real rated speed and the smoother breaking procedure are implemented to the “validated design model” by using the in Figure 4.21 displayed generator control strategy.

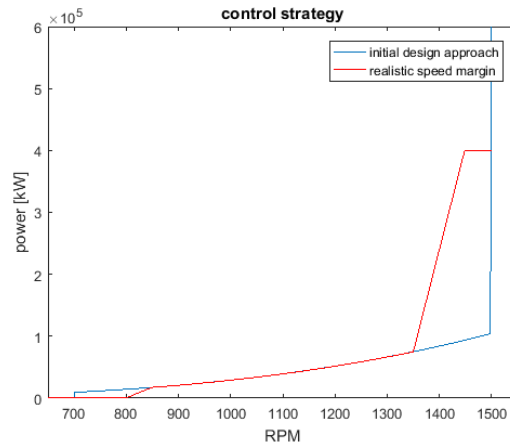


Figure 4.21 Rotational speed margin and breaking procedure [real (red); theoretical approach (blue)]

Real control strategy

In Figure 4.22 the red curve displays the theoretical in (Falcao, 2002) proposed optimal control strategy, which was used for the initial predictions. As stated before in Chapter 4. 3.2. the real device operation with it is hardly possible due to constant aerodynamic stall events.

The blue curve corresponds to the “best practice” real operation strategy. Both curves are directly applicable to the system because the rated speed is already reduced to 1350 RPM and the smooth breaking procedure is implemented. Whilst the curves match at about rated speed the optimal curve aims to extract significantly more power at lower speed, which the turbine is apparently not able to deliver. Therefore the power is drawn from the flywheel, which reduces the rotational speed. The reduced rotational speed in turn provokes further aerodynamic stall, which causes a further dramatic loss of turbine power from which the system is unable to recover. The avoidance of this determining feedback loop is done by the implementation of the “best practice” blue curve that can also be obtained in Figure 4.22 .The curve corresponds to the empirically in operation found and since than generally used control strategy, which enables relatively smooth plant operation. It is implemented to the “validated model” and the “validated design model”.

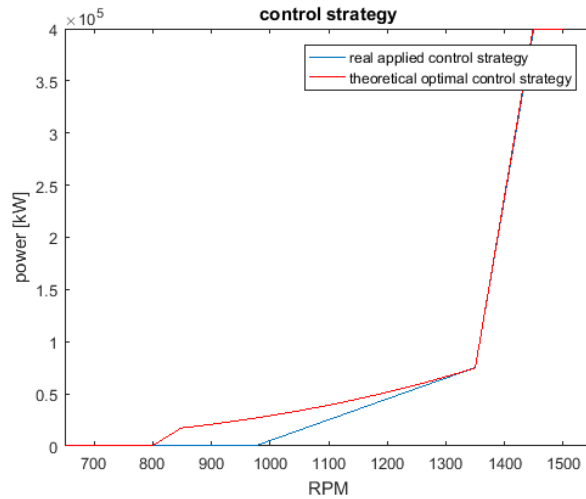


Figure 4.22 Control strategy [theoretically optimal (red); real “best practice” (blue)]

Turbine performance deficit

The turbine performance deficit is modeled once for the use with the proposed optimal control strategy and a second time with the in reality used “best practice” strategy. The reduced rated speed and the smoother breaking procedure are always assumed. Here the turbine curve that was found for the “validated model” is used and displayed green in Figure 4.23. The figure corresponds with Figure 4.7 and as explained there it is the real measured turbine curve that is multiplied by an empirically found factor of 1,5. The higher power values on the right side of the curve compared to the designed curve were found in the measurements. They are likely to be caused by the absence of the rotor guide vanes downstream of the rotor. In (Brito-Melo, Gato and Sarmento 2002) a similar effect is described. The rotor guide vanes do increase the peak height but also narrow the range with a higher turbine efficiency. However, as explained in Appendix 3 the missing guide vane does not appear to be the cause of the lower turbine peak.

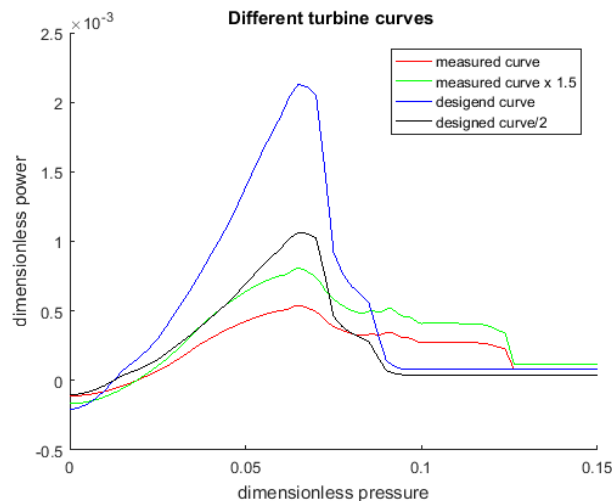


Figure 4.23 Characteristic turbine curve comparison

Electrical losses (direct and indirect)

Real machine operation in low energetic sea conditions often causes negative net power, because the losses and the background energy consumption is higher than the generated power. The result is a net draw of power from the grid. In these sea conditions the machine is not operated, though the generated power is still positive. In average over a large number of operation periods these direct electrical losses are in the range of 8 kW. For small generated power the losses increase and another negative effect occurs. It was found that device operation with generated power average below 12 kW caused negative or zero net power and additionally in operation periods with negative net power the device produces inductive reactive power. Because inductive reactive power is billed negatively operation below 12 kW average generated power was stopped. In the consequence all periods with generated average power below 12 kW do not contribute to the annual power production anymore.

The direct electrical losses are consequently modeled by reducing the generated power about 8 kW in average.

Further indirect electrical losses are modeled by not counting the operation periods, in which the generated power is below 12 kW.

The influence of the indirect electrical losses is only modeled for the “validated model” and the “validated model” with implemented designed turbine curve.

Hydrodynamic defects

The detailed analysis of this effect can be found in Chapter 4. 3.3. .

3.5. POWER EVALUATION

As explained in Chapter 4. 3.4. the Pico plant was theoretically expected to produce an annual average grid power of about 96 kW. In comparison to the predictions the real Pico plant reached its maximum annual average production in 2016, when an average of 5,1 kW was fed to the grid. This low value was essentially influenced by technical machine down time. As already shown in Chapter 4. 3.3. by superposition for the technical machine down time the annual average grid power for full machine availability was estimated to be approximately 11,5 kW. The “validated model”, which reproduces the real device reasonable, returned 23 kW annual average grid power. This model was fed with the “computed theoretical wave input” similar as was done for the initial predictions. The validated model uses the hydrodynamic conversion of the designed device and therefore existing defects in the chamber structure are not taken into account.

Because here additional hydrodynamic losses caused by the the structural defects are expected to be likely in the range of the unexplained 11,5 kW, the performance appears to be analyzed sufficiently.

In order to provide standardized performance results a performance evaluation that follows the in (Pecher *et al*, 2011) proposed Equimar Methodology is executed. This methodology allows the comparison to other WEC' s such as the evaluation of the device performance in other wave climates.

Because, as already in Chapter 3. 4. stated, the only available wave data at the time of this study was offshore forecast data, the same methodology as introduced in Chapter 4. 3.3. Step 6 was applied for this purpose.

In order to enable a more precised sea state classification here a much larger set of 493 predefined sea states was used. These 493 local sea states cover the range of 0,5- 4,5 m H_s and 8- 15 sec T_e with a accuracy of 0,5 m in H_s and 0,25 sec in T_e .

This enabled the relation of operation periods into sea states with a tolerance of only 10 % for the spectral values H_s , T_e and m-1 moment of the chamber surface elevation.

For the presentation in a scatter diagram the large number of sea states was reduced again by merging them into a set of 107 sea states with an accuracy of 0,5 m for H_s and 1 sec for T_e .

In the scatter diagram of Figure 4.24 the real produced generator power and the generator power results of the “validated model” are shown. It can be obtained that the trend is similar and the power levels of the model results are approximately 10 kW higher in most sea states. This matches with the expectations. Here the generated power instead of grid power was chosen to enable a direct comparison to the prior performance evaluation presented in (Pecher *et al*, 2011).

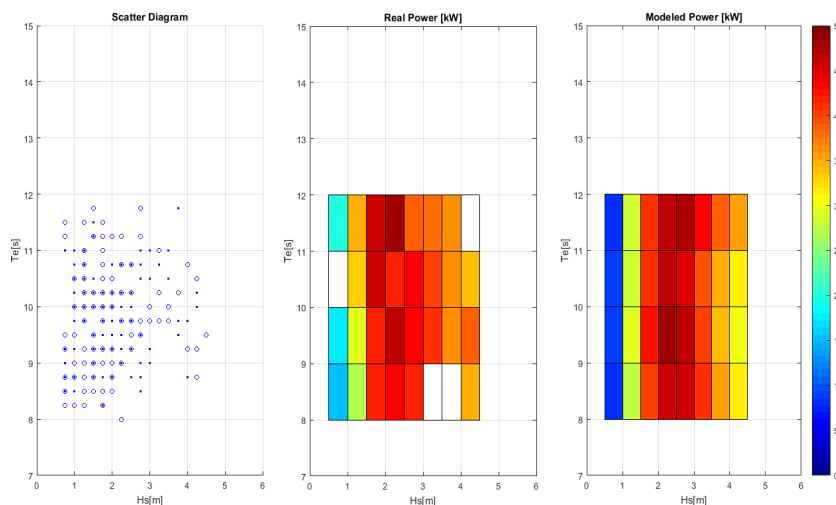


Figure 4.24 General scatter diagram of the Pico device today (Left: the used performance points (The filled and empty dots both indicate one performance point. Due to the classification procedure the points are sometimes overlapping. Therefore two different point types are used.); Middle: the real device average power per sea state; Right: Validated model average power per sea state)

CHAPTER 4. DATA ANALYSIS AND RESULTS

Though the found low performance is real, it should not be forgotten that it appears to be caused widely by only one system malfunction. Further as will be shown in Chapter 5. 3.1. this malfunction appears to be correctable within reasonable means.

In order to show what appears to be achievable when only the detected turbine performance deficit can be removed a second scatter diagram is shown in Figure 4.25. It shows again the generated power results of the “validated model” just as Figure 4.24 but additionally shows the expected increased generated power of the “Model with corrected turbine”.

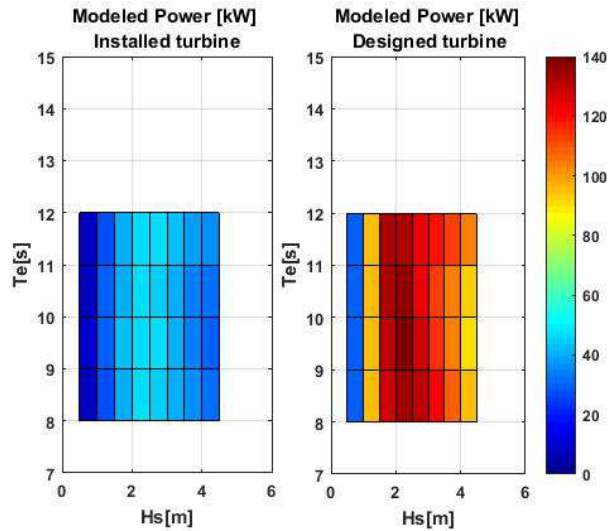


Figure 4.25 Pico scatter diagram for the device with corrected turbine efficiency (Left: modeled average power per sea state for the “Validated model”; Right: modeled average power per sea state for the “Model with corrected turbine”)

3.6. DISCUSSION OF UNCERTAINTIES

The conversion from pressure inside the air chamber to generated power can be reproduced reasonable by the numerical model. The average error here is in the range of 4 kW. Here uncertainties are introduced by several assumptions but the only assumption with a large influence to the model results is the chosen turbine performance curve. This turbine curve of the real turbine could only be captured with a fairly low data quality, which required filtering. This is likely to compress the peak of the captured curve too much. Therefore the shape of the captured curve is likely not exactly correct and therefore introduces uncertainties. However the captured curve shows an even lower peak height than the one that returns the good model match. This corresponds with the assumption of the peak compression due to the filtering.

Without the modeled turbine underperformance it was impossible to achieve a somehow reasonable model match for this part of the conversation. Therefore either the turbine deficit or another still unknown effect with a similar influence appears proven. The hydrodynamic conversion is not included in this model therefore additional losses in the hydrodynamic conversion cannot cause these losses.

Further uncertainties are introduced due to the missing real time wave measurements. Therefore for the annual power observation it has to be assumed that the used local wave climate is reasonable, the annual variations of the wave climate in the observed production interval was not too large and the used assumptions for the superposition are reasonable.

Also for the analysis of the specific sea conditions uncertainties are introduced by the chosen sea state classification method. However, a wrong sea state classification does not change the pure device power production but only shifts the performance point in the scatter diagram of Figure 4.24 into another box. But as can be obtained there, all high performance points are missing in the entire diagram for the real device.

Both analysis show the similar, plausible results independently from each other. The model shows clearly that the largest power losses appear in the conversion from pressure in the chamber to electric power. Here it only remains not 100% proven that the reason is really the turbine curve alone. In relation only smaller losses are not explained in the part of the conversion and therefore are assumed to be caused by the hydrodynamics. Here the uncertainties are rather high but the influence of these uncertainties is low due to the rather small losses in this part.

Plausible analysis results:

- The theoretical initial annual power predictions could be reproduced by the use of the prior validated model, the local wave climate and the assumption that the hydrodynamic performance is as designed.
- With the same assumption, also based on the local wave climate the validated model returns a power short fall of about 73 kW from the the initial predicted 96 kW annual average grid power down to 23 kW annual average grid power.
- Superposition of real device production data indicates an annual average power of approximately 11,5 kW, which corresponds to a power shortfall of 84,5 kW.
- From the annual power observation additional hydrodynamic losses in the range of 11,5 kW can be expected.
- The performance evaluation of the real device in specific wave conditions with again assumed designed hydrodynamic conversion confirms this result independently from uncertainties in the local wave climate. In average over all observed sea conditions the difference between validated model and real device is in the range of 10 kW.

3.7. DISCUSSION OF THE PERFORMANCE ANALYSIS RESULTS

The results appear plausible due to the coherence between the real device results and the model results.

For further interpretation of the found results they are set in context with two prior analysis of the Pico converter. One is the already introduced performance evaluation of the Pico plant (Pecher et al, 2011) and the other is another also already mentioned study about the correction of the pressure asymmetry at the Pico plant (Monk, Winands and Lopes, 2018).

The in (Pecher et al, 2011) in 2010 executed performance evaluation of the Pico plant is based on the Equimar methodology, which widely corresponds to the here executed overall performance analysis. The analysis in (Pecher et al, 2011) is based on offshore wave measurements of an at this time still existing wave rider buoy in the region. The used power data is obtained from event based measurements on converter level of the Pico plant. As can be seen in Figure 4.26 compared to Figure 4.24 the in (Pecher et al, 2011) presented results show in average approximately 10 kW higher real power results. The data in (Pecher et al, 2011) was obtained from an unofficial data acquisition system, which depend on the data acquisition system configuration and the calibrations. The here presented data is based on grid records. It cannot be said if plausibility verification with grid measurements were executed at the time. However, the author was the Pico plant operator in 2010 and never experienced only a single operation period with grid power values of the presented level. In 2010 the main DAQ system was not correctly functional. That is why the event based data stored in the control unit was used for the study. This data is usually not used due to its inaccuracy. Further evidence for overestimation of the generated power in (Pecher et al, 2011) can be found in observations of the grid power records of 2010. Though the records of the utility contain problems and do not cover the entire period it can be seen that the found higher power results are most likely a calibration problem because not a single record of any higher power periods can be found. The different results in the here presented performance evaluation of 2016 and the one 2010 are here regarded to be no sign for a decreasing device performance, because no evidence could be found for it.

Never the less the trend of the scatter diagram is similar. Additionally the magnitude of the overall power levels is fairly similar. It can further be obtained that the power levels are shifted towards higher H_s values. Such a result has to be expected because the used classification is based on offshore measurements and the significant wave height H_s decreases from offshore waves to near shore waves.

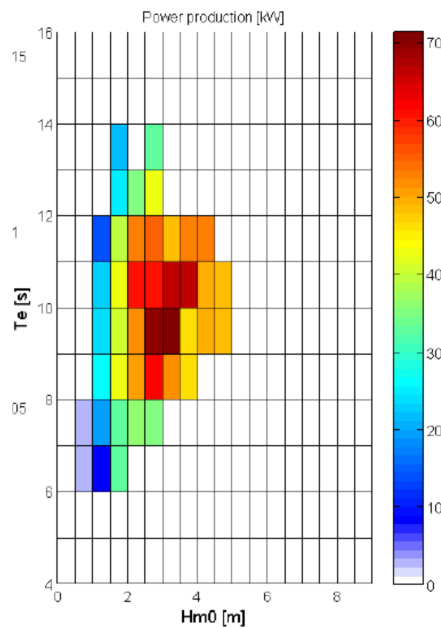


Figure 4.26 Pico performance scatter diagram presented in (Pecher et al, 2011)

In (Monk, Winands and Lopes, 2018) a study was executed about the partially correction of the chamber pressure asymmetry by the use of a passive one way valve installed in series with the installed turbine bypass valve. The conclusion is that up to approximately 45 % power increase can be achieved in the more energetic sea

CHAPTER 4. DATA ANALYSIS AND RESULTS

states by using the proposed passive valve to reduce the pressure skewness. Due to the low production levels the found 45 % correspond with approximately 12 kW. Further it can be seen that the system only shows an influence at very large sea conditions. This is obviously caused by the type of system, which can only operate at large sea conditions and which further is only a correction system of the pressure asymmetry that cannot remove the asymmetry completely. However in the here presented thesis the assumed influence of hydrodynamic conversion problems is 11,5 kW, which is in the range of the maximal found modeled power increase in the passive valve study. Therefore the paper results are assumed to backs the results of the here presented study.

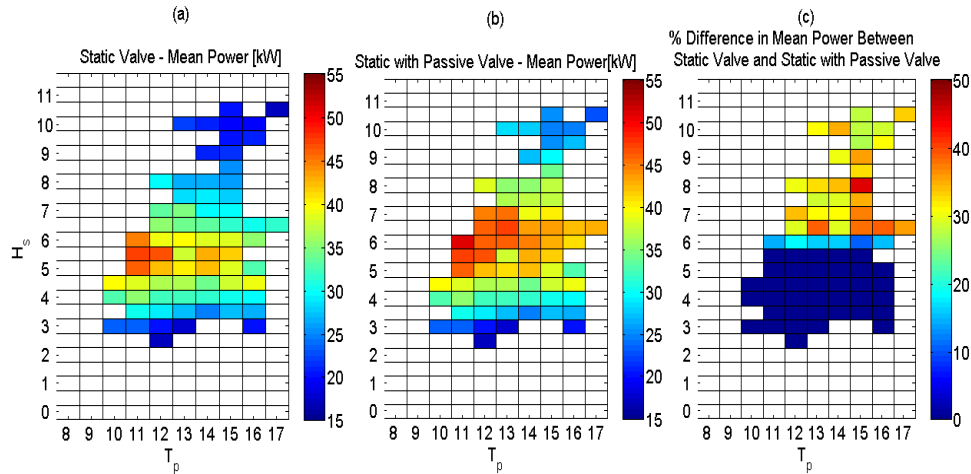


Figure 4.27 Pico scatter diagram with passive rectification valve (Monk, Winands and Lopes, 2018) (H_s and T_p values correspond to excitation flow surface elevation and not to outside wave).

3.8. CONCLUSIONS FROM THE PERFORMANCE ANALYSIS

For the Pico plant in its current conditions

- The present analysis can explain the occurrences, which cause the underperformance of the Pico converter.
- Theoretically the concept of the Pico project could be proven by the reasonable fit from real to modeled performance.
- The real device was able to produce about 12 % of the initial power predictions for grid power which are accounted with 96 kW (full machine availability assumed).
- The prior as main contributor of the large device underperformance expected additional hydrodynamic losses, which are caused by structural defects, could be found to cause rather small losses in the range of 12 % of the initial power predictions.
- A turbine performance deficit, which could not fully be understood for its root causes, was found to be the major contributor. It appears to cause losses of about 69 % of the initial power predictions.
- Another 7 % of the initial power predictions are lost due to reduced rotational speed.
- Frequently occurring aerodynamic stall events are assumed to be partly caused by the low turbine efficiency and are assumed to decrease when achieving the designed turbine performance.
- The influence of the designed optimal control strategy could be found to be unappropriated and detrimental to the machine in its current state due to the underperforming turbine. For the machine with corrected turbine performance it appears to have a positive influence in low energetic sea conditions. Due to the small influence it was not analyzed further here. Once the designed turbine is installed a proper analysis is recommended.

Perspective for a device with removed turbine performance deficit

The consequent final step of the Pico project should have been the correction of the turbine performance deficit, which appear technical possible with reasonable means and effort. Therefore the model predictions for this case are shown as well. In this approach the power losses due to hydrodynamic defects and rotational speed limitation are assumed similar as for the real machine with turbine underperformance.

In Figure 4.28 the power losses of the device in its current conditions is displayed and the possible benefit when removing the turbine performance deficit is displayed by the use of the “ Model with corrected turbine”. Similar to Figure 4.20 the length of the beams corresponds to the size of the displayed values.

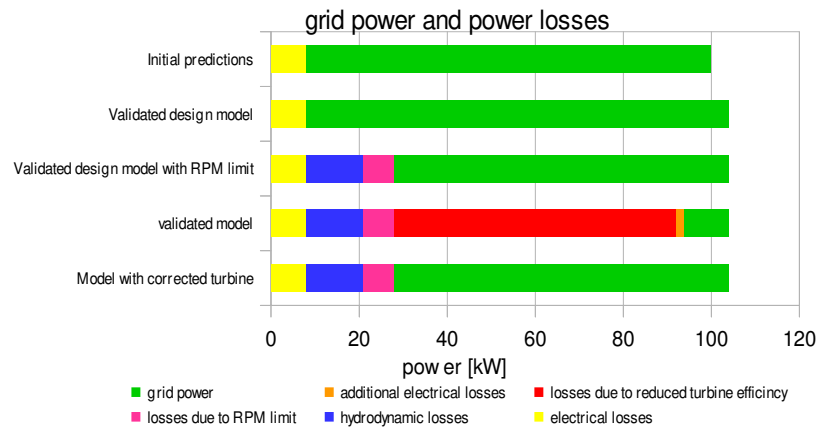


Figure 4.28 Expected power increase

CHAPTER 4. DATA ANALYSIS AND RESULTS

- In Figure 4.28 it can be obtained that the grid power increases about the factor of 6,7 to about 77,5 kW. *Note: This high multiplication factor is essentially influenced by the currently very low power production.*
- If the additional hydrodynamic losses are not considered, for generated power an increase about the factor 2,9 from 33 kW to 97 kW can be obtained. This increase can be seen when comparing the model results. Similar to the method that was applied in Chapter 4. 3.3. , in Figure 4.29 results for both the “validated model” and the “Model with corrected turbine” are plotted in the 44 sea states. In Figure 4.30 a plot of a random operation period is given. The factor of approximately 2,9 can be obtained in both figures.

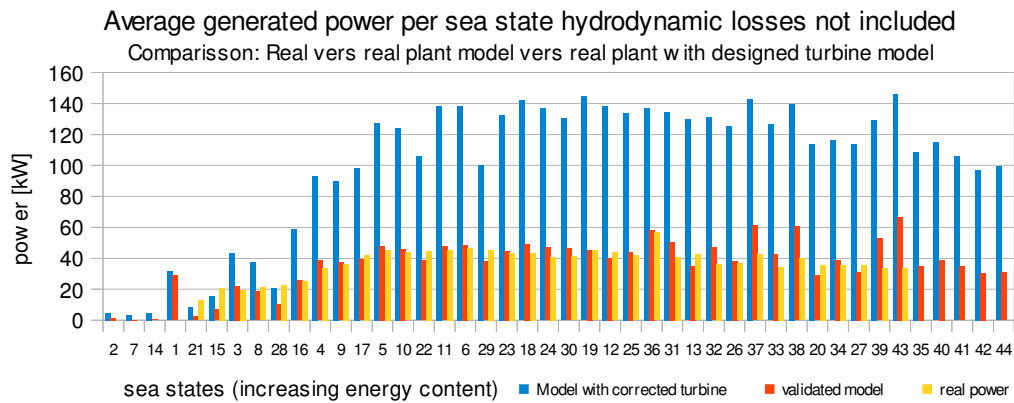


Figure 4.29 Generated power comparison per sea state

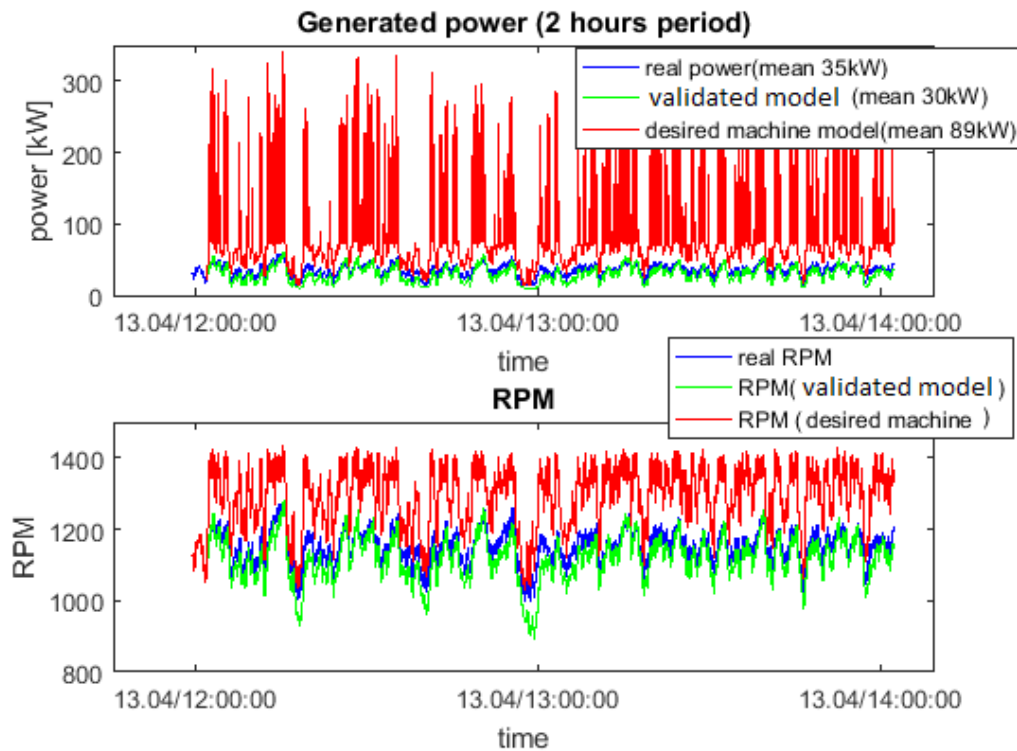


Figure 4.30 Factor 2,9 verification in real operation interval of 2 hours (Figure corresponds to Figure 4.8)

CHAPTER 5. CONCLUSIONS

1. CONCLUSIONS RELATED TO THE THESIS OBJECTIVES

The objective to explain the reasons for the initial project problems could be achieved.

With the executed root cause analysis it could be shown in a transparent way that the initial project struggled mainly because existing reliable design solutions were not applied in various subsystems. By presenting the solutions to overcome the problems it could be shown that the application of existing common engineering solutions solved the problems. Therefore it could be shown that the majority of the determining problems could have been avoided.

The objective to share the continuous operation experience has been achieved.

The technical problems and the related solutions are shared.

The Pico project delivers a fully functional OWC system, including the necessary detail designs such as component choices, suitable protection systems such as a suitable maintenance plan and plant control procedures. Further many low cost solutions for sensors and detail designs were developed.

Based on the gathered experience of the Pico project it is possible to build a next generation device, which is supposed to operate from the right beginning without large technical problems.

By sharing the production figures and comparing it to other devices it could be shown that since 2010 the Pico project is a rather positive example for wave energy converters. This is concluded from the following achieved success which are presented.

- Different from most other large scale devices the Pico plant could be operated in long term continuous operation for a period of 7 years.
- The device operated reliable automatically and remote controlled.
- The used machinery could be fully understood in terms of operation and maintenance requirements.
- The in reality achieved production figures are noteworthy and enough to cover spare parts and consumables costs. Though the production remained far below the expectations the overall efficiency appears to be still in a similar range as for the Mutriku OWC, which is the WEC that had reached the highest accumulated power of all WECs.
- The Pico plant could prove its survivability on an especially in winter time very energetic coast line. The device remained more than 18 years.

The objective to present the detection of the main reason for the large device underperformance could be achieved.

It is shown that the executed performance analysis could reveal the main reason for the large underperformance of the real device to be a turbine underperformance. In Chapter 5. 3.1. Further development on the Pico plant it will also be shown that it appears theoretically and practically possible to implement new turbine blades and possibly new guide vanes to remove the turbine performance deficit. This change alone enables reasonable perspectives in terms of economical viability. It appears possible to reach a load factor of 0,19, which corresponds to annual average production of 77,5 kW and an annual income from energy revenues of more than 180.000 €.

Because these predictions are based on a prior validated model the risk to fail appears rather low. The same applies for other new determining technical failure because the device was already in long term operation.

The global objective to reinforce the sector of wave energy by providing a positive example for a full scale WEC could only partly be achieved.

It could be shown that after having passed a complicated realization and troubleshooting period the device has delivered more than most other full scale WECs. Beside that it was possible to proof the theory with an reasonable match between the real device performance and a validated numerical model. Further the reasons for the production deficit could theoretically been discovered. Also the technical solutions to remove the turbine underperformance and finally turn the Pico plant into an indeed successful full scale WEC, which performs close to its predictions are suggested.

However, the suggested turbine underperformance correction could not be realized at the real device, even though the problem was detected and the technical solutions internally presented already in 2016 when the device structure was still in conditions, which allowed the proposed intervention. Without the verification of the

CHAPTER 5. CONCLUSIONS

model results at the real device the results cannot be assumed as 100 % proven, neither can the Pico plant be called a full success.

If it would have been possible to confirm the theoretic findings of the performance analysis with real plant tests with corrected turbine performance it would have been realistic to believe that a next generation device based on similar technology can deliver power levels in the range of the 100 kW annual average. These power levels would correspond to a load factor of 0,25 when assuming similar rated power.

Finally the Pico project remains another full scale WEC, which could in reality not fulfill its production predictions. But at least it could be shown that it is indeed possible to operate such a full scale WEC in very harsh conditions without the need of a large budget. And at least theoretically it appears proven that the power output could have been increased almost to the initial predictions even with the old and outdated device.

2. SCIENTIFIC INNOVATION

2.1. SCIENTIFIC INNOVATION OF THE FIELD STUDY

Before the beginning of this field study hardly any real long term operation results existed for the latest generation of full scale OWC wave energy converters equipped with Wells turbines. The same applies for most of the other PTO types but this is not the topic here. At the time the Mutriku OWC device was not yet build, the Limpet 500 OWC device could only reach long term continuous operation with significantly smaller turbines, the Osprey OWC device was destroyed during installation, the Pico device was more or less nonoperational and still today very few details are known about the Vinzinhim OWC.

The in this thesis presented work during this field study enabled continuous long term operation of a full scale OWC device, which could not be reached before and is still unique when regarding the installed turbine size. This operational full scale device enabled unique learning about the system and several scientific studies.

Beside others the following studies were enabled:

- The in 2011 executed performance analysis of the Pico device (Pecher *et al*, 2011).
- The studies about short term forecasting by using neuronal networks (Monk *et al*, 2015).
- A study about the correction of pressure skewness caused by structural defects (Monk, Winands and Lopes, 2018)
- The fatigue analysis in OWC rotor guide vanes caused by aerodynamic stall (Vieira, 2014).

2.2. SCIENTIFIC INNOVATION OF THE THESIS

In this thesis it was possible to analyze and explain the occurrences, which caused the OWC with the largest turbine that ever reach continuous operation to be economically absolutely not viable.

- The real device performance could be quantified and revealed a significant difference to a prior evaluation presented in (Pecher *et al*, 2011).
- The total before not understood losses of almost 90 % compared to the predicted power could be analyzed and explained.
- A before undiscovered malfunction of the turbine could be detected, which makes up for about 70 % of the total losses.
- A concept to turn the at the time of the study still existing Pico OWC and future device into economical viable devices could be proposed in Chapter 5. 3.1. .
- Large parts of the wave to wire theory could finally be confirmed on a large scale OWC. This could be achieved by the development of a time domain model that can reasonably return the instantaneous real device performance and the annual power predictions.
- The developed model can now be used as a base for reliable power predictions for future OWC's.

Before this thesis it was assumed in (Monk *et al*, 2015) that the poor performance of the Pico OWC was most likely caused by structural defects, which cause hydrodynamic losses. This assumption was based on the results of a time domain model, which modeled the conversion from excitation flow to generated power confirm to the instantaneous real device performance. Following these prior model results, the in operation visible and in (Pecher *et al*, 2011) quantified large performance deficit in annual average was expected to not be caused in this part of the conversion. This theory could be disproven in the here presented thesis.

With the detection of the turbine malfunction the question for the reasons is raised. A first during this study executed analysis for the root causes of the turbine malfunction revealed some evidence that a scaling problem for monoplane Wells turbines exist. This should be subject of future studies to remove remaining uncertainties.

3. FUTURE WORKS

3.1. FURTHER DEVELOPMENT ON THE PICO PLANT

This part was written before the device finally collapsed. At this time it was strongly recommended to correct the here detected turbine performance deficit.

This would have enabled the following opportunities

- The above concluded power increase could be realized.
 - This would be a great success for wave energy because the Pico plant would become a WEC, which provides about 80 % of the initial power predictions.
 - The device would be economically fairly viable
 - The device testing and learning could be completed by
 - gaining experience in continuous operation with designed power levels
 - studying the suggested optimal control strategy in the predicted power range.

Suggestions to realize the turbine performance correction

The rotor of the Pico turbine was designed with the possibility to exchange the rotor blades, therefore it was not required to substituted the main structure of the turbine. The question why the turbine performance was so much lower than the designed turbine should be studied and answered. However even without this study it appeared possible to reach a turbine performance in the desired range. This was assumed because in (Falcao, Henriques and Gato, 2016) a recent monoplane Wells turbine similar to the Pico turbine type is presented and already theoretically adapted to the Pico plant. The characteristic curve of this for Pico adapted turbine can be obtained in Figure 5.1. In Figure 5.2 the curve is compared to the in Chapter 2. 2.3. shown characteristic turbine curve of the designed Pico turbine(Figure 2.6). It is visible that the peak of the curve is about the factor 1,6 higher. This turbine could have been directly implemented to the Pico device. However this would have implemented some slightly deeper changes because the rotor only consists of 5 blades and additionally new rotor guide vanes would be required. Therefore it was suggested to study if it would have been possible without to large performance losses to adapt the turbine to a 8 blade rotor without guide vanes.

Even in the case that the performance deficit of the Pico turbine was caused by a scaling problem, which might apply for all mono plane Wells turbines it would have still been possible to increase the performance of the Pico plant essentially.

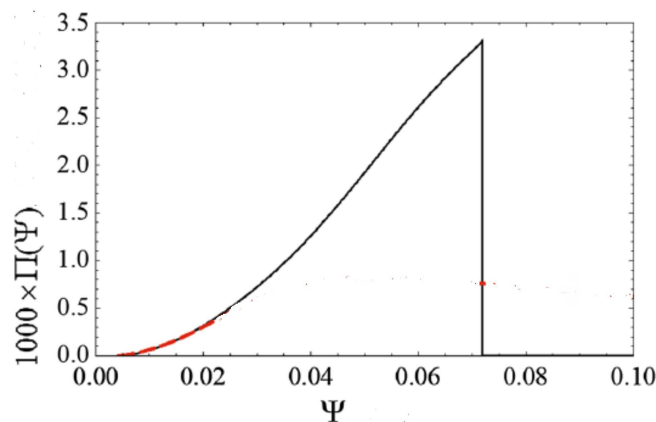


Figure 5.1 Turbine curve of a recent Wells turbine which is adapted to the Pico plant (presented in (Falcao, Henriques and Gato, 2016)).

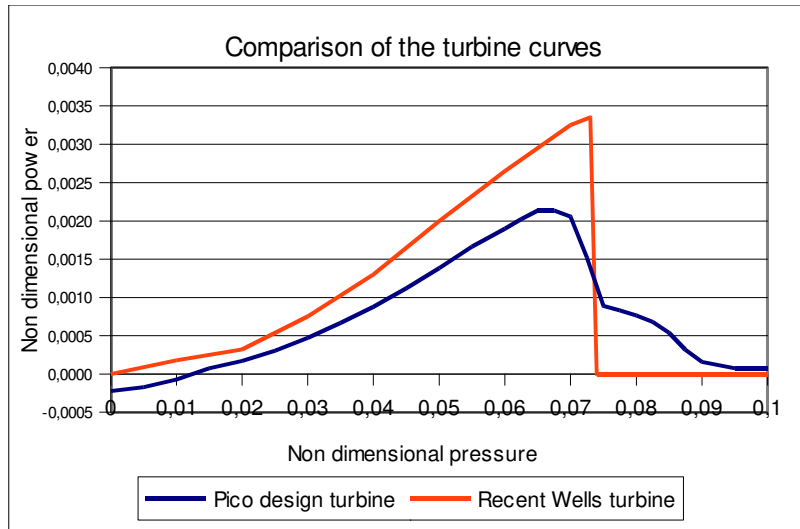


Figure 5.2 Curve comparison: Recent turbine to Pico design turbine

3.2. SCIENTIFIC STUDIES

Wells turbine

The reason for the here detected turbine performance deficit of the Pico turbine should be studied. A first analysis during the field study revealed some evidence that a scaling problem might be the cause. This is required to be verified because it is essential to this turbine type and OWC technology. Therefore it is proposed to execute the following analysis steps.

- Capture the real Pico plant turbine curve with suitable equipment to reduce uncertainties (Due to the device collapse this is not possible anymore).
- Capture the turbine curve of the mini turbine that was used for the Pico turbine design process again for certainty in the results.
- Possibly degrade the mini turbine artificially to the conditions of the real turbine and capture the turbine curve again.

4. ADVISES FOR FUTURE PROJECTS

4.1. ALL PTO TYPES

Here it is assumed essential for all device types of near future WECs to find the right balance between reliability and performance. Here it is suggested to not go for the most efficient machine if this involves an elevated risk to fail but also not to go for a very reliable system, which is not obviously showing a chance of economic viability in the near future.

In the design process it is strongly recommended

- To reduce own new design solutions to an absolute minimum and instead use and adapt proven solutions from other systems or applications.
- To design the entire system in a way that all components can be accessed, maintained and replaced within reasonable means even in the installed location.
- Design should be executed rather conservative to ensure reliable prototypes. The design can be optimized when the function is proven.

For the project management it is recommended

- To involve persons with different professional background in the design process to reduce the risk of unnecessary failures
- To consult local knowledge about the location and infrastructural conditions
- To be prepared for unexpected failures with budget and a troubleshooting concept. Here it is assumed required to foresee an engineering / troubleshooting team on location for the first project period.

4.2. OWC IN PARTICULAR

Here the learning process with onshore OWCs with large mono plane Wells turbines is not considered to be completed. Though onshore OWCs with mono plane Wells turbines are here not considered as the end of the line in wave energy technology it is recommended to complete the learning process before taking the next step. The underlying theory still waits for its final prove in real full scale device operation. Further operation experience with the elevated power levels has to be gained to ensure the results with reduced turbine performance can be confirmed. Though today other recent turbine types appear more efficient, as for example the be radial turbine that is analyzed in (Falcao, Henriques and Gato, 2016) , it is suggested to prove the correct transfer from mini to real turbine on the already build mono plane Wells turbines first to reduce the risk of similar problems with other turbine types.

5. PERSONAL CONSIDERATION

In the authors opinion the struggling of the Pico project and the reason why the final operation period could not be reached are not caused by missing technical solutions.

LITERATURE LIST

- Adams, A.S. and Keith, D.W. (2013) 'Are global wind power resource estimates overstated?', *Environmental Research Letters*, 8 (2013) 015021 (9pp)
- AW- Energy (2017) Waveroller. Available at: <http://aw-energy.com/> (Viewed: 23.02.2017)
- Brito- Melo, A., Gato, L.M.C. and Sarmento, A.J.N.A. (2002) 'Analysis of Wells turbine design parameters by numerical simulation of the OWC performance', *Ocean Engineering*, 29 (2002), pp 1463–1477.
- Brito- Melo, A., Hoffman, T., Sarmento, A.J.N.A., Clement, A.H. And Delhommeau, G. (2001) 'Numerical Modelling of OWC-Shoreline Devices Including the Effect of Surrounding Coastline And Non-flat Bottom', *ISOPE*, 11 (2)
- Brook, J. (2003) 'Wave energy conversion' *Elsvier Ocean Engineering Book Series*, vol.6
-
- Cargas, M. (2006) 'The Pelamis Wave Energy Converter A phased array of heave + surge point absorbers'. Available at: http://hydropower.inl.gov/hydrokinetic_wave/pdfs/day1/09_heavesurge_wave_devices.pdf (Downloaded: 23 February 2017)
- Carnegie (2017). Available at: <https://carnegiewave.com/> (Viewed: 23.02.2017)
- Cement, A., Mc Cullen, P., Falcao, A., Fiorention, A., Gardner, F., Hammarlund, K., Lemonisa, G., Lewish, T., Nielsen, K., Petroncinij, S. and Pontes, T. (2002) 'Wave energy in Europe: current status and perspectives', *Renewable and Sustainable Energy Reviews*, 6 ,issue 5, October (2002), pp 405-431.
- Edinburgh wave power group (1984) *Narrow tank introduction* (video), Available at: <http://www.homepages.ed.ac.uk/v1ewaveg/Videos.htm> (viewed 18.03.2017)
- EVE (2016) *The wave energy plant in Mutriku reaches a production milestone with the renewable energy of waves by generating more than 1GWh*. Available at: <http://www.eve.eus/Noticias/La-planta-de-las-olas-de-Mutriku-alcanza-un-hito-d.aspx?lang=en-GB> (viewed 20.02.2017)
- Falcao, A.F.O. (2000) 'The shoreline OWC wave power plant at the Azores', In: Proceedings of the Fourth European Wave Power Conference, Energy Centre Denmark, Danish Technological Institute, Tastrup, 42–48, Denmark, paper B1.
- Falcao, A.F.O. (2002) 'Control of an oscillating-water-column wave power plant for maximum energy production', *Applied Ocean Research*, 24 (2002), pp 73-82.
- Falcao, A.F.O., Henriques, J.C.C. And Gato, L.M.C. (2016) 'Air turbine optimization for a bottom-standing oscillating-water-column wave energy converter', *Journal of Ocean Engineering and Marine Energy*, February 2016
- Global wind energy council, (2016)'Global wind statistic 2015' Available at: http://www.gwec.net/wp-content/uploads/vip/GWEC-PRstats-2015_LR.pdf (Downloaded: 23.02.2017)
- Gunn, K. and Stock- Williams, C. (2012) 'Quantifying the global wave power resource', *Renewable Energy*, 44 (2012), 296-304
- Illawarran Mercury (2014) *Port wave generator removal in doubt*. Available at: <http://www.illawarramercury.com.au/story/2193950/photos-port-wave-generator-removal-in-doubt/> (viewed 25.01.2017)
- INSTITUTO SUPERIOR TECNICO (1998) 'EUROPEAN WAVE ENERGY PILOT PLANT ON THE ISLAND OF PICO, AZORES, PORTUGAL. PHASE TWO: EQUIPMENT', *Contract JOR3-CT95-0012 PUBLISHABLE REPORT*. Available at: <http://cordis.europa.eu/documents/documentlibrary/47698021EN6.pdf> (Downloaded: 23 February 2017)
- International Energy Agency (2015) '2015 Key world Energy Statistics' Available at: <https://www.iea.org/newsroom/news/2015/november/key-world-energy-statistics-2015-available-for-download-in-time-for-climate-talk.html> (Downloaded: 23 February 2017)
- IRENA, International renewable energy agency, (2014), *Wave energy technology brief 4*, Available at http://www.irena.org/DocumentDownloads/Publications/Wave-Energy_V4_web.pdf (viewed 13.03.2017)
- Jayashankar, V., Mala, K., Kedarnath, S., Jayaraj, J., Omezhilan, U. and Krishna V (2011) 'Design of a 100 GWh wave energy plant', in: Proceedings of the World renewable energy congress 2011 – Sweden *Marine and Ocean Technology (MO)*, 8-13 May 2011, Linköping, Sweden
- Justino, P.A.P. And Falcao, A.F.O. (1999) 'Rotational speed control of an OWC plant', *J. Offshore Mech. Arct. Eng.* 121(2), 65-70 (May 01, 1999)
- Kenny, C., Findlay, D., Lazakis, I., Shek, J. and Thies, P. (2017) 'Lessons Learned from 3 Years of Failure: Validating an FMEA using Historical Failure Data', EWTEC 2017: 12th European Wave and Tidal Energy Conference, 27 August - 1 September 2017, Cork, Ireland

- Le Crom I., Brito-Melo, A., Neumann, F., Sarmento, A.J.N.A. (2009) 'Numerical Estimation of Incident Wave Parameters Based on the Air Pressure Measurements in Pico OWC Plan', in *Proceedings of the 8th European Wave and Tidal Energy Conference EWTEC 2009, Uppsala, Sweden- 7-10 September 2009*.
- Mäki, T., Vuorinen, M and Much, T. (2014) 'WaveRoller – One of the Leading Technologies for Wave Energy Conversion', in: *Proceedings of the International conference of ocean energy, Halifax, 2014*.
- Marquis, L., Kramer, M. and Frigaard, P. (2010) 'First Power Production figures from the Wave Star Roshage Wave Energy Converter', in: *Proceedings of the Proceedings of the International conference of ocean energy, Bilbao, 2010*.
- Mohamed, M and Shaaban, S (2013) 'Optimization of blade pitch angle of an axial turbine used for wave energy conversion', *Energy*, 56 (2013) 229-239
- Monk, K. (2012) 'A review of the Pico project 2010 to 2012- mistakes, milestones and the future '. Available at: http://www.pico-owc.net/files/33/cms_e8432fb72c61c9066957124e5a420a05.pdf (Downloaded: 23.02.2017)
- Monk, K., Conley, D., Winands, V., Lopes, M., Zou, Q. and Greaves, D. (2015) 'Simulations and Field Tests of Pneumatic Power Regulation by Valve Control Using Short-term Forecasting at the Pico OWC', in *Proceedings of the EWTEC conference, Nantes, 2015*.
- Monk, K., Winands, V. and Lopes, M. (2018) 'Chamber pressure skewness corrections using a passive relief valve system at the Pico OWC' *Renewable Energy*, Volume 128 (2018) 230-240
- Mork, G., Barstow, S., Kabuth, A. and Pontes, M.T. (2010) 'Assessing the global wave energy resource', in: *Proceedings of the OMAE 2010 29th International Conference of Ocean, Offshore Mechanics and Arctic Engineering, June 6-11 2010, Shanghai*
- Mucha, T. (2014) 'WaveRoller Demonstration Project in Portugal: From Lab to Sea', in: *Proceedings of the International conference of ocean energy, Halifax, 2014*.
- Neumann, F. and Brito- Melo, A. (2009) 'MOERI - WavEC Collaboration Research for Safety Design and Optimal Operation of OWC-WEC Pilot Plant in Korea', Report prepared by WAVEC for a project in Korea
- Neumann, F. and Le Crom, I.(2011) 'Pico OWC - the Frog Prince of Wave Energy? Recent autonomous operational experience and plans for an open real-sea test centre in semi-controlled environment', in: *Proceedings of the 9th European Wave and Tidal Energy Conference (EWTEC 2011), Southampton, UK, 05-09 September 2011*.
- Neumann, F., Brito-Melo, A. and Sarmento, A.J.N.A. 'Grid connected OWC wave power plant at the Azores, Portugal', In: *Proceedings Int. Conf. Ocean Energy: from innovation to industry, OTTI, ISBN 3-934681-49-2, pp. 53-60, 2006*.
- New Atlas (2009) *Ocean-power installation up and running*. Available at: <http://newatlas.com/wave-power-owc/11122/> (viewed 25.01.2017)
- Nunes, N.N. and Claudio, R.D. (2006) 'Avaliação do Estado de Condição da Central de Energia das Ondas do Pico por Análise de Vibrações' Analysis executed by the Escola Superior Technolgia Setubal requested by WAVEC
- Ocean Energy Council (no date), *What are the anticipated wave energy costs?*, Available at: <http://www.oceanenergycouncil.com/ocean-energy/wave-energy/> (viewed 13.03.2017)
- Parmeggiani, S., Fernandez Chozas, J., Pecher, A., Friis- Madsen, E., Soerensen, H.C. And Kofoed, J.P. (2011), 'Performance Assessment of the Wave Dragon Wave Energy Converter Based on the EquiMar Methodology', in *Proceedings of the 9th EWTEC conference, Southampton, 2015*.
- Pecher, A. and Kofoed, J.P. (2016) *Handbook of Ocean Wave Energy*. Available at: <http://textpdfbook.org/pdf/?book=3319398881#Download> (Downloaded: 23 February 2017)
- Pecher, A., Kofoed, J. P., Le Crom, I., Neumann, F., and Azevedo, E. de B. (2011) 'Performance Assessment of the Pico OWC Power Plant Following the Equimar Methodology', In: *Proceedings of the Twenty-first International Offshore and Polar Engineering Conference, 19-24 June, Maui, Hawaii, USA , ISOPE*.
- Prado, M.G. De Sousa, Gardner, F., Damen, M. and Polinder, H.(2006) 'Modelling and test results of the Archimedes wave swing'. in: *Proceedings of the Institution of Mechanical Engineers Vol.220 (Part A)Journal of Power and Energy*
- Robertson, S. (2014) *A case study of wave energy: Port Kembla Australia*, Available at: <http://coastalenergyandenvironment.web.unc.edu/ocean-energy-generating-technologies/wave-energy/wave-energy-case-studies/a-case-study-on-wave-energy-port-kembla-australia/> (Viewed: 23.02.2017)
- Sarmento, A. J. N. A., Brito- Melo, A. and Neumann, F. 'Results from sea trials in the OWC European wave energy plant at Pico, Azores', in *Invited paper for WREC-IX, Florence, Italy, 2006, pp. 1–6*.
- Sarmento, A.J.N.A (2006) 'Engineering, analysis and monitoring of full-scale and prototype plants (performance, safety and environmental impacts)', Deliverable 06 report for the FP7 ITN 215414 – wavetrain2 project.

- The carbon trust (2005) 'Marine Energy Challenge *Oscillating Water Column Wave Energy Converter Evaluation Report*'
- The Globe and Mail. Inc. (2011) *Germany's RWE pulls out of world's biggest wave energy plan*. Available at: <https://www.theglobeandmail.com/report-on-business/industry-news/energy-and-resources/germanys-rwe-pulls-out-of-worlds-biggest-wave-energy-plan/article599534/> (viewed 15.01.2018)
- The Guardian (2014) *Scottish government accused of abandoning wave power*, Available at: <https://www.theguardian.com/environment/2014/dec/09/scottish-government-accused-abandoning-wave-power> (viewed 25.01.2017)
- Tidal Energy Today (2015) *Oceanlinx sinks into liquidation*. Available at: <https://tidalenergytoday.com/2014/12/23/oceanlinx-goes-into-liquidation/> (viewed 25.01.2017)
- Torresi, M., Camporeale, S.M., Strippoli, P.D. And Pascazio, G. (2008) 'Accurat numerical simulation of a high solidity Wells turbine', *Renewable Energy*, 33 (4) 735-747
- Torre-Enciso, Y., Ortubia, I.; Lopes de Aguilera, L.I. and Marqués, J. (2009) 'Mutriku Wave Power Plant: From the Thinking out to the Reality', in the Proceedings of the 8th European Wave and Tidal Energy Conference, Uppsala, Sweden.
- Valerio, D., Beriao, P. and da Costa, J.S. (2007) 'Optimisation of wave energy extraction with the Archimedes Wave Swing', *Ocean Engineering*, 34 (2007) 2330- 2344
- Venu, M. (2012) *Innovation Lost To The Waves ; The remnants of the decommissioned wave energy plant at Vizhinjam represent more than just another project that failed to take off*, Available at: <http://www.yentha.com/news/view/features/innovation-lost-to-the-waves> (viewed: 23.02.2017)
- Vieira, M., Monk, K., Sarmiento, A.J.N.A. and Reis, L. (2013)'The Pico Power Plant as an Infrastructure for Development, Research and Graduation' in the Proceedings of the Congresso de Ciência e Desenvolvimento dos Açores, Angra do Heroísmo, Azores, Portugal, 2013.
- Vierira (2014) 'Análise da Integridade Estrutural das Pás Directrizes da Turbina da Central de Ondas dos Açores' *Master Thesis at the I.S.T. Lisbon*
- Wave Star A/S. (2013) 'Wavestar Prototype at Roshage' Performance Data for ForskVE Project No 2009-1-10305 Phase 1 & 2. Report by Wave Star A/S. pp 23.
- WAVEC (2014 a) *February 2014: The master returns and the machine roars*. Available at: <http://www.pico-owc.net/news.php?cat=83&newid=318&wnsid=bde8e621058950805180d6e3e9f98b40> (viewed: 31.01.2017)
- WAVEC (2015) *April and May 2015: A reasonably good month of production followed by RPM sensor failure*. Available at: <http://www.pico-owc.net/news.php?cat=85&newid=328&wnsid=e3a675e59fd2b42f4f7ba145171ca1e6> (viewed: 31.01.2017)
- WAVEC, (2014 b) *December 2014: Maintenance work*. Available at: <http://www.pico-owc.net/news.php?cat=83&newid=325&wnsid=f13e0889a75ea81f5ad5a413ffbe2d46> (viewed: 31.01.2017)
- Wikipedia (2017 a) Seeschlange Available at: [https://de.wikipedia.org/wiki/Seeschlange_\(Wellenkraftwerk\)](https://de.wikipedia.org/wiki/Seeschlange_(Wellenkraftwerk)) (Viewed: 23.02.2017)
- Wikipedia (2017 b) *Fail-safe*. Available at: <https://en.wikipedia.org/wiki/Fail-safe> (viewed 30.01.2017)
- Wikipedia (2017 c) Wave Power, Available at: https://en.wikipedia.org/wiki/Wave_power (viewed 13.03.2017)
- Wikipedia (2018) *Wavegen*. Available at: <https://en.wikipedia.org/wiki/Wavegen> (viewed 15.01.2018)
- Winands, V. and Fester, F. (2013) 'Challenging times for wave energy:Reasons and Solutions', in the Proceedings of the *EWTEC* conference, Aalborg, 2013
- World energy Council, (2016)' World Energy Resource 2016' Available at: <https://www.worldenergy.org/publications/2016/world-energy-resources-2016/> (Downloaded: 23 February 2017)
- Wordpress (no date) Renewable Energy, Salters nodding duck, Available at: <https://baonguyen1994.wordpress.com/introduction-to-wave-energy/ocean-wave-technologies/terminators/salters-nodding-duck/> (viewed: 13.03.2017)
- Yao, S.X. and Gerwick, B.C. (no date) 'Underwater Concrete: Mix design and construction practices'. Available at: <ftp://dfi.org/OneMine/Marine%20Foundations%20Book%20-%20individual%20papers/29-5.4%20Underwater%20Concrete%20-%20Mix%20Design%20and%20Construction%20Practices.pdf> (Downloaded: 23.02.2017)

ISSN (online): 2446-1636
ISBN (online): 978-87-7210-525-3

AALBORG UNIVERSITY PRESS